

1-1-1994

## Thermal considerations in the drift due to the emplacement of a horizontal high level nuclear waste container

Akshay Bhargava  
*University of Nevada, Las Vegas*

Follow this and additional works at: <https://digitalscholarship.unlv.edu/rtds>

---

### Repository Citation

Bhargava, Akshay, "Thermal considerations in the drift due to the emplacement of a horizontal high level nuclear waste container" (1994). *UNLV Retrospective Theses & Dissertations*. 432.  
<http://dx.doi.org/10.25669/spm-t-gsu6>

This Thesis is protected by copyright and/or related rights. It has been brought to you by Digital Scholarship@UNLV with permission from the rights-holder(s). You are free to use this Thesis in any way that is permitted by the copyright and related rights legislation that applies to your use. For other uses you need to obtain permission from the rights-holder(s) directly, unless additional rights are indicated by a Creative Commons license in the record and/or on the work itself.

This Thesis has been accepted for inclusion in UNLV Retrospective Theses & Dissertations by an authorized administrator of Digital Scholarship@UNLV. For more information, please contact [digitalscholarship@unlv.edu](mailto:digitalscholarship@unlv.edu).

## **INFORMATION TO USERS**

**This manuscript has been reproduced from the microfilm master. UMI films the text directly from the original or copy submitted. Thus, some thesis and dissertation copies are in typewriter face, while others may be from any type of computer printer.**

**The quality of this reproduction is dependent upon the quality of the copy submitted. Broken or indistinct print, colored or poor quality illustrations and photographs, print bleedthrough, substandard margins, and improper alignment can adversely affect reproduction.**

**In the unlikely event that the author did not send UMI a complete manuscript and there are missing pages, these will be noted. Also, if unauthorized copyright material had to be removed, a note will indicate the deletion.**

**Oversize materials (e.g., maps, drawings, charts) are reproduced by sectioning the original, beginning at the upper left-hand corner and continuing from left to right in equal sections with small overlaps. Each original is also photographed in one exposure and is included in reduced form at the back of the book.**

**Photographs included in the original manuscript have been reproduced xerographically in this copy. Higher quality 6" x 9" black and white photographic prints are available for any photographs or illustrations appearing in this copy for an additional charge. Contact UMI directly to order.**

# **UMI**

A Bell & Howell Information Company  
300 North Zeeb Road, Ann Arbor, MI 48106-1346 USA  
313/761-4700 800/521-0600



**THERMAL CONSIDERATIONS IN THE DRIFT DUE TO  
THE EMPLACEMENT OF A HORIZONTAL HIGH  
LEVEL NUCLEAR WASTE CONTAINER**

by

**Akshay Bhargava**

A thesis submitted in partial fulfillment  
of the requirements for the degree of

**Master of Science**

in

**Mechanical Engineering**

Department of Mechanical Engineering  
University of Nevada, Las Vegas  
December 1994

UMI Number: 1361119

---

UMI Microform Edition 1361119  
Copyright 1995, by UMI Company. All rights reserved.


This microform edition is protected against unauthorized  
copying under Title 17, United States Code.

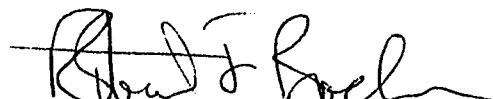
---

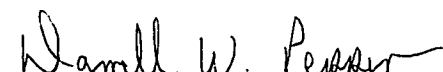
UMI

300 North Zeeb Road  
Ann Arbor, MI 48103


The Thesis of Akshay Bhargava for the degree of Master of Science in Mechanical Engineering is approved.

 9/14/94  
Chairperson, Dr. Samir Moujaes, Ph.D., P.E.

 9/15/94  
Examining Committee Member, Dr. Robert Boehm, Ph.D., P.E.

 9/15/94  
Examining Committee Member, Dr. Darrell Pepper, Ph.D.

 9/15/94  
Graduate Faculty Representative, Dr. Moses Karkouzian, Ph.D., P.E.

  
Dean of the Graduate College, Dr. Ronald Smith, Ph.D.

University of Nevada, Las Vegas  
December 1994

## **ABSTRACT**

The Yucca Mountain Site Characterization Project is investigating the feasibility of locating a high level radioactive nuclear waste repository at Yucca Mountain, Nevada. The design of waste containers to be used for the long term storage of the high level nuclear waste has progressed from the borehole model indicated in the original site characterization plan to drift emplaced multi-placed containers. The removal of decay heat is important in the first 1000 years as Zircaloy degradation temperature of 350°C is not to be exceeded.

In this study a two dimensional finite element thermal analysis has been completed for two scenarios for the in-drift emplacement scheme i.e. drift without backfill and drift with inverted backfill. Transient and steady state simulations have been carried out for a period of 1000 years and the peak temperatures at the walls of the drift and at the center of the container have been determined. The effects of natural convection and radiation are also discussed.

## TABLE OF CONTENTS

ABSTRACT .....	iii
LIST OF FIGURES .....	vi
ACKNOWLEDGEMENTS .....	viii
CHAPTER 1 INTRODUCTION.....	1
Nuclear Power History.....	1
Background.....	1
Charcterizing the Waste Forms.....	2
Literature Search.....	3
Objective.....	3
CHAPTER 2 THERMAL MODEL.....	4
CHAPTER 3 TRANSIENT HEAT CONDUCTION IN THE ROCK .....	14
Computational Domain.....	14
Simulation Approach.....	16
Results.....	18
CHAPTER 4 STEADY STATE ANALYSIS OF HEAT TRANSFER INSIDE THE DRIFT.....	32
Computational Domain.....	32
Simulation Approach.....	34
Results.....	38
CHAPTER 5 STEADY STATE ANALYSIS OF HEAT TRANSFER INSIDE THE DRIFT WITH BACKFILL.....	50
Computational Domain.....	50
Simulation Approach.....	52
Results.....	56
CHAPTER 6 CONCLUSION.....	74
APPENDIX 1 INPUT FILE FOR THE TRANSIENT HEAT CONDUCTION PROBLEM.....	75



APPENDIX 2 INPUT FILE FOR STEADY STATE HEAT TRANSFER INSIDE THE DRIFT WITHOUT BACKFILL.....	84
APPENDIX 3 INPUT FILE FOR STEADY STATE HEAT TRANSFER INSIDE THE DRIFT WITH BACKFILL.....	92
BIBLIOGRAPHY.....	100

## LIST OF FIGURES

Figure 1	Thermal Model.....	5
Figure 2	Waste Packages in the Drift.....	7
Figure 3	Variation of Heat Source.....	8
Figure 4	Computational Domain for Transient Heat Conduction in the Rock....	15
Figure 5	Variation of Time Increments.....	19
Figure 6(a)	Mesh Plot.....	20
Figure 6(b)	Zoomed Plot for the Mesh.....	21
Figure 6(c)	Zoomed Plot for the Mesh.....	22
Figure 7	Location of Nodes on the Model.....	24
Figure 8	History of Temperature on the Drift Wall.....	25
Figure 9(a)	History of Temperature at 10 m.....	26
Figure 9(b)	History of Temperature at 50 m.....	27
Figure 9(c)	History of Temperature at 150 m.....	28
Figure 10(a)	Temperature Variation at 22 Years.....	29
Figure 10(b)	Temperature Variation at 73 Years.....	30
Figure 10(c)	Temperature Variation at 951 Years.....	31
Figure 11	Computational Domain for the Steady State Analysis Inside the Drift Without Backfill.....	33
Figure 12	Mesh Plot.....	39
Figure 13(a)	Temperature Contours at 30 Years.....	42
Figure 13(b)	Temperature Contours at 130 Years.....	43
Figure 14(a)	Velocity Vector at 30 Years.....	44
Figure 14(b)	Velocity Vector at 130 Years.....	45
Figure 15	Streamline plot.....	46
Figure 16	Variation of Drift Wall Temperature.....	47
Figure 17 (a)	Zoomed Plot of Temperature Contours at 30 Years .....	48
Figure 17 (b)	Zoomed Plot of Temperature Contours at 130 Years .....	49
Figure 18	Computational Domain for the Steady State Analysis Inside the Drift With Backfill.....	51
Figure 19	Calculation of Hydraulic Diameter.....	55
Figure 20	Mesh Plot.....	57
Figure 21(a)	Temperature Contours at 10 Years.....	60
Figure 21(b)	Temperature Contours at 30 Years.....	61
Figure 21(c)	Temperature Contours at 130 Years.....	62
Figure 21(d)	Temperature Contours at 600 Years.....	63
Figure 22(a)	Temperature Contours at 10 Years (Only Conv) .....	64

Figure 22(b)	Temperature Contours at 30 Years (Only Conv).....	65
Figure 22(c)	Temperature Contours at 130 Years (Only Conv).....	66
Figure 22(d)	Temperature Contours at 600 Years (Only Conv).....	67
Figure 23	Temperature Contours at 10 Years (L=35 ft).....	68
Figure 24	Temperature Contours at 10 Years (L=35 ft, Only Conv).....	69
Figure 25	Vector Plot at 10 Years.....	72
Figure 26	Streamline Plot.....	73

## **ACKNOWLEDGEMENTS**

I would like to express my profound gratitude to Dr. Samir Moujaes for his contribution to this thesis project. But for his brilliant ideas and guidance at each step, this would not have been possible.

I would like to thank Dr. Samaan Ladkany, Professor of Civil & Environmental Engineering for offering me financial aid to complete this project. I would also like to thank Dr. Robert Boehm, Chairman of the Department of Mechanical Engineering and Dr. Darrell Pepper, Associate Professor of the Department of Mechanical Engineering for their valuable advice regarding this project.

I am also grateful to Mr. Raveen Abhishetty for the help rendered by him during the course of this project. Last, but not the least, I would appreciate the whole hearted support of my wife, Mrs. Nidhi Bhargava, for the completion of my thesis.

## **CHAPTER 1**

### **INTRODUCTION**

#### **Nuclear Power History**

On December 2, 1942, a team of scientists at the University of Chicago, led by Enrico Fermi, created man's first controlled, self sustaining nuclear chain reaction. Today, more than 100 nuclear power plants generate about 19% of the electricity used in the United States.

The spent fuel and the high-level radioactive waste produced by these plants is currently stored in steel-lined concrete pools at power plant sites in more than 30 states. Although spent fuel and high-level radioactive waste lose about 50% of their radioactivity after three months of storage, and about 80% after one year of storage, radioactivity remains for thousands of years. For this reason, the waste requires permanent disposal to isolate it from the public and the environment.

#### **Background**

The Lawrence Livermore National Laboratory (LLNL) is responsible for the design and development of the waste container to be used for the permanent disposal

of high-level nuclear waste. As part of the Nevada Nuclear Waste Storage investigations (NNWSI), this task also is a part of the U.S. Department of Energy's (DOE) Civilian Radioactive Waste Management Program. The waste package - that is, the container and the waste form - is being designed specifically for safe, permanent disposal in the proposed tuff rock layer at the Yucca Mountain repository. Tuff is rock composed of compact volcanic ash). Yucca Mountain, Nevada, is adjacent to the southwestern boundary of the Nevada Test Site, about 100 miles northwest of Las Vegas.

### **Characterizing the Waste Forms**

High-level waste is of two types: spent fuel discharged from approximately 100 commercial nuclear power plants and waste resulting from production of U.S. defense program materials. Spent fuel is in the form of pellets encapsulated with zirconium-alloy cladding, while reprocessing waste is contained in borosilicate glass. Tests are in progress to measure effects on radioactivity release rates from such variables as ground water flow rates and composition over a range of temperatures. The extent to which spent fuel cladding can be expected to delay the access of the ground water to the fuel is being studied, as is the rate of radioactivity release from fuel with flawed or breached cladding. The data from this work will be used to evaluate whether the expected release rates from the waste package will meet performance objectives established by the Nuclear Regulatory Commission.

### **Literature Search**

Ruffner<sup>2</sup> presented thermal calculations of the effects of radioactive waste decay heat on the potential repository at Yucca Mountain in conjunction with Yucca Mountain Site Characterization Project at Lawrence Livermore National Laboratory. Drift emplacement of waste containers resulted in lower rock temperatures than borehole emplacement. The peak drift wall temperature did not exceed 160°C for an Areal Mass Loading of 138 MTU/acre ( 157 kW/acre). Holland<sup>6</sup> performed calculations to examine the systems implications of various thermal loadings on the near- and far-field repository environments. Local areal power densities of 57, 80 and 100 kW/acre were used in the calculations. Radiation and convective heat transfer across the drifts were simulated by using a material that has a high conductivity and low specific heat. The centerline temperature of the waste container was predicted to exceed the performance goal limit of 350°C for the 100 kW/acre thermal loading.

### **Objective**

The objective of this study is to conduct a two dimensional finite element analysis of heat transfer around a nuclear waste container placed horizontally in the drift and to determine the peak temperatures on the drift and inside the nuclear waste container. Thermal analysis has been performed for two scenarios: drift without backfill and drift with inverted backfill.

## CHAPTER 2

### THERMAL MODEL

The thermal model is shown in Figure 1. The model extends 300m above the center of the drift (ground surface) and 300m below the center of the drift (water table). The repository drifts are 6.7 m in diameter and spaced 40m center to center. Each waste package is 1.67 m in diameter and contains 30 kW of heat. Its length is 4.45 m and the spacing between the waste packages is 21.21 m as shown in Figure 2. The heat decays<sup>3</sup> with time over a period of 1000 years as shown in Figure 3. Table 1 shows the value of heat content for a period of 1000 years. The waste containers have been considered as infinitely long cylinders of uniform heat source and a section has been modelled with heat flux imposed on the walls of the waste container. The heat source has been assumed to be smeared over the length of 21.21m. The heat flux on the canister has been calculated as follows:

Heat smeared  $q_l$  (W) over the length of 21.21m is given by,

$$q_l = q \frac{l}{L} \quad (1)$$

where,

$q$  = actual heat (W)

$l$  = length of the waste container (m)

$L$  = distance between the centers of the containers (m)



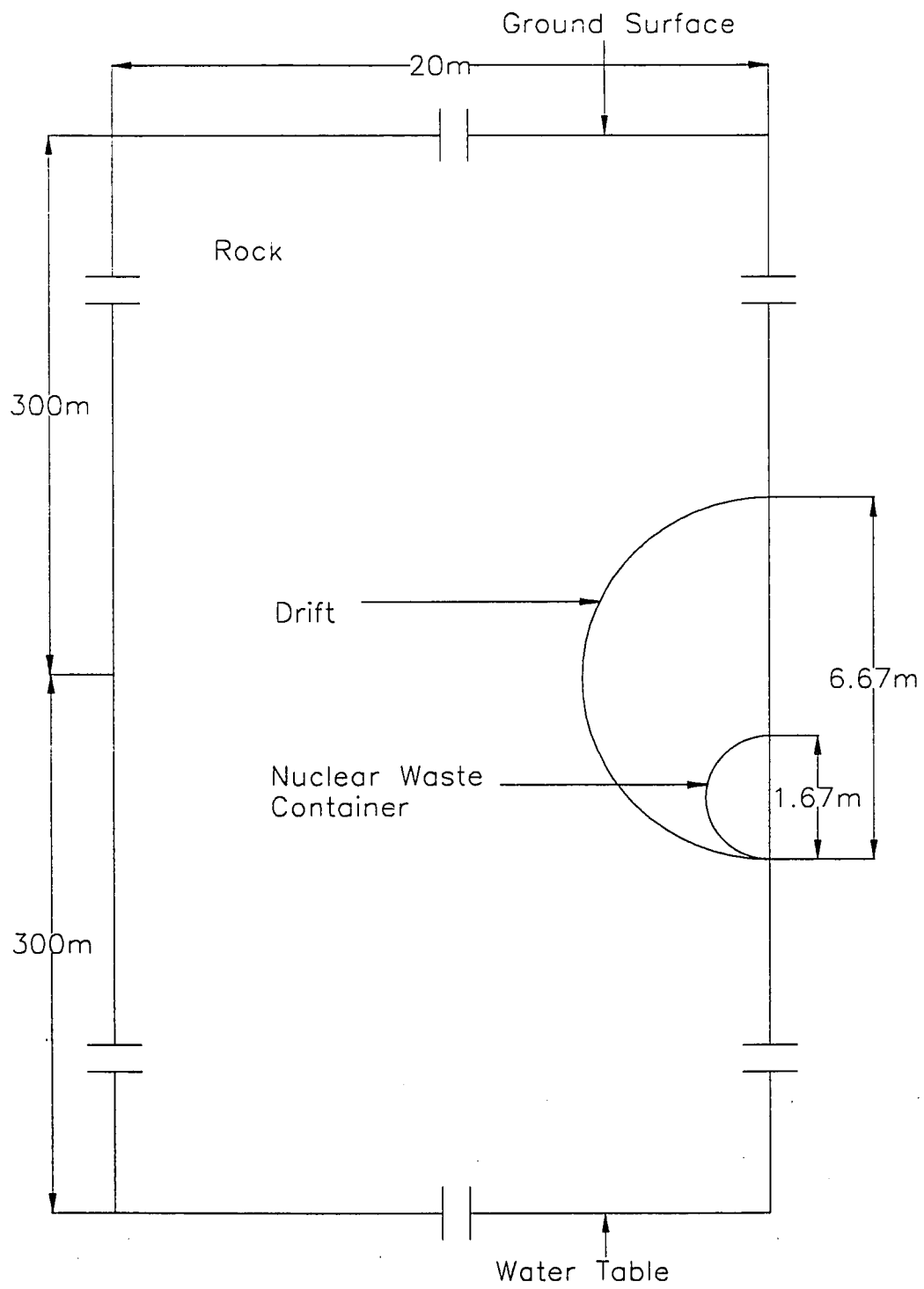


Figure 1 Thermal Model

For this case,  $q = 30,000 \text{ W}$

$$l = 4.45 \text{ m}$$

$$L = 21.21 \text{ m}$$

Therefore,  $q_1 = 6294.2 \text{ W}$

Heat per unit volume  $q'''$  ( $\text{W}/\text{m}^3$ ) is given by,

$$q''' = \frac{q_1 l}{\frac{\pi}{4} d^2 l} \quad (2)$$

where,

$d$  = diameter of the waste container (m)

For this case,  $d = 1.67 \text{ m}$

Therefore,  $q''' = 645.74 \text{ W}/\text{m}^3$

Heat content for a unit length of the waste container,

$$q_2 = q''' \cdot \frac{\pi}{4} \cdot d^2 \cdot l \quad (3)$$

Therefore,  $q_2 = 1414.43 \text{ W}$

Heat flux  $q_c''$  ( $\text{W}/\text{m}^2$ ) is given by,

$$q_c'' = \frac{q_2}{\pi \cdot d \cdot l} \quad (4)$$

Therefore,  $q_c'' = 270 \text{ W}/\text{m}^2$

Table 2 shows the variation of heat flux on the walls of the waste container for a period of 1000 years.

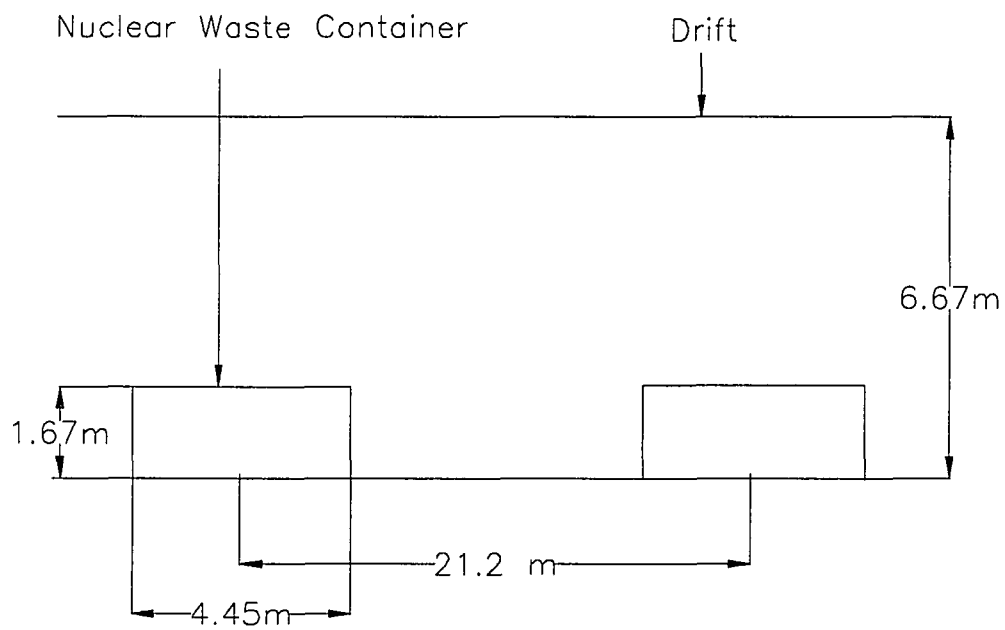


Figure 2 Waste Package in the Drift

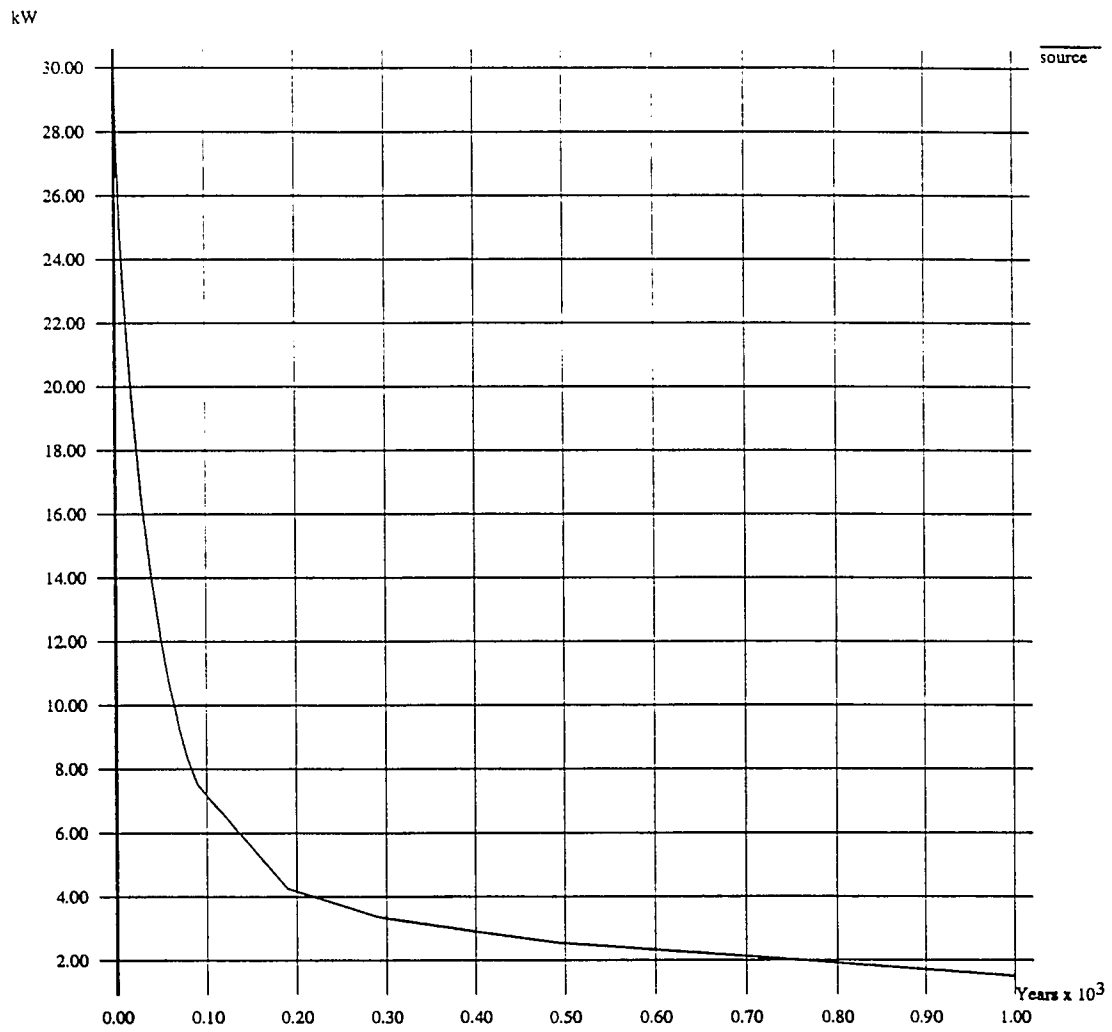


Figure 3 Variation of Heat Source

Table 1 Variation of Heat Source<sup>3</sup>

Years	Heat (kW)
0	30.00
6	25.11
8	24.03
10	23.07
15	20.99
20	19.22
30	16.31
40	14.00
50	12.15
60	10.60
70	9.24
80	8.29
90	7.51
190	4.25
290	3.36
390	2.93
490	2.55
1000	1.49

Table 2 Variation of Heat Flux on the Canister

Years	Heat flux (W/m <sup>2</sup> )
0	270.00
6	225.99
8	216.27
10	207.66
15	188.97
20	172.99
30	146.76
40	126.05
50	109.39
60	95.94
70	83.66
80	75.01
90	67.94
190	38.44
290	30.41
390	26.07
490	22.69
1000	13.26

The rock type at Yucca Mountain consists of four major layers of porous and non-porous tuff, a dense form of volcanic ash produced more than 13 million years ago. The rock<sup>1</sup> has been modelled as a continuum with average properties.

$$\text{Thermal conductivity} = 3.0 \text{ W/m/K}$$

$$\text{Density} = 2640 \text{ kg/m}^3$$

$$\text{Specific heat} = 800 \text{ J/kg/K}$$

The properties of the air<sup>1</sup> have been selected at a temperature of 325°C .

$$\text{Thermal conductivity} = 2.816 \times 10^{-2} \text{ W/m/K}$$

$$\text{Density} = 1.086 \text{ kg/m}^3$$

$$\text{Specific heat} = 1006 \text{ J/kg/K}$$

$$\text{Dynamic viscosity} = 1.962 \times 10^{-5} \text{ N-s/m}^2$$

Constant properties have also been assumed for the nuclear waste<sup>1</sup>.

$$\text{Thermal conductivity} = 2.79 \text{ W/m/K}$$

$$\text{Density} = 4705.2 \text{ kg/m}^3$$

$$\text{Specific heat} = 422.8 \text{ J/kg/K}$$

All the calculations have been performed using FIDAP<sup>5</sup>, a fluid dynamics analysis package that uses the finite element method (FEM) to simulate many kinds of fluid flows such as two-dimensional, axi-symmetric and three-dimensional steady state or transient simulations in complex geometries including the effects of temperatures. FEM is becoming as powerful a tool in fluid dynamics as it is in structural analysis. In FEM the flow region is subdivided into a number of small regions called finite elements. The partial differential equations of fluid mechanics covering the region as a whole are

replaced by ordinary differential or algebraic equations in each element. The system of these equations is then solved by sophisticated numerical techniques to determine the velocities, pressures, temperatures and other unknowns throughout the region.

The great advantage of FEM over other methods is its inherent flexibility in treating arbitrarily complex flow domains and boundary conditions. Unstructured grids can be designed which allow areas of interest to be studied in greater detail without the need for excessively many grid points throughout the entire flow domain. FEM allows the natural and correct imposition of boundary conditions on curved boundaries. In addition, FEM has an elegant mathematical formulation which allows the derivation of comprehensive error estimates and the determination of accurate solutions to within user-prescribed tolerances. At the same time, fluid simulation with FEM allows access to the wealth of powerful graphics pre- and post-processing packages available in the structural engineering field.

Initially, transient state simulations were done for a combined mode of heat transfer inside the drift: conduction, free convection, and radiation. However, the timestep for the transient problem turned out to be very small, of the order of 0.1 second, due to the presence of free convection. Since the simulation has to run for 1000 years, that time step was extremely small. Therefore, the thermal problem is broken into two steps:

- 1) Heat flux is imposed on the walls of the drift (to eliminate the waste container and the air portion) and the model is solved in the transient state for heat conduction inside the rock. This model is discussed in chapter 3.
- 2) Steady state simulation is done for a combined mode of heat transfer inside the



drift surrounded by the part of the rock. Boundary conditions have been selected at 10 m from the center of the drift as in step 1. This model is discussed in chapter 4. Results have been presented for 30 years and 130 years.

One more model is discussed in chapter 5. The waste container is placed on the inverted backfill inside the drift. The boundary conditions have been selected at 10 m from the center of the drift as in step 1. Results have been presented for 10 years, 30 years, 130 years and 600 years. Simulations have also been done for the case when free convection was the only mode of heat transfer inside the drift. The effects of radiation and free convection have been discussed. Two more cases are discussed when it is assumed that the heat source is smeared over half the distance between the centers of the waste container i.e. the heat is smeared over 10.6 m instead of 21.2 m.

## CHAPTER 3

### TRANSIENT HEAT CONDUCTION IN THE ROCK

#### Computational Domain

The computational domain for the thermal model is shown in Figure 4. The model extends 300 m above the center of the drift and 300 m below the center of the drift. Constant temperature boundary conditions have been imposed on the top and bottom of the thermal model. The temperature<sup>7</sup> at the top of the model (ground surface) is set at 25°C and the temperature<sup>7</sup> at the bottom of the model (water table) is set at 35°C. The vertical boundaries of the model are planes of symmetry and are treated as adiabatic surfaces. The heat flux is imposed on the walls of the drift instead of being imposed on the waste container. It has been assumed that the heat flow from the waste container is equal to the heat flow imposed on the walls of the drift. The heat flux on the drift wall  $q_d''$  has been calculated as follows:

$$q_d'' = q_c'' \cdot \frac{d}{D} \quad (5)$$

where,

$q_c''$  = heat flux on the canister (W/m<sup>2</sup>)

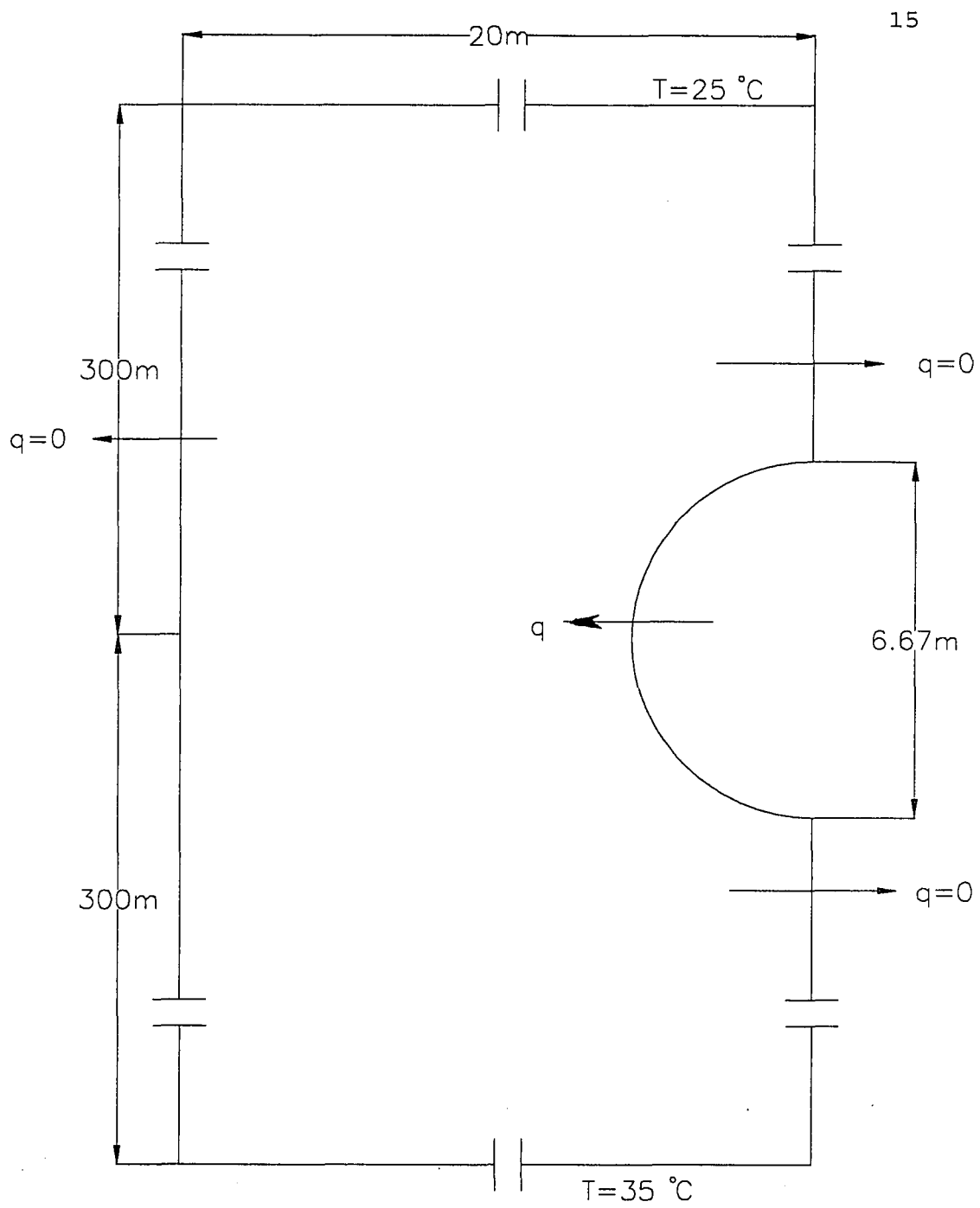


Figure 4 Computational Domain for the Transient  
Heat Conduction in the Rock

$d$  = diameter of the nuclear waste container (m)

$D$  = diameter of the drift (m)

For this case,

$$q_c'' = 270 \text{ W/m}^2$$

$$d = 1.67 \text{ m}$$

$$D = 6.67 \text{ m}$$

Therefore,  $q_d'' = 67.5 \text{ W/m}^2$

Table 3 shows the variation of heat flux over the period of 1000 years. A transient state thermal analysis with a time varying heat flux has been performed for the heat conduction in the rock to determine the temperatures at different levels of the rock and on the drift. The initial condition for the temperature has been taken as 25°C at all nodes in the rock.

### **Simulation Approach**

A transient analysis has been performed and a first order backward Euler implicit time integration scheme has been implemented with a variable time increment integration scheme. This scheme allowed a small time increment to track the transient behaviour of the solution during the early years of simulation and a much larger time increment during the later years of the simulation. The transient analysis started with an initial time step of 100,000 seconds. For the first few time steps time increments were of the order of initial time increment but as the temperature field built up, the time increments gradually became large, of the order of  $4.72 \times 10^{10}$  seconds.

Table 3 Variation of Heat Flux on the Drift Wall

Years	$q_d''$ (W/m <sup>2</sup> )
0	67.5
6	56.49
8	54.09
10	51.92
15	47.24
30	36.69
40	31.51
60	23.98
80	18.75
90	16.98
190	9.61
290	7.60
390	6.52
490	5.67
1000	3.32

The period of 1,000 years was simulated in 42 time steps. The plot of the time step number versus time is shown in Figure 5. The time increment (DT) on the y-axis is in seconds and the time step number is on the x-axis.

The Successive Substitution Iterative method with an acceleration factor of 0.8 has been selected to obtain the solution at each time step of the time dependent problem. The equations are expressed in Cartesian coordinates and only the energy equation has been solved with no convective terms. Clipping has been employed for the temperature variable to prevent temperatures from being less than 298°C as the iteration procedure may not recover from such undershoots and the solution diverges.

Paved mesh with quadrilateral elements has been generated. Figure 6(a) shows the mesh plot for the thermal model. Figures 6(b) and 6(c) show zoomed plots for the mesh with the drift in the center. The total number of nodal points is 5094 and the total number of elements is 4773. Appendix 1 describes the input file to generate the mesh and to obtain the solution field for the above model.

## Results

Figure 7 shows the location of a few nodes for which the history of temperatures has been plotted. The different levels in the rock reach the peak temperatures at different times. Figure 8 shows the history of the temperatures on the drift wall (node 12). The temperature on the y-axis is in K while the time on the x-axis is in seconds. The drift reaches a peak temperature of 208.7°C at around 37 years. The maximum temperatures on the nodes 5 and 20 are 207.55°C and 207.7°C

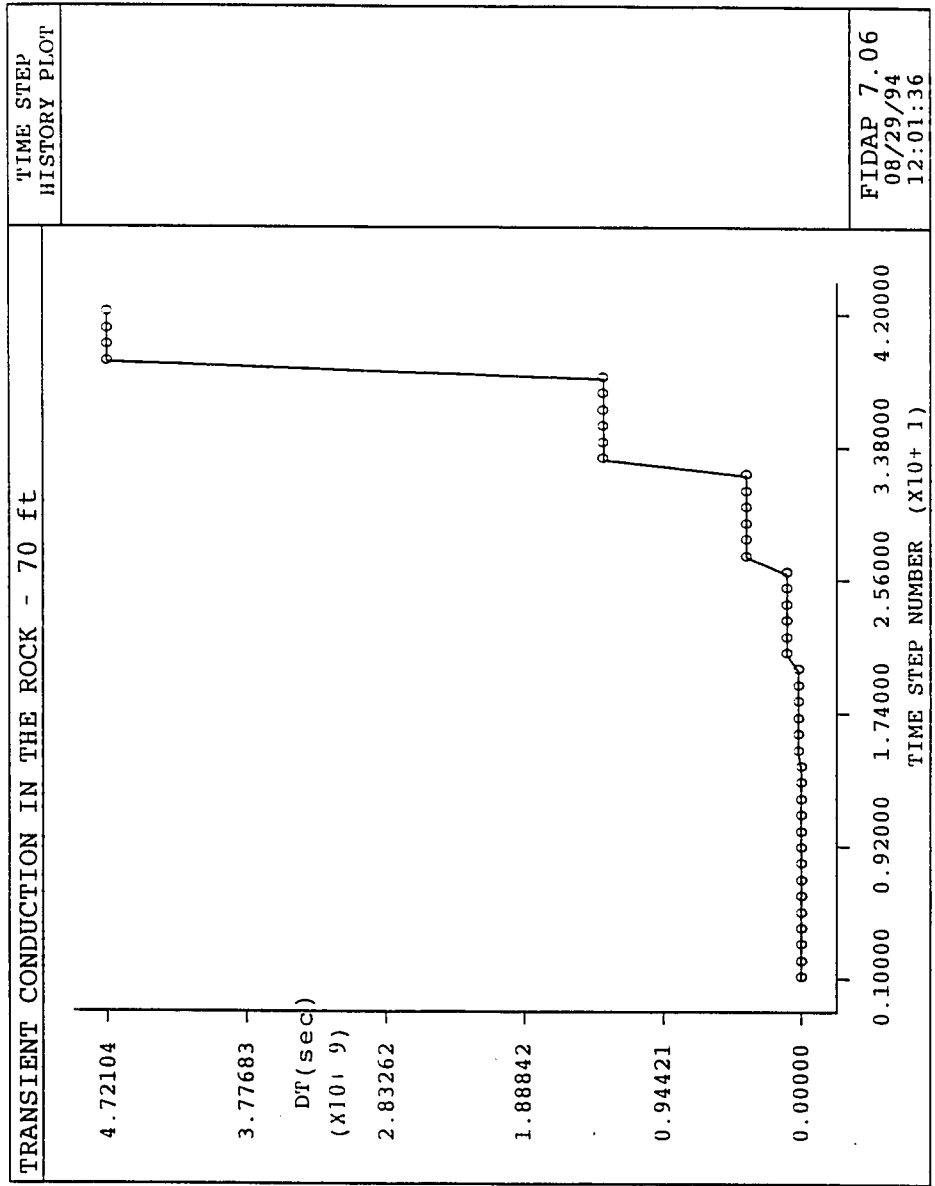


Figure 5 Variation of Time Increments

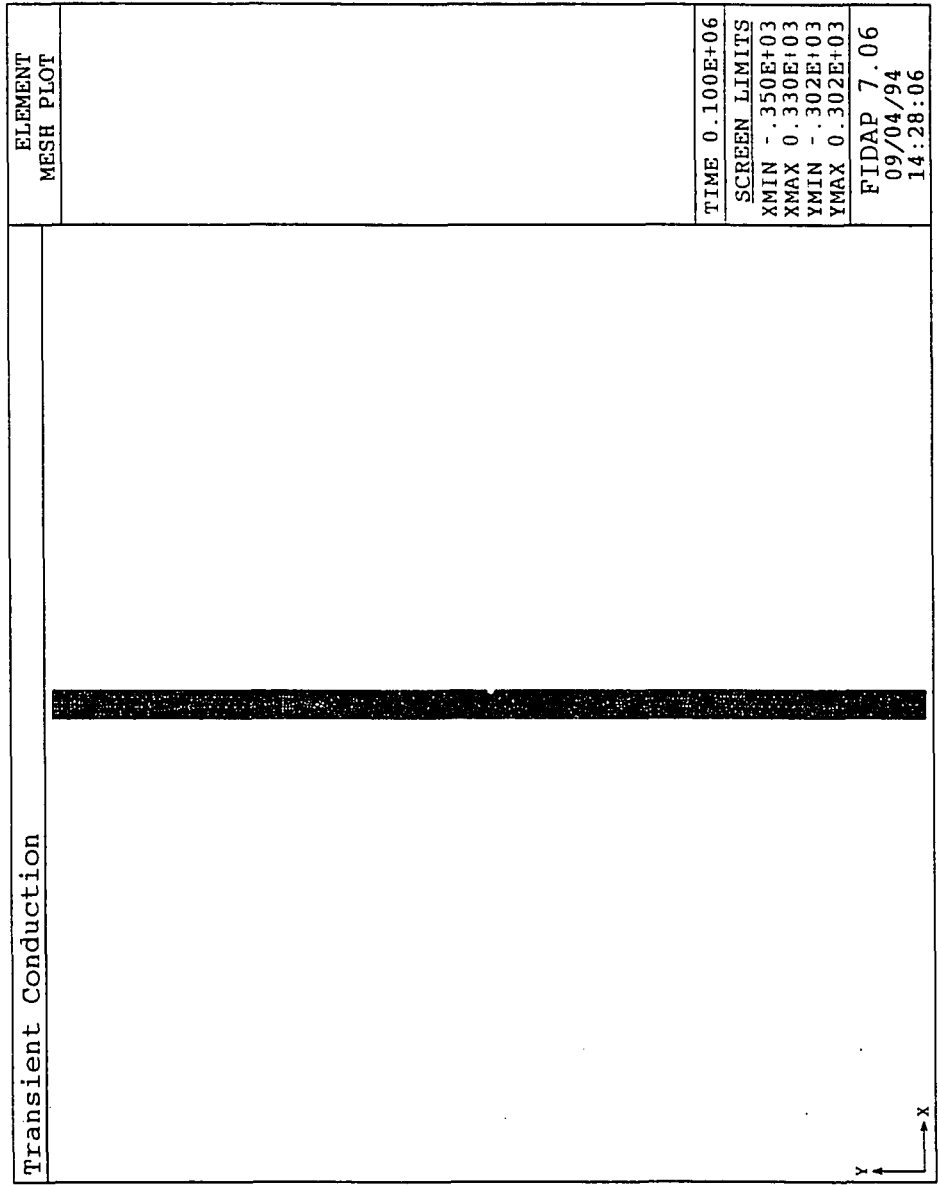


Figure 6(a) Mesh Plot



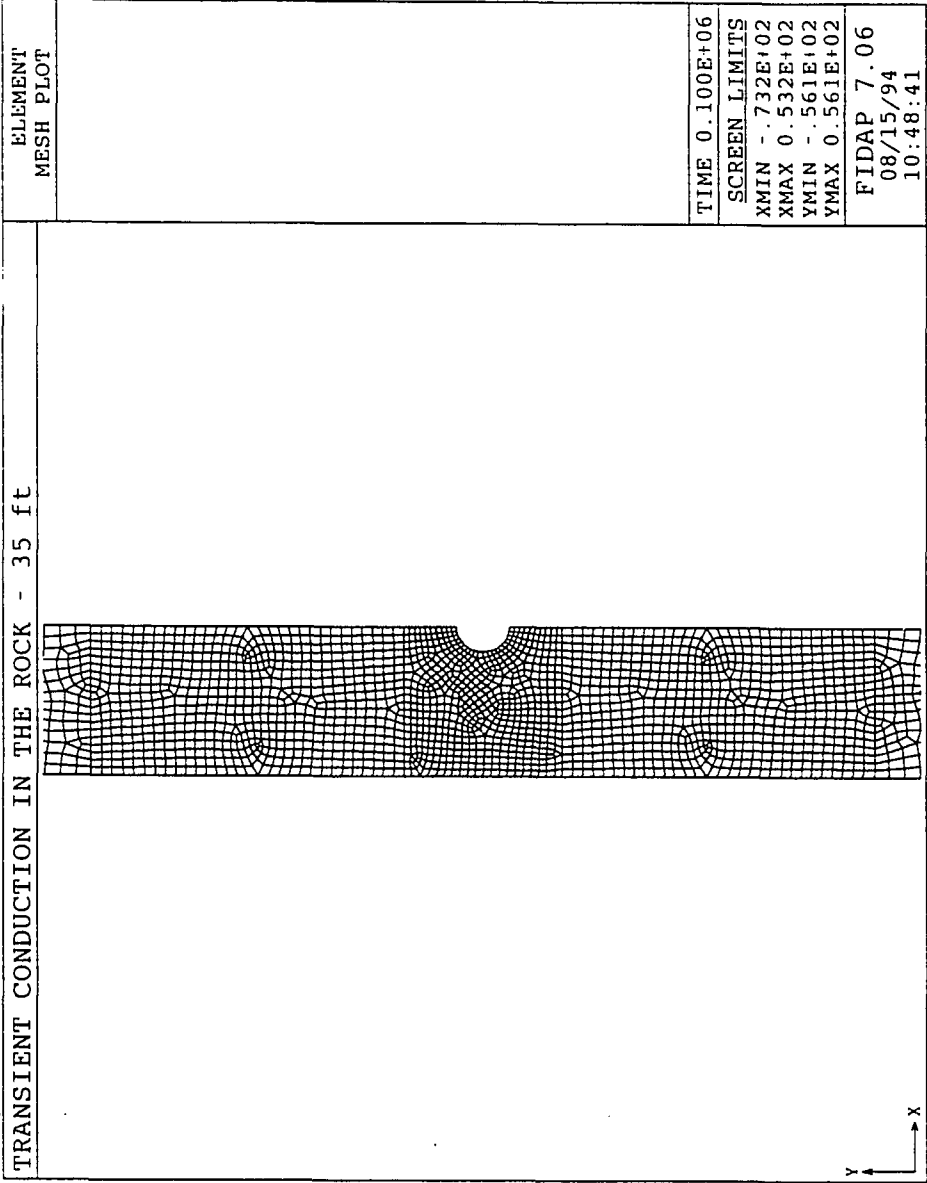


Figure 6(b) Zoomed Plot for the Mesh

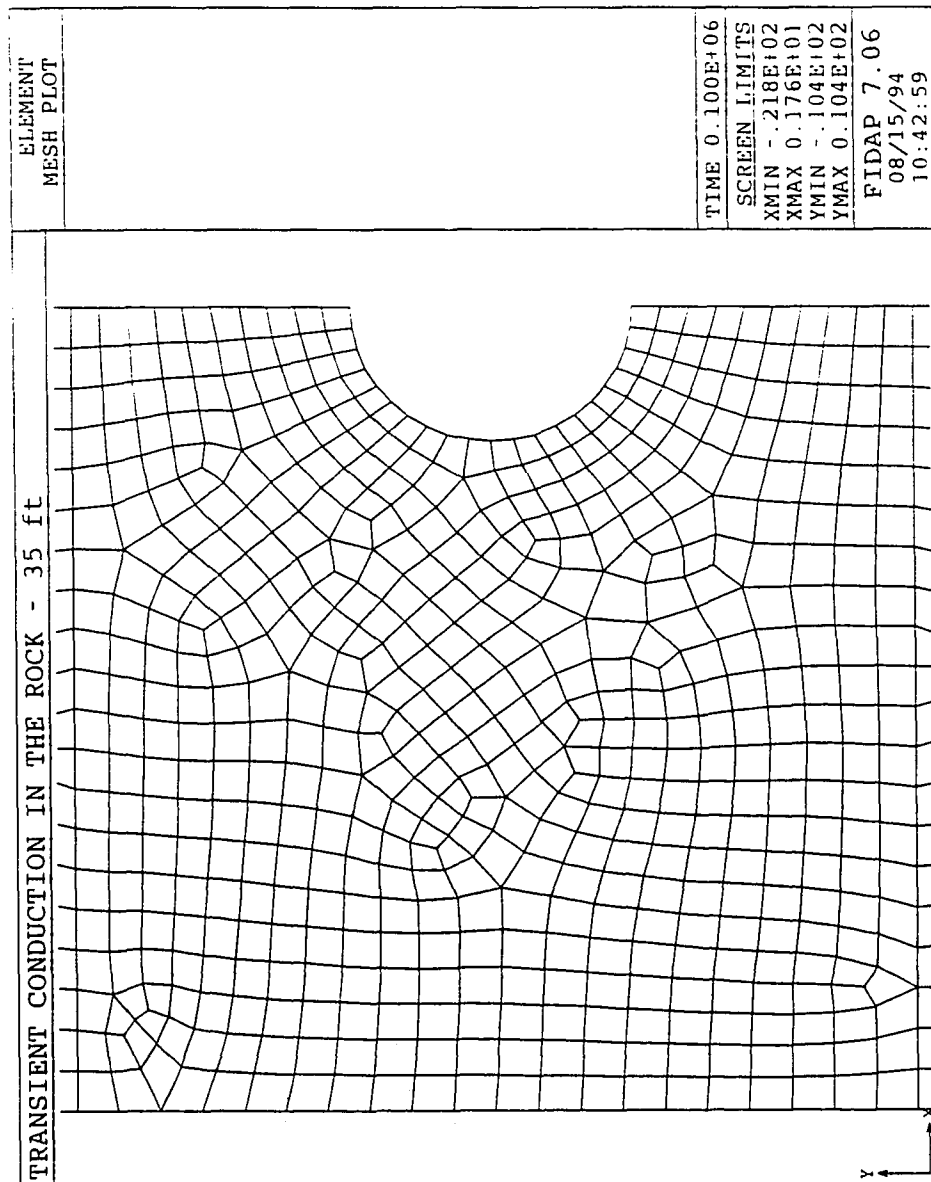


Figure 6(c) Zoomed Plot for the Mesh

respectively. This indicates that the temperatures on the drift wall are almost uniform.

Figure 9(a), 9(b), and 9(c) show the history of temperatures at 10 m (node 714), 50 m (node 751) and 150 m (node 786) above the center of the drift. The temperature on the y-axis is in K while the time on the x-axis is in seconds. The maximum temperatures at node 714, node 751 and node 786 are  $169.5^{\circ}\text{C}$ ,  $137.4^{\circ}\text{C}$ , and  $89.6^{\circ}\text{C}$  respectively at times (approximately) 148 years, 360 years and 655 years respectively. A distinct maximum is observed in the temperature history curve at the drift, at 10m and at 50m but no obvious maximum is observed at 150 m. This is probably due to the large storage effect in the rock. There is a significant difference in the temperatures between the node on the left side (node 721), at the center (node 714) and on the right side (node 703) at the 10 m level at any time as node 703 is closest to the walls of the drift. The maximum temperatures at the nodes 721, 714 and 703 are  $168.6^{\circ}\text{C}$ ,  $170.3^{\circ}\text{C}$  and  $175.3^{\circ}\text{C}$  respectively. However, at 50 m level and 150 m level the temperatures are almost the same. A slight difference is also observed between the temperatures at the nodes at 10 m above the center of the drift and at 10 m below the center of the drift. The temperature variation in the rock 300m above and 300m below the center of the drift at 22 years, 73 years and 951 years is shown in Figure 10(a), 10(b) and 10(c) respectively. The temperatures are in K. The temperature contours are concentrated around the drift in early years but as the time progressed the temperature contours gradually spread out in the whole domain. Maximum temperature is at the walls of the drift.

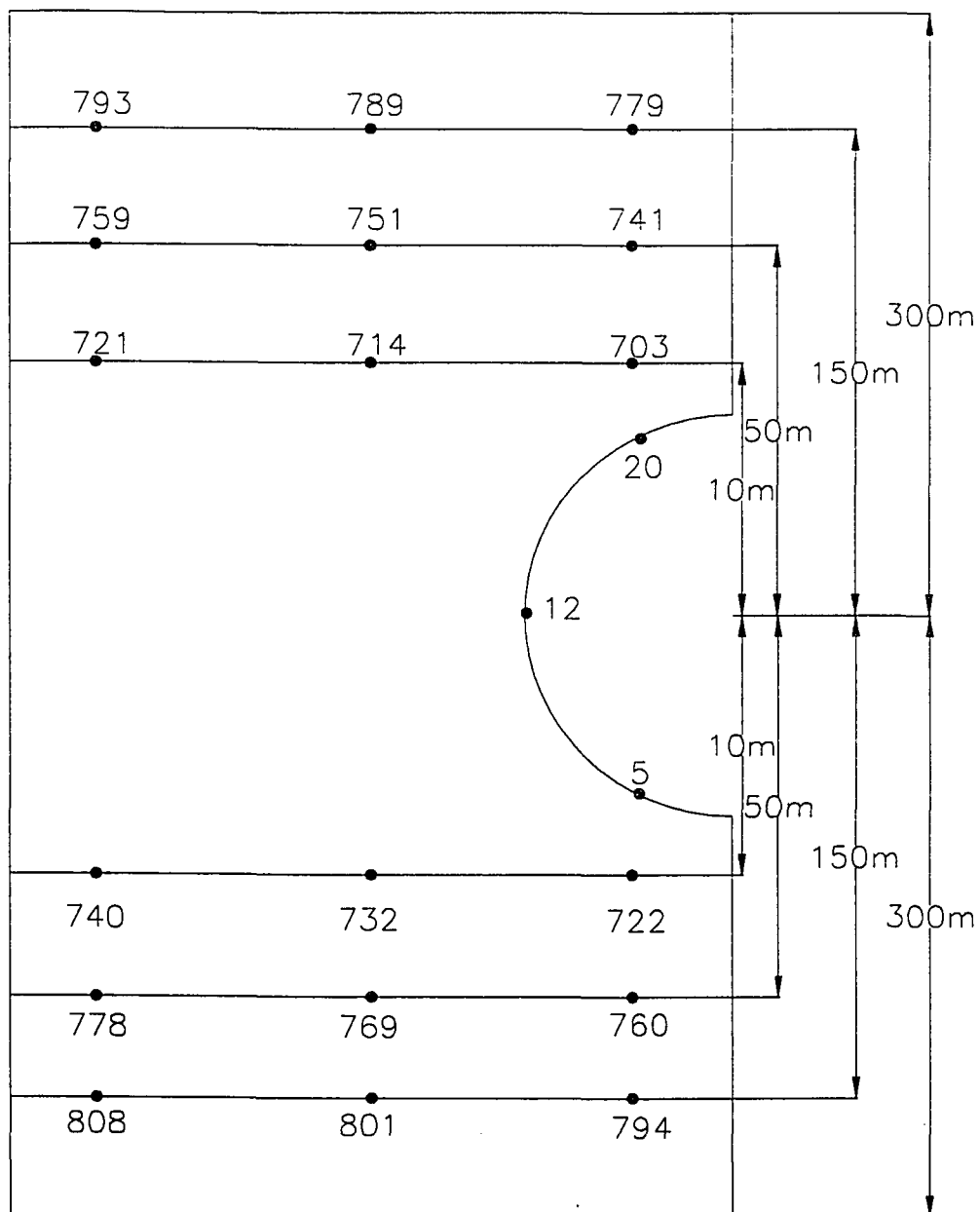


Figure 7 Location of Nodes on the Model

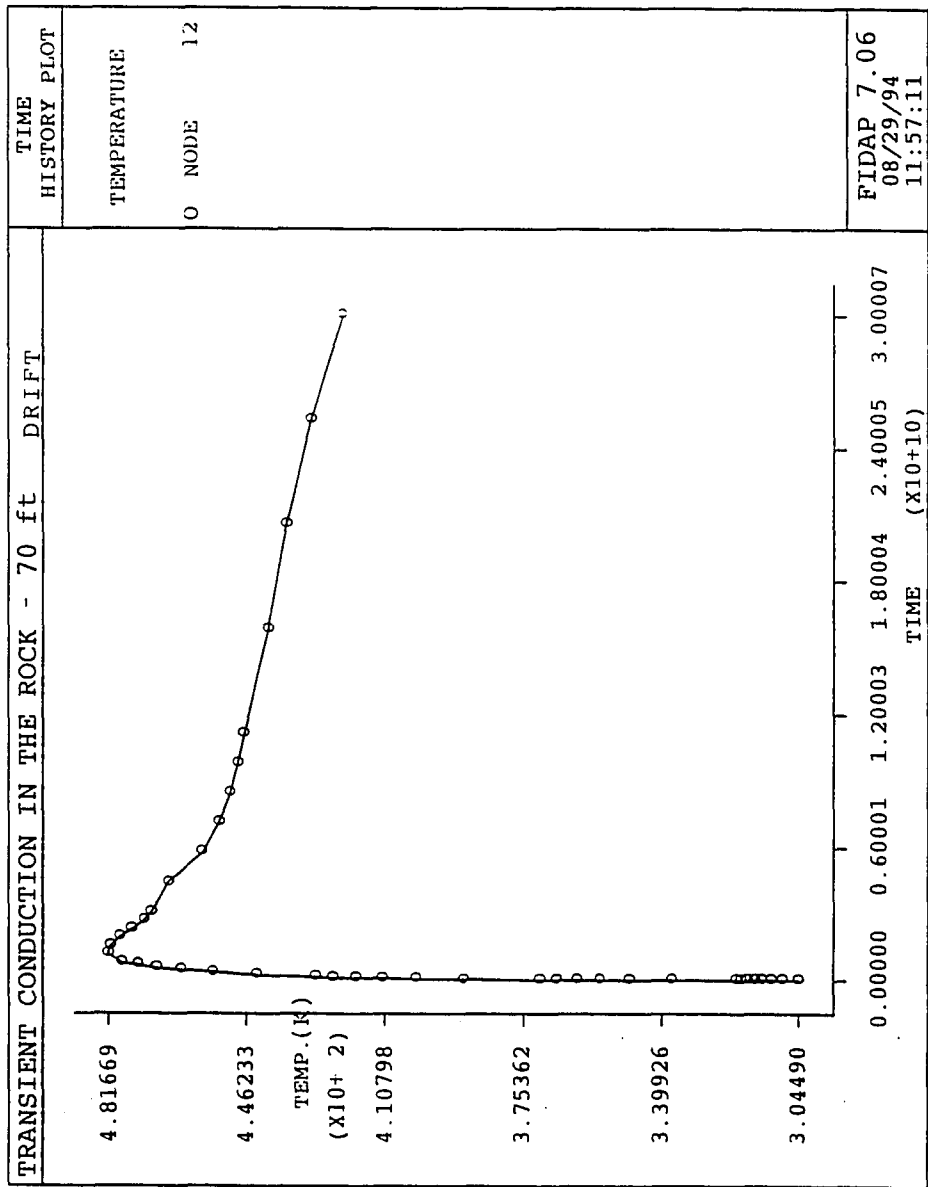


Figure 8 History of Temperature on the Drift Wall

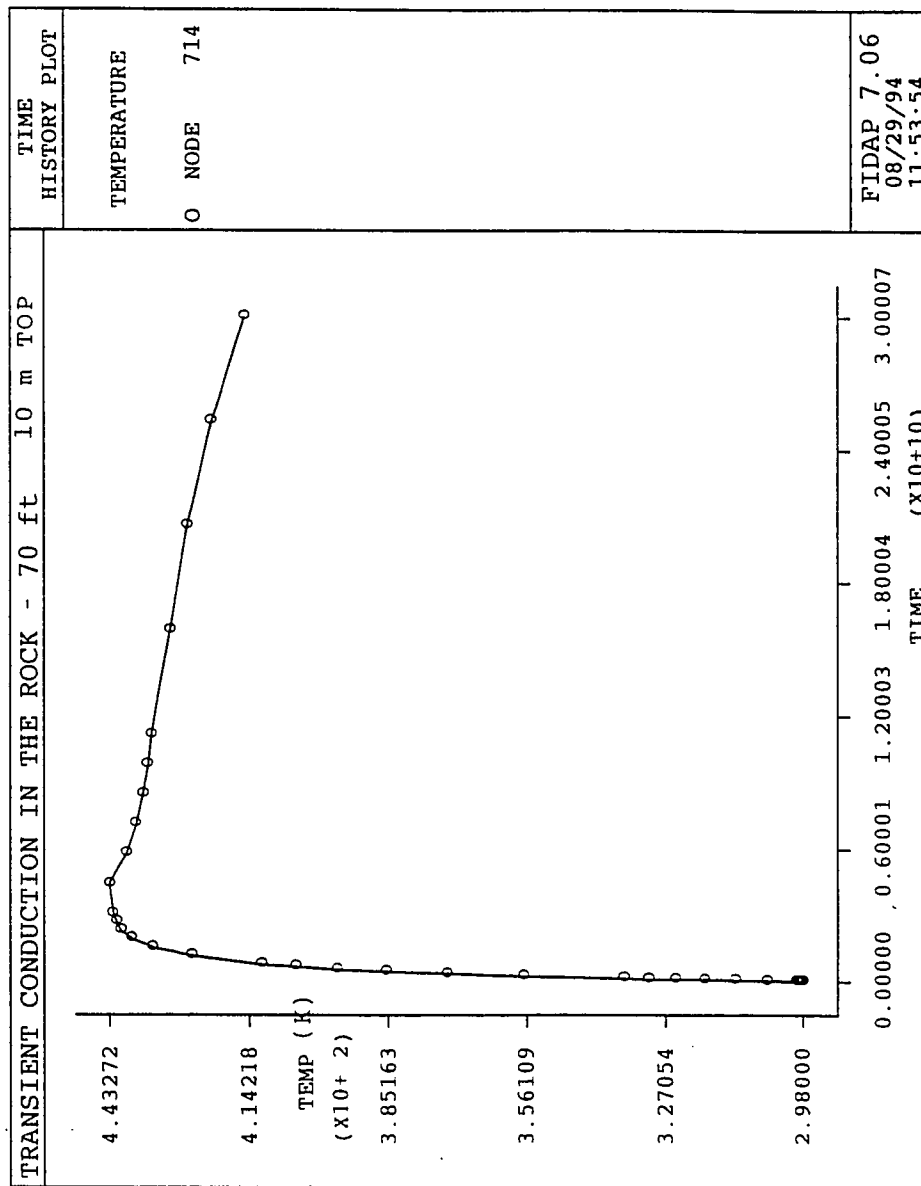


Figure 9(a) History of Temperature at 10 m

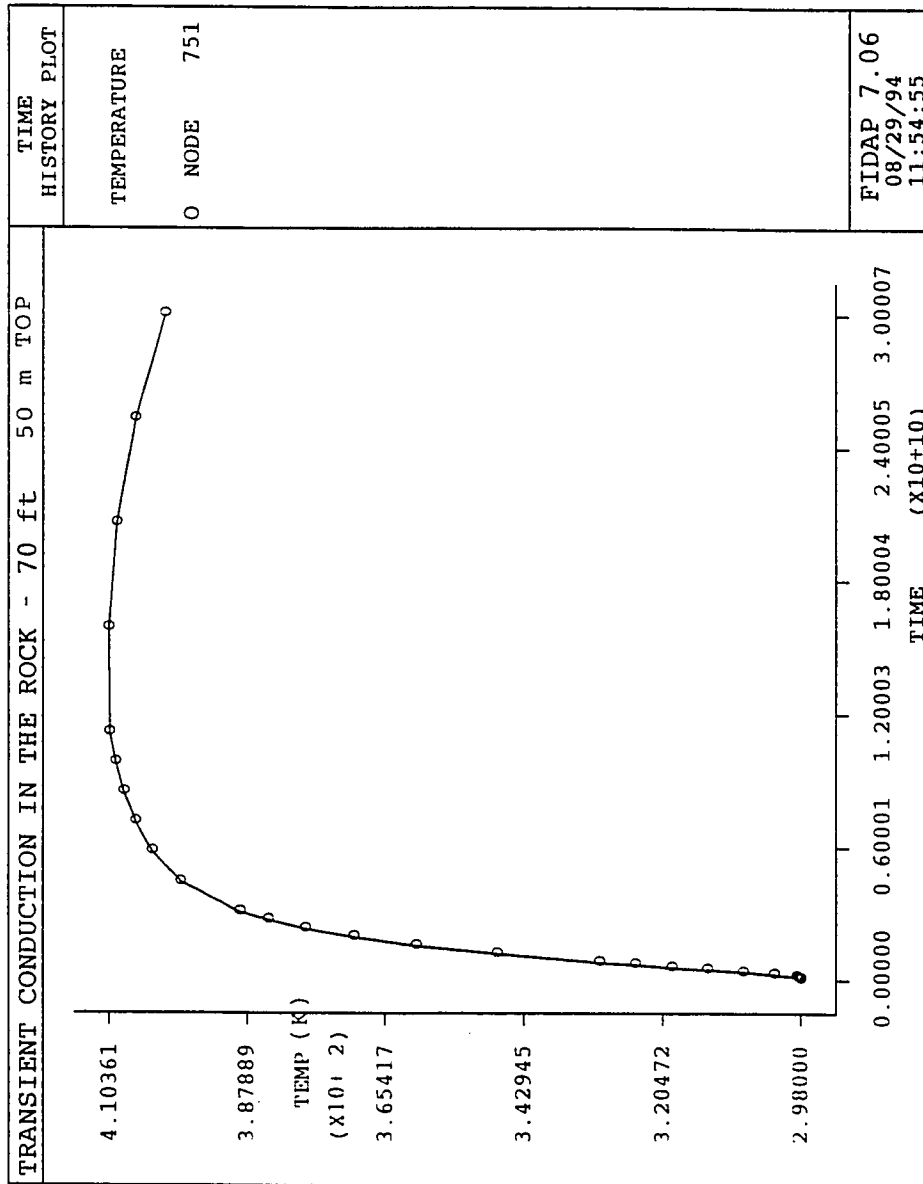


Figure 9(b) History of Temperature at 50 m

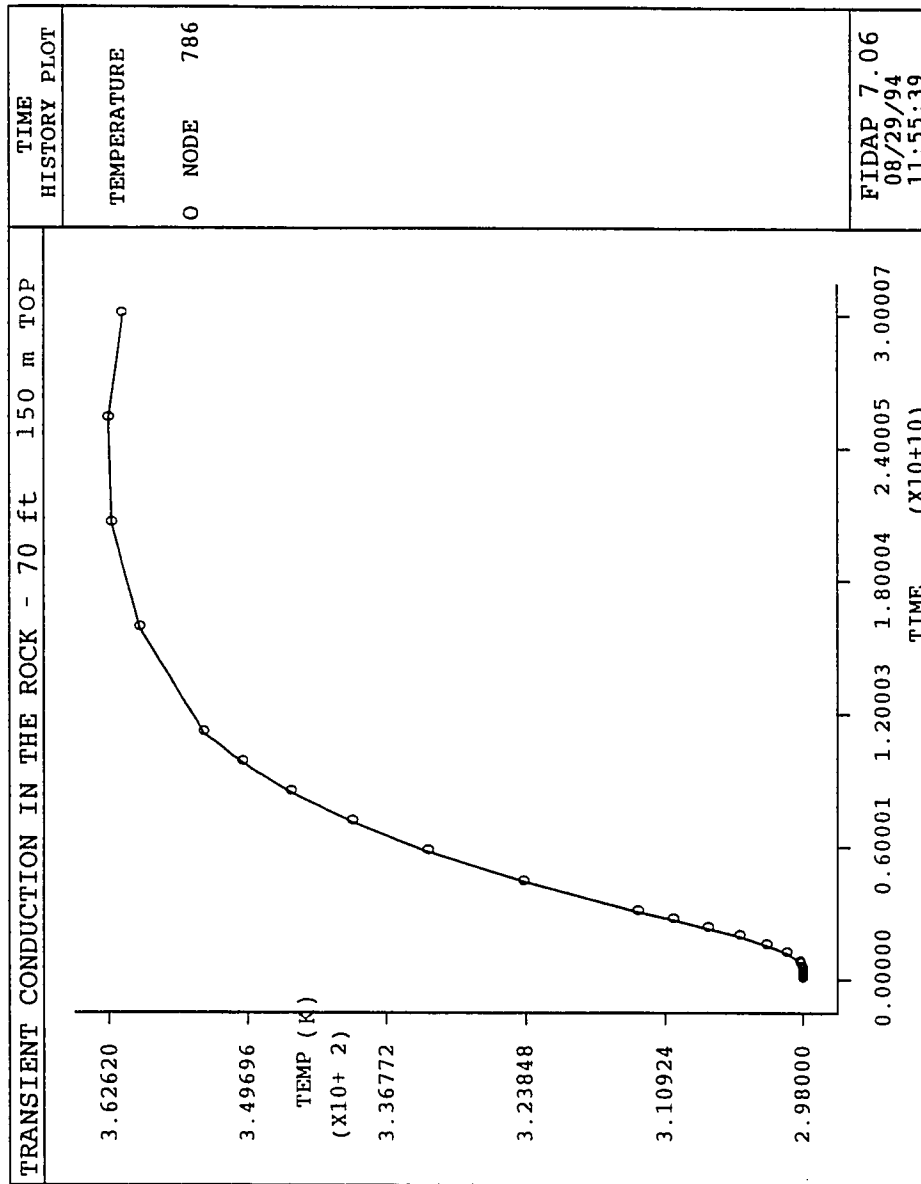


Figure 9(c) History of Temperature at 150 m



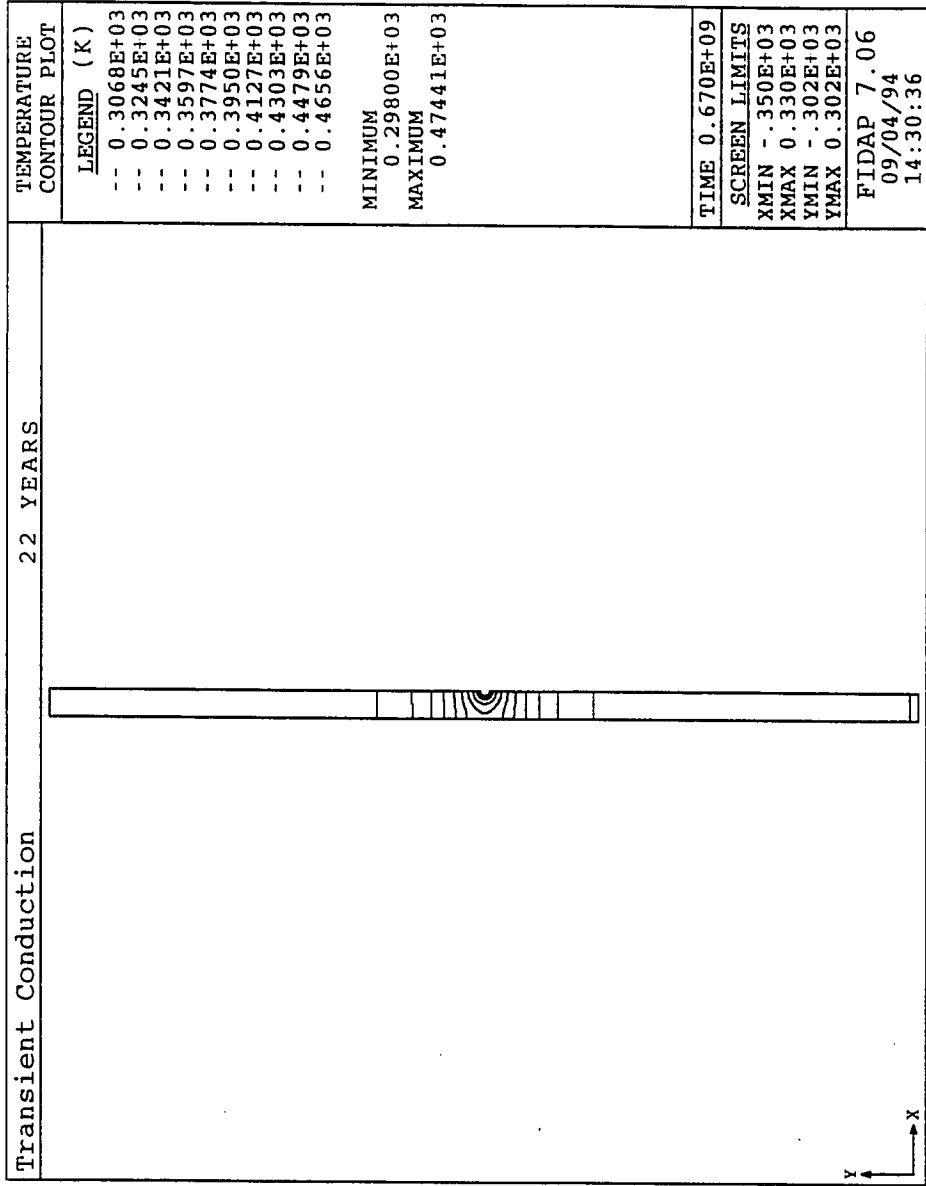


Figure 10 (a) Temperature Contours at 22 Years

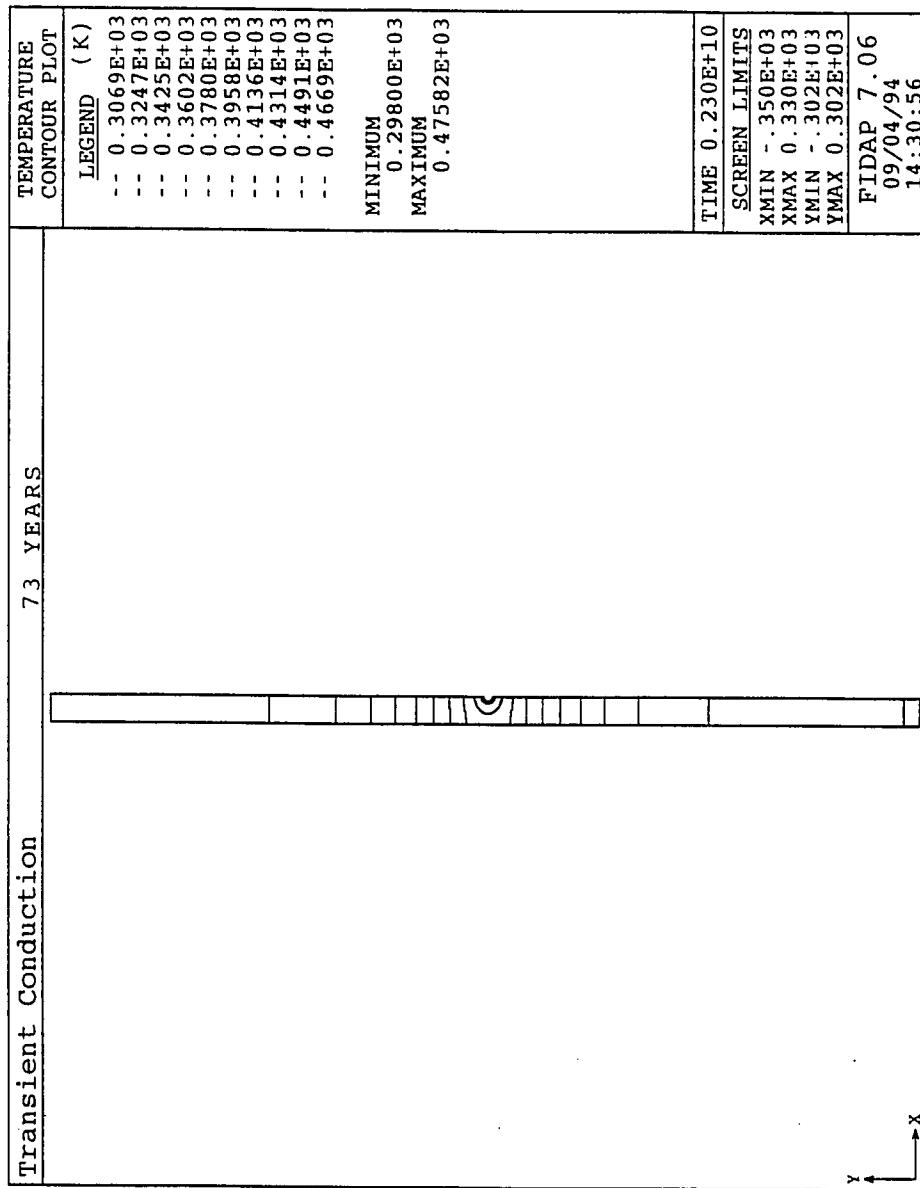


Figure 10(b) Temperature Contours at 73 Years

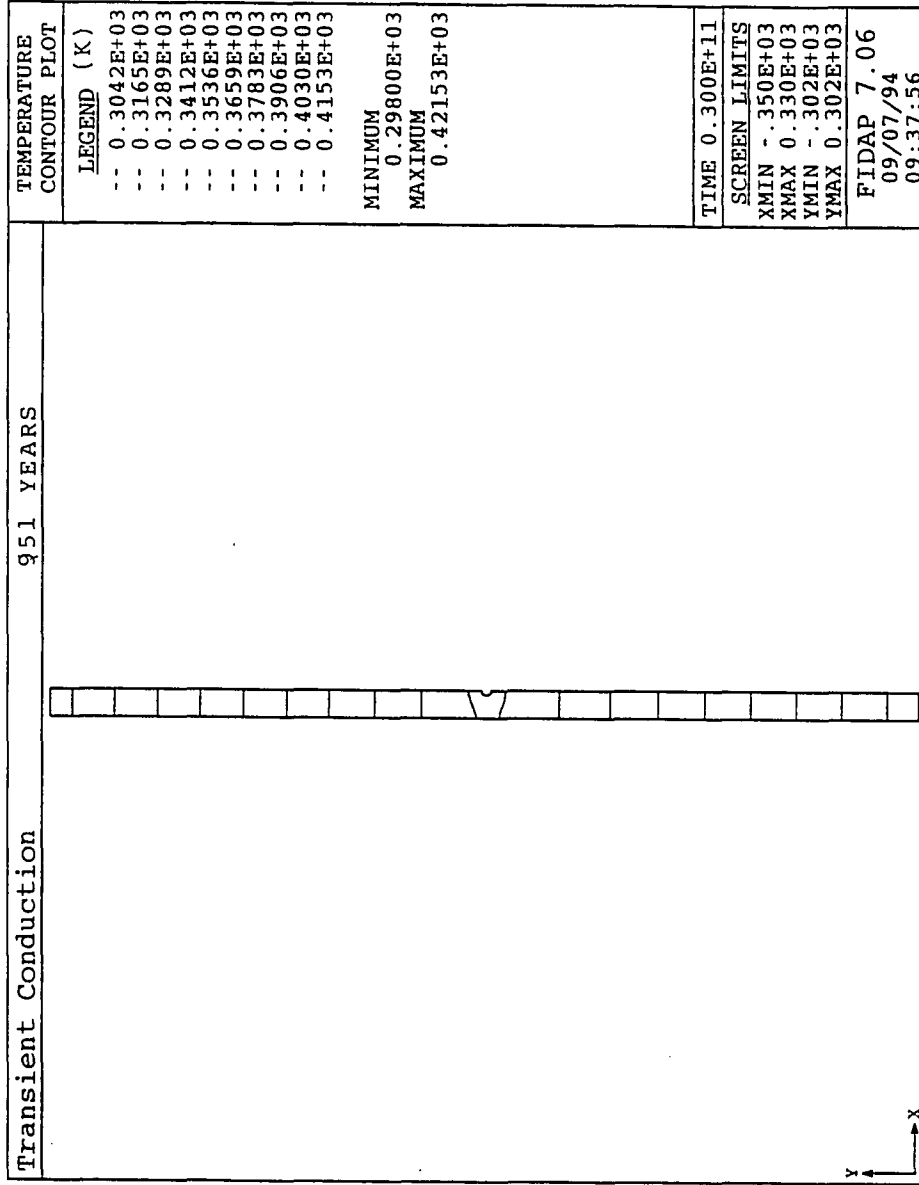


Figure 10(c) Temperature Contours at 951 Years

## **CHAPTER 4**

### **Steady State Analysis of Heat Transfer Inside The Drift**

#### **Computational Domain**

The heat transfer inside the drift has been modelled as a steady state problem imposing the temperatures obtained from the transient conduction model (chapter 3) as the boundary conditions. The computational domain for this model is shown in Figure 11. The drift is in the center with the waste container placed on the floor of the drift and is surrounded by rock. The top and bottom horizontal boundaries are 10 m from the center of the drift and a constant temperature boundary condition is imposed on them. The left and right vertical boundaries are also 10 m from the center of the drift and again a constant temperature boundary condition is imposed on them. Heat flux has been imposed on the walls of the waste container. The temperatures from the transient conduction run have been selected as the boundary conditions at 10m from the center of the drift at different time steps. Table 4 shows the boundary conditions for this model at 30 years and 130 years.

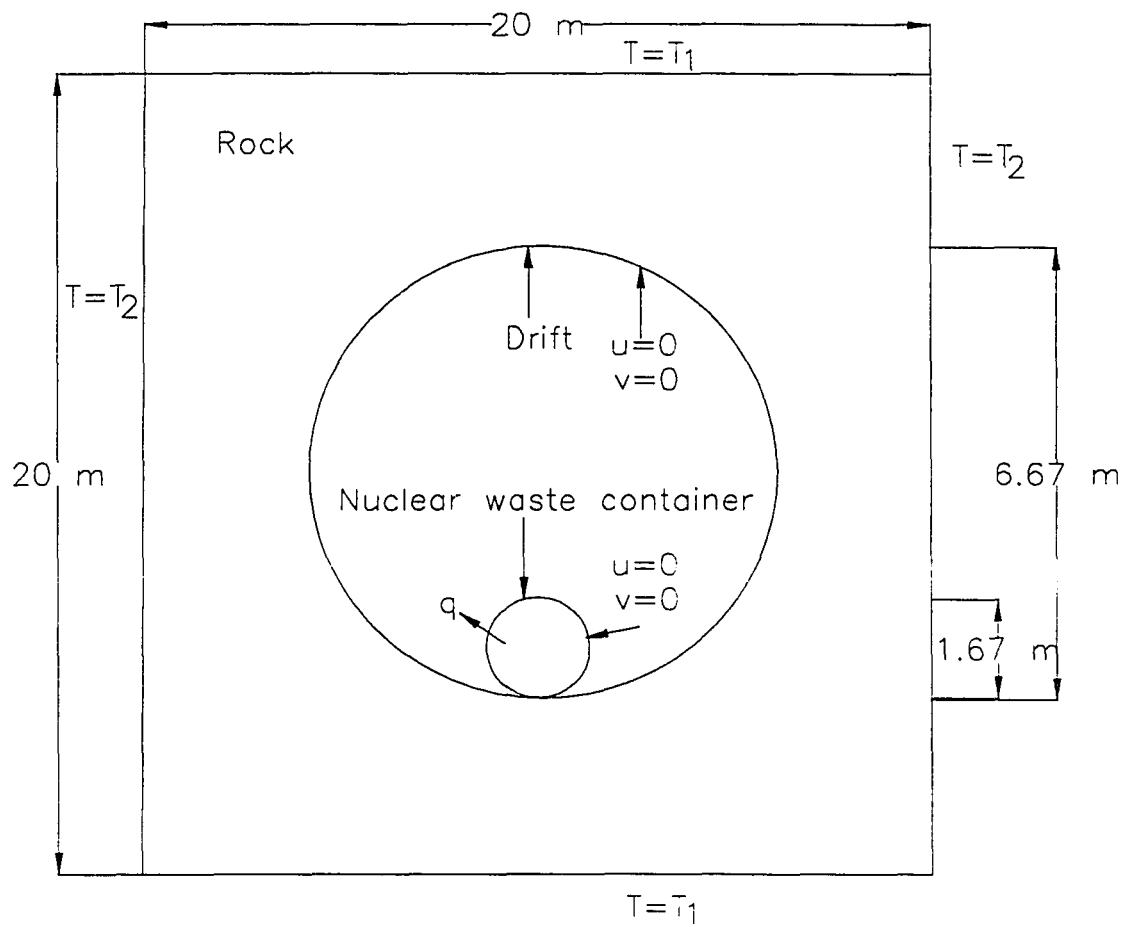


Figure 11 Computational Domain for the Steady State Analysis Inside the Drift Without Backfill

Table 4 Boundary Conditions

Year	Horizontal Boundary $T_1$	Vertical Boundary $T_2$	Heat Flux $q$
30	417 K	423 K	146 (W/m <sup>2</sup> )
130	437 K	421 K	57 (W/m <sup>2</sup> )

### Simulation Approach

A steady state analysis is performed for the heat transfer between the waste package and the drift. Combined modes of heat transfer using conduction, free convection and radiation have been modelled. The problem has been defined as steady state, non-linear, turbulent and strongly coupled. The equations are expressed in Cartesian coordinates. For strongly coupled flows, the complete momentum and energy equations are solved and the buoyancy term is included in the momentum equation. The Boussinesq approximation models the presence of the buoyancy force caused by density variation resulting from the variations in temperature. The form of this buoyancy force term is

$$(\rho - \rho_0) g_i = -\rho_0 [\beta_T (T - T_0)] g_i \quad (6)$$

where,

$\rho_0$  = density of air at the reference temperature (kg/m<sup>3</sup>)

$T_0$  = reference temperature (K)

$\beta_T$  = coefficient of thermal expansion ( $K^{-1}$ )

$g_i$  = gravity vector ( $m/s^2$ )

$\rho$  = density ( $kg/m^3$ )

$T$  = temperature (K)

$\rho_0$  has been taken as  $1.17 \text{ kg/m}^3$  at a reference temperature of  $25^\circ\text{C}$ . The coefficient of thermal expansion has been modelled as a constant with an average value of  $0.00335 \text{ K}^{-1}$ . The gravity vector has also been taken as a constant ( $9.81 \text{ m/s}^2$ ) and specifies globally the magnitude and direction of gravity.

The Rayleigh numbers are of the order of  $10^{12}$ , indicating that the flow in the drift is in the turbulent<sup>4</sup> region. The Rayleigh number has been defined as follows:

$$Ra = \frac{\rho \cdot \beta \cdot g \cdot L^4 \cdot q_{ref}}{\mu \cdot \alpha \cdot k} \quad (7)$$

where,

$L$  = characteristic length (m)

$q_{ref}$  = heat flux ( $W/m^2$ )

$\alpha$  = thermal diffusivity ( $m^2/s$ )

The characteristic length has been defined as the distance between the centers of the drift and canister.

$$L = \frac{D - d}{2} \quad (8)$$

where,

$D$  = diameter of the drift (m)

$d$  = diameter of the waste container (m)

For this model,

$$D = 6.67 \text{ m}$$

$$d = 1.67 \text{ m}$$

Therefore,  $L = 2.5 \text{ m}$

At 325°K,

$$\rho = 1.086 \text{ kg/m}^3$$

$$\beta = 0.0031 \text{ K}^{-1}$$

$$g = 9.81 \text{ m/s}^2$$

$$\alpha = 2.578 \times 10^{-5} \text{ m}^2/\text{s}$$

$$k = 2.816 \times 10^{-2} \text{ W/m/K}$$

$$\mu = 1.962 \times 10^{-5} \text{ N-s/m}^3$$

Table 5 shows the Rayleigh numbers obtained at different years.

The Reynold's averaged equations have been solved. The two equation  $k$ - $\epsilon$  model has modelled the turbulence viscosity, using the eddy viscosity concept. The effective viscosity  $\mu_e$  is computed by

$$\mu_e = \mu_0 + \mu_t$$

where  $\mu_0$  is the laminar viscosity of the air and  $\mu_t$  is the turbulent viscosity. The turbulent viscosity is computed by solving two additional transport equations, one for the turbulent kinetic energy ' $k$ ', and another for the turbulent dissipation ' $\epsilon$ ' and then using the formula:



$$\mu_t = \frac{\rho C_\mu k^2}{\epsilon} \quad (10)$$

The initial values for the turbulent kinetic energy and the turbulent dissipation has been input as 0.002 each.  $C_\mu$  is set<sup>5</sup> at 0.09 . The laminar viscosity<sup>1</sup> of the air is taken as  $1.8 \times 10^{-5}$  N.s/m<sup>2</sup> at a reference temperature of 25°C.

Table 5 Rayleigh Numbers

Years	Heat flux (W/m <sup>2</sup> )	Rayleigh number
0	270.0	$2.43 \times 10^{13}$
30	146.0	$1.3 \times 10^{13}$
130	57.0	$5.13 \times 10^{12}$
1000	13.26	$1.19 \times 10^{12}$

For the radiation problem, the air has been taken as a non - participating medium. Grey body radiation has been specified for the calculation of view factors. The emissivities<sup>2</sup> have been taken as constant, 0.6 for the canister and 0.75 for the walls of the drift. The penalty approach<sup>5</sup> is chosen to discretize the pressure variable.

The iterative Successive Substitution method solves the nonlinear steady state solution. A value of 0.8 for the acceleration factor improved the convergence characteristics for the simulation. The iteration for the steady state solution is terminated when two convergence criteria are satisfied simultaneously:

$$\left[ \frac{U_i - U_{i-1}}{U_i} \right] < DTOL \quad (11)$$

and

$$\left[ \frac{R_i}{R_o} \right] < RTOL \quad (12)$$

where,

- U = solution vector
- R = residual force vector
- DTOL = tolerance for the velocity convergence
- RTOL = tolerance for the residual convergence

A tolerance of 0.01 is specified for DTOL and RTOL.

Paved mesh with quadrilateral elements has been generated. Figure 12 shows the mesh plot for the above model. The waste container is raised a bit from the floor of the drift to facilitate the generation of mesh. The total number of nodes for the solution is 3021 and the total number of elements is 3240. The mesh inside the drift is dense to catch the minute physical details. Appendix 2 describes the input file to generate mesh and to obtain a solution field for the problem.

## Results

The temperature and velocity fields at 30 and 130 years are shown in Figure 13(a) and Figure 13(b) respectively. At 30 years the average temperatures on the walls of the canister and the drift are 196°C and 190°C respectively. The temperature is maximum

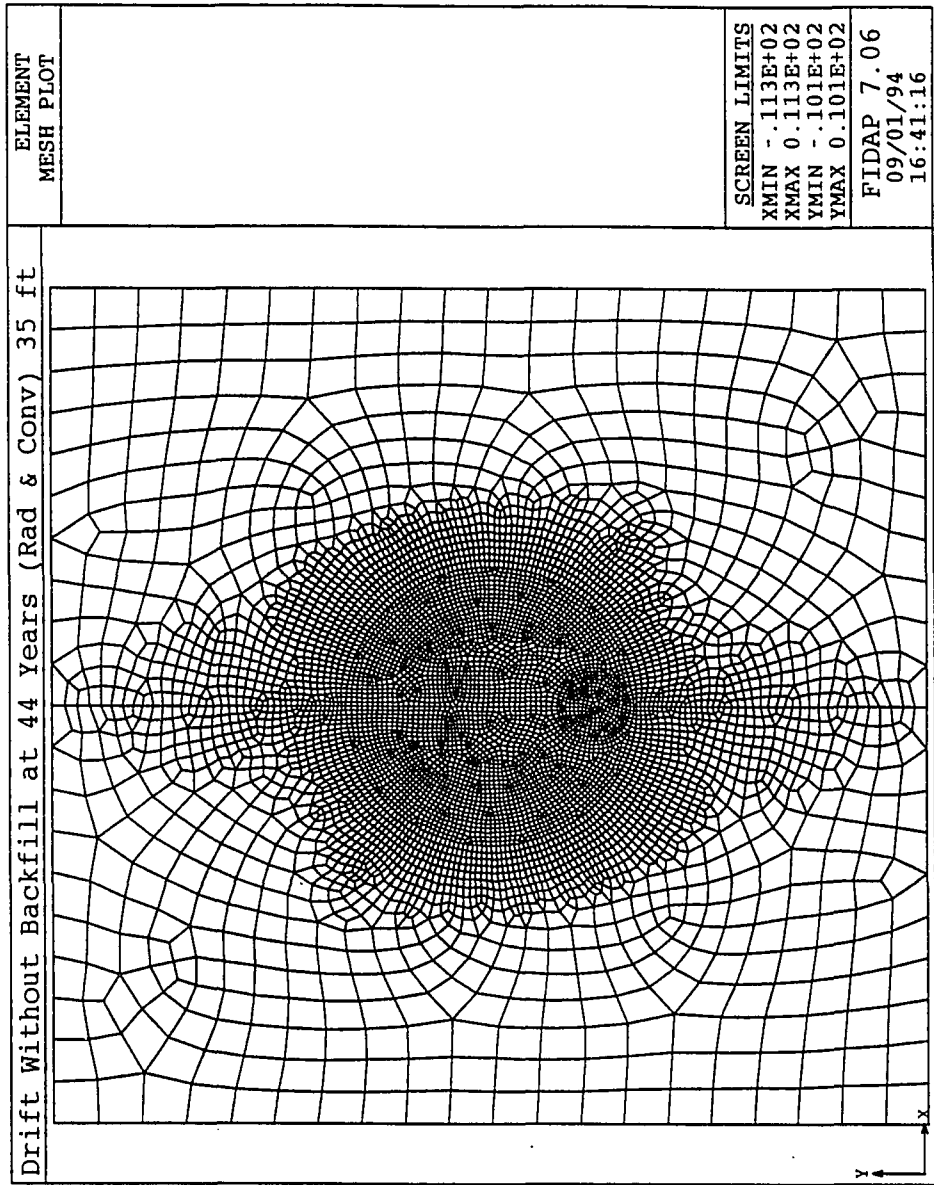


Figure 12 Mesh Plot

at the bottom of the drift as the waste container is placed on the floor of the drift and the maximum difference of temperatures at the top and the bottom of the drift is about  $10^{\circ}\text{C}$ . The maximum velocity of air due to natural convection at this time is  $0.21\text{ m/s}$  beneath the waste container and the drift wall as the waste container has been raised slightly to facilitate the generation of mesh. Figure 14(a) and Figure 14(b) show the vector plots at 30 years and 130 years respectively. As the time progressed average temperature differences between the drift and the waste container were reduced. This is evident in the velocity vector plots which show a trend of decreasing velocities as the time progressed because the heat flux reduced with time, thus reducing the Rayleigh numbers and consequently the turbulence. The difference of temperatures between the top and the bottom of the drift also reduced with time because of the reduction in the value of heat flux. Two asymmetric cells were obtained for the streamline plot, indicating that the problem cannot be treated as a symmetric one along the vertical center line of the drift. Figure 15 shows a typical plot of the streamlines obtained at 10 years. There were two flow cells at all times.

The variation of the average drift wall temperatures for a period of 1000 years for the combined heat transfer is shown in Figure 16. The maximum temperature on the drift is  $192^{\circ}\text{C}$  which means that condensation is not likely in this scenario. Figure 17(a) and 17(b) show temperature contours inside the drift at 30 years and 130 years. These figures are zoomed plots of Figure 13(a) and 13(b) respectively. The difference in the temperatures due to natural convection is evident by the contours in the drift which show a maximum temperature inside the canister and the temperatures decrease as the contours

move up towards the walls of the drift. The maximum temperature obtained inside the canister is about 200°C at around 30 years. This temperature decreased as the time progressed and the maximum temperature inside the canister is around 140°C at 1000 years.

The comparison of the temperature distribution in Figure 11 and Figure 16 exhibits the effect of free convection and radiation as modes of heat transfer. The maximum drop in the average temperature is about 13°C. The maximum velocity achieved is around 0.21 m/s. The maximum temperature inside the canister is around 200°C, which is well below the thermal goal of 350°C for the zirconium alloy cladding.

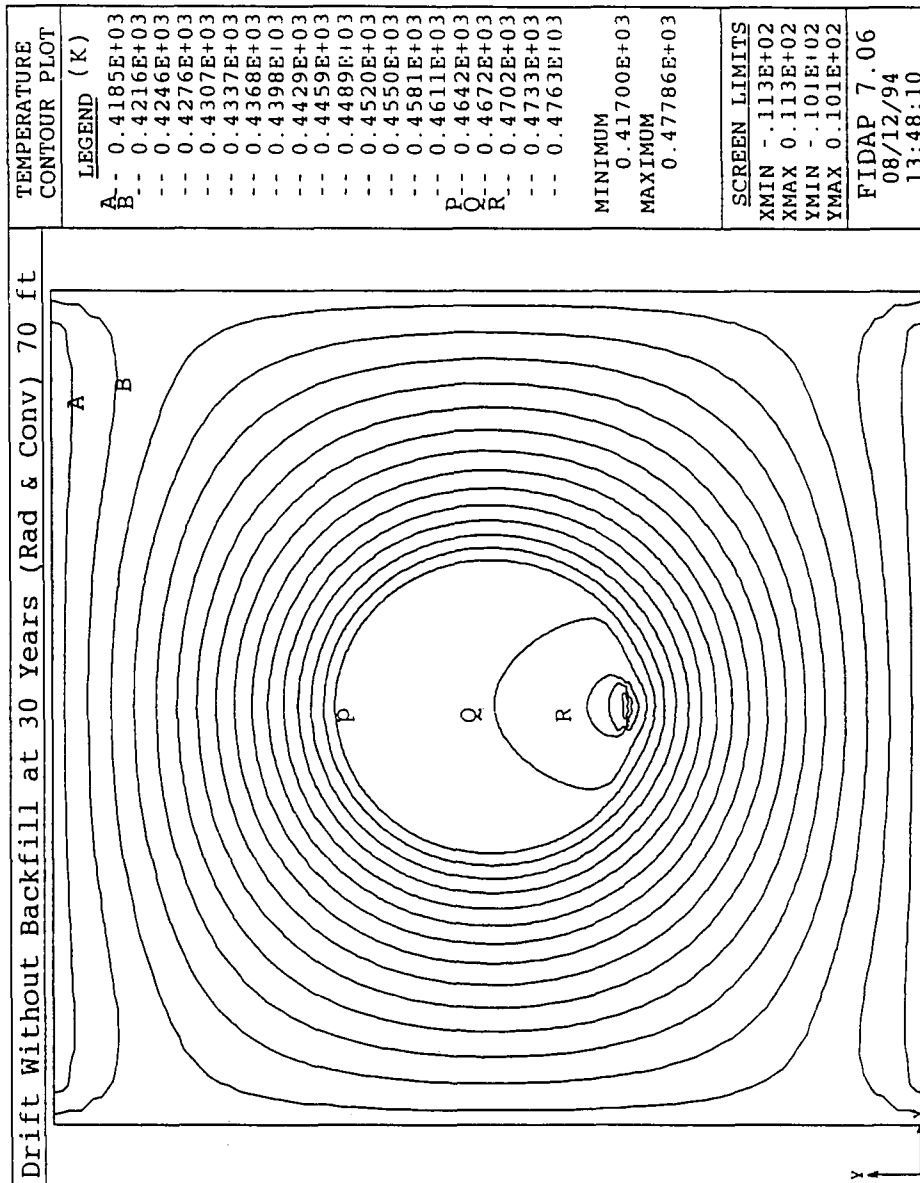


Figure 13(a) Temperature Contours at 30 Years

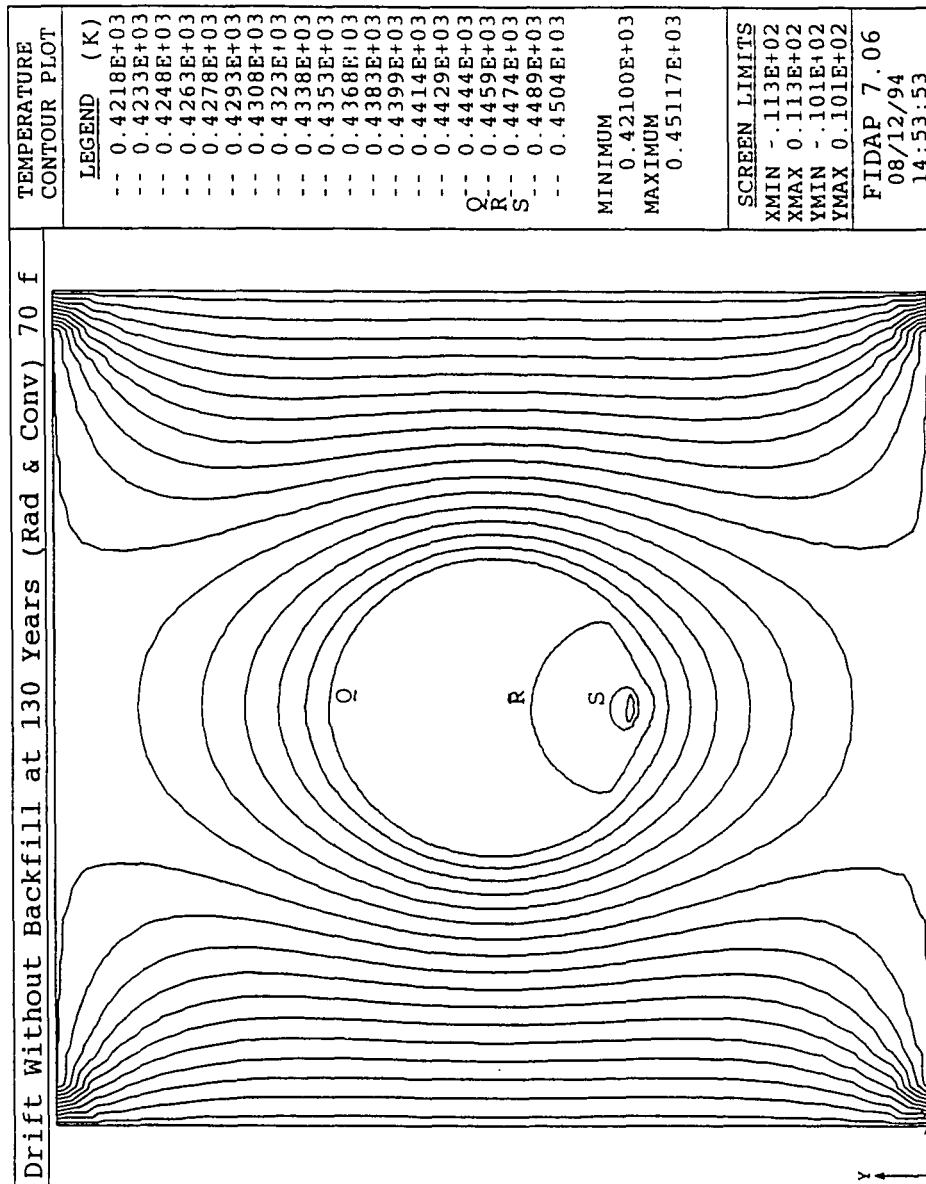


Figure 13(b) Temperature Contours at 130 Years

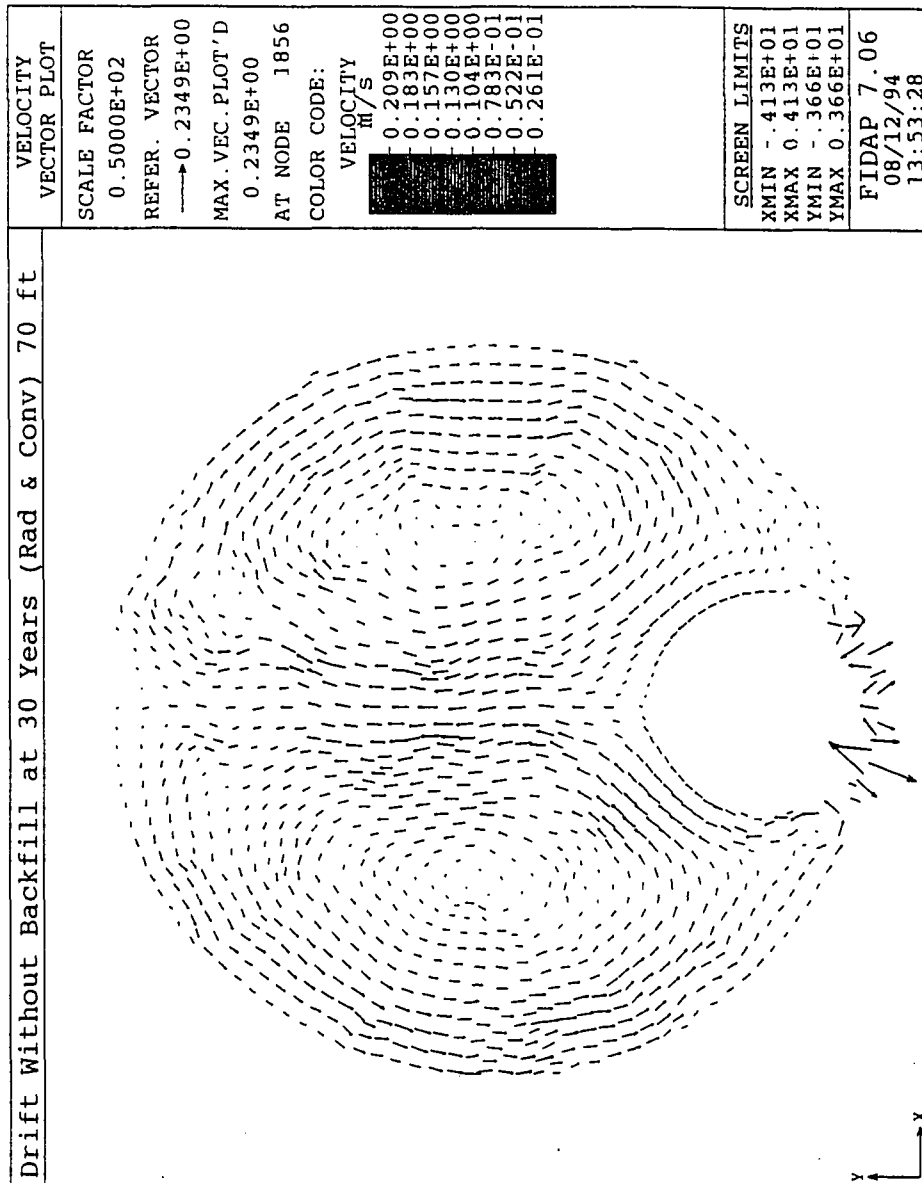


Figure 14(a) Vector Plot at 30 Years





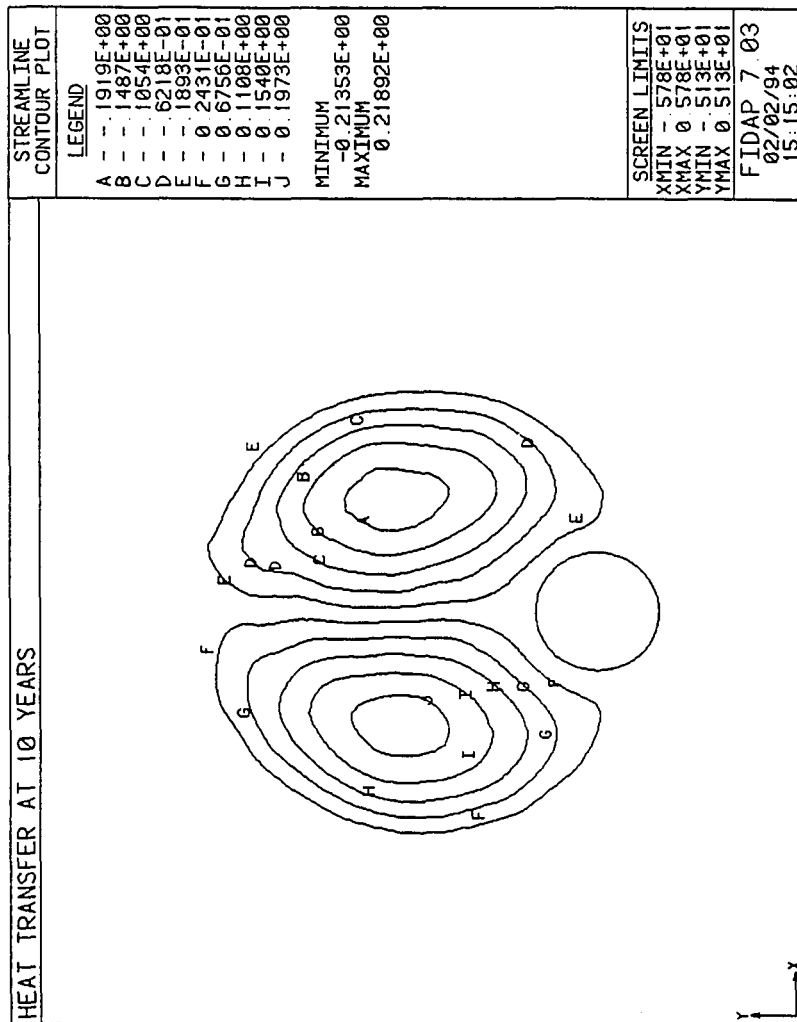


Figure 15 Streamline Plot

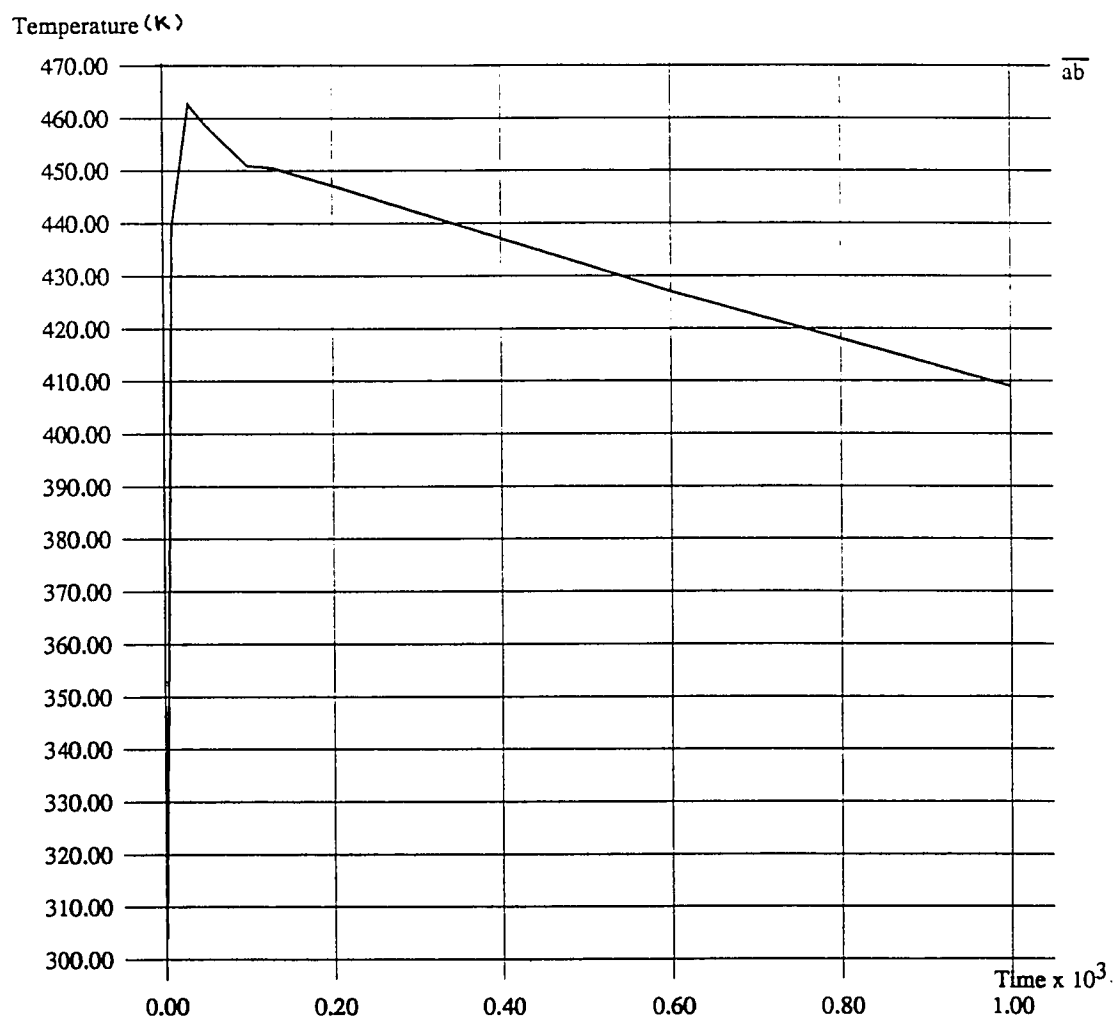


Figure 16 Variation of Drift Wall Temperature for Steady State Analysis

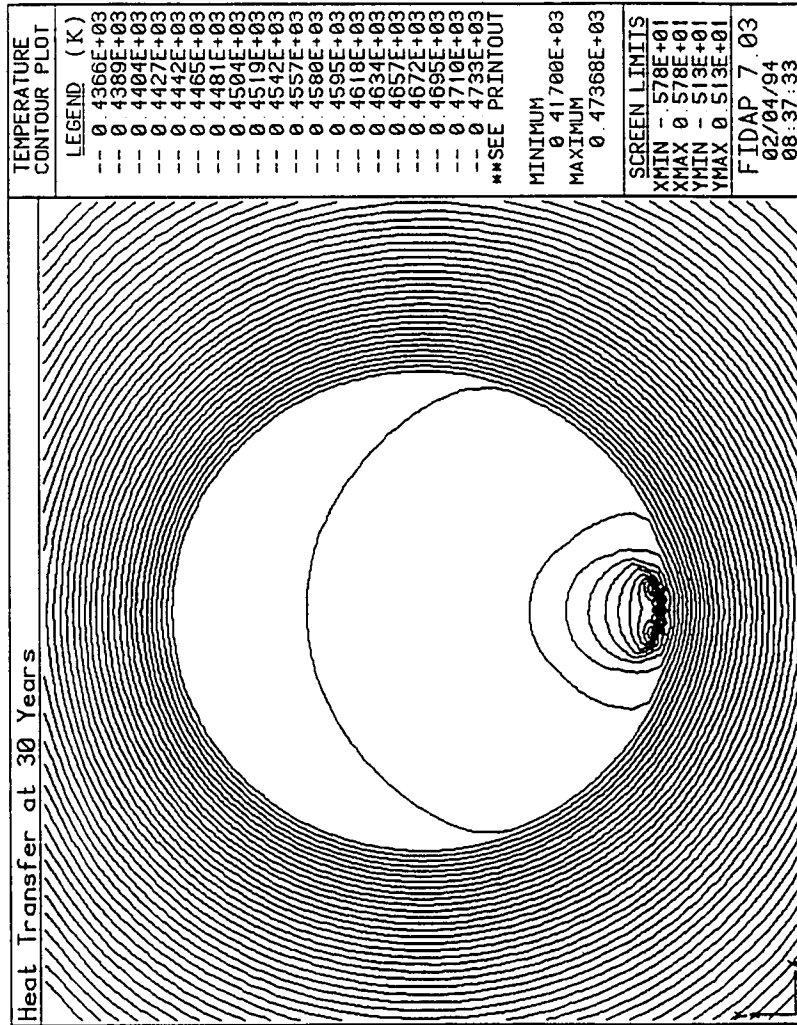


Figure 17(a) Zoomed Plot of Temperature Contours at 30 Years

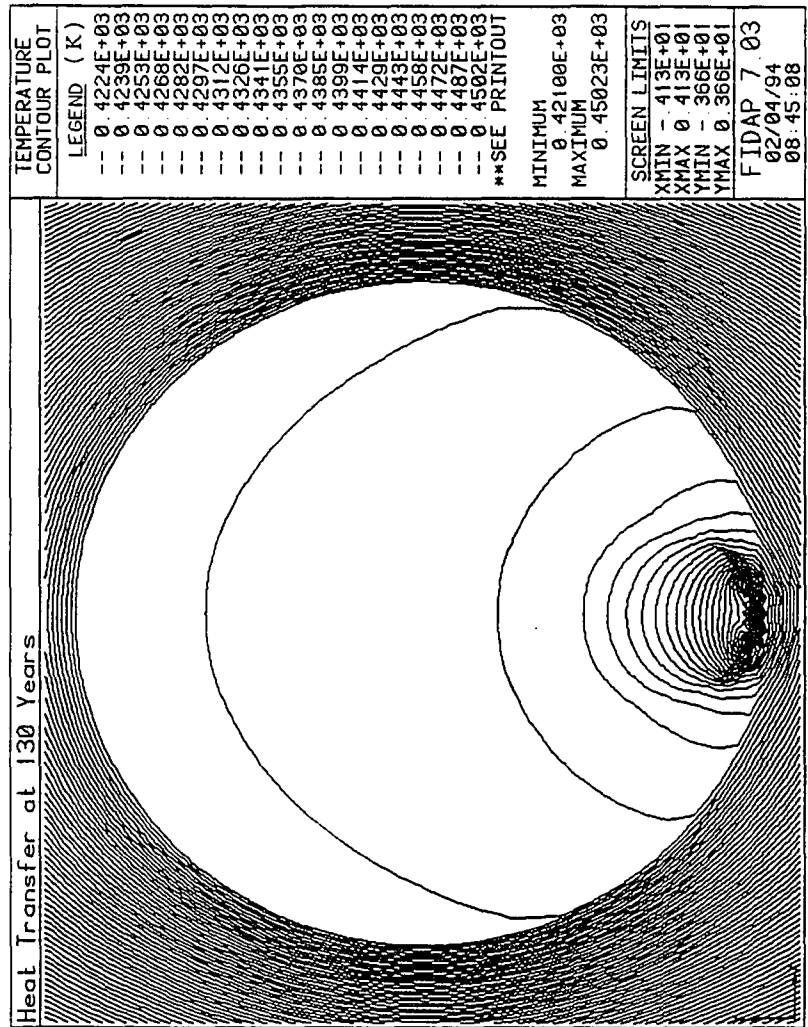


Figure 17(b) Zoomed Plot of Temperature Contours at 130 Years

## **CHAPTER 5**

### **STEADY STATE ANALYSIS INSIDE A DRIFT WITH INVERTED BACKFILL**

#### **Computational Domain**

A two-dimensional finite element thermal analysis is performed for the heat transfer around a nuclear waste container placed horizontally in the drift. The nuclear waste containers are placed on the backfill above the floor of the drift and exchange heat with the walls of the drift and with the air circulating through the repository. The backfill material is assumed to be composed of a non-compact crushed tuff.

The computational domain of the thermal model is shown in Figure 18. The drift is in the center of the thermal model with the nuclear waste container placed horizontally on the backfill which is between the nuclear waste container and the floor of the drift. The drift is surrounded by the rock. The individual waste containers are collectively modelled as an infinitely extended (along the drift axis) smeared source with a circular cross section consistent with the proposed package design and a section has been modelled with heat flux imposed on the boundary of the nuclear waste container. The top and bottom horizontal boundaries extend 10 m from the center of the drift and constant temperature boundary conditions are imposed on them. The left and right vertical boundaries also extend 10 m from the center of the drift and the temperature boundary conditions are constant.

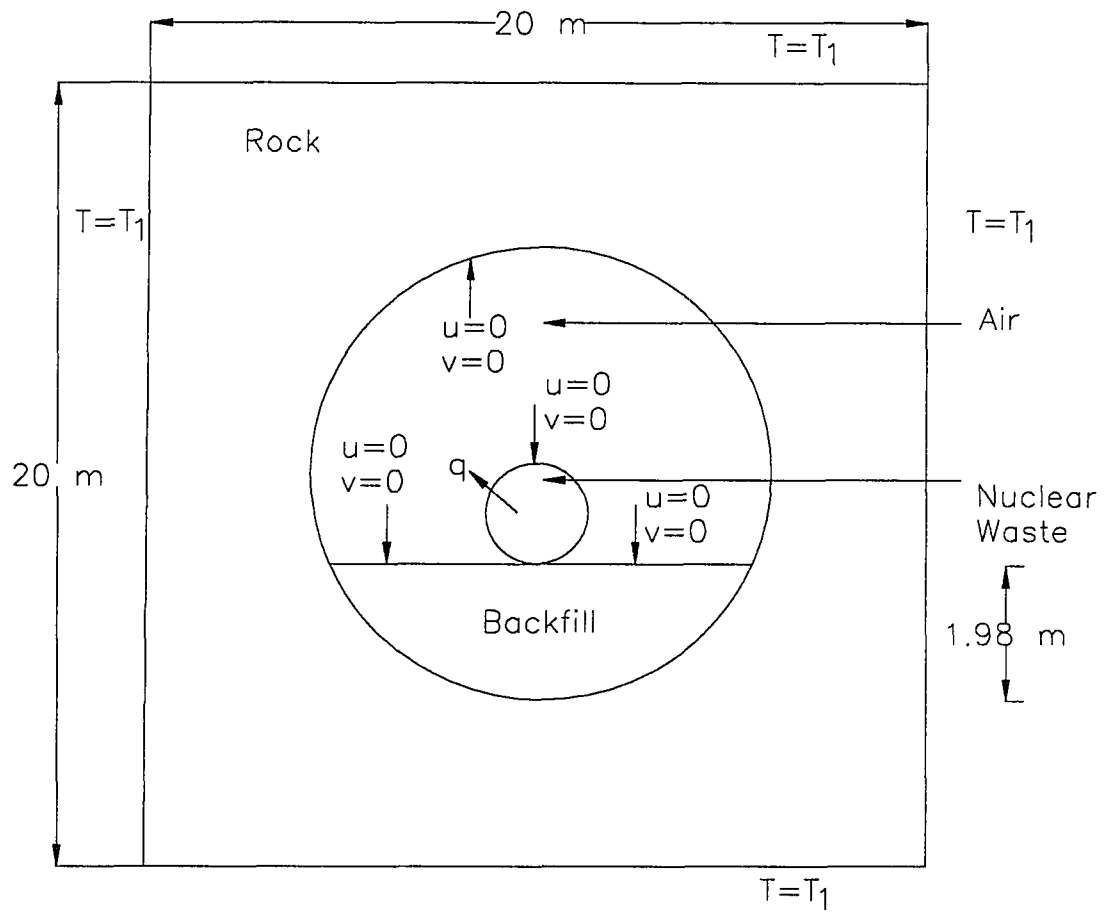


Figure 18 Computational Domain for the Steady State Analysis Inside the Drift with Backfill

The properties of the rock, air and nuclear waste have been discussed in chapter 2. The effective porosity of the backfill material is assumed to be 40%. Air is the only medium present inside the drift. Table 6 shows the boundary conditions for the heat flux imposed on the walls of the waste container and for the constant temperatures imposed on the horizontal and vertical boundaries of the computational domain.

### Simulation Approach

A steady state analysis is performed for the heat transfer between the waste package and the drift. Combined mode of heat transfer affects the cooling of the waste containers in the repository drifts. Conduction through the backfill and the rock, natural convection to the air and radiation between the container surface and the drift wall contribute to the removal of the heat from the nuclear waste container. The flow in the drift is strongly coupled and the buoyancy term is included in the momentum equation. The problem is defined as steady state, non-linear, turbulent and strongly coupled.

Figure 19 shows the nomenclature used for calculating the hydraulic diameter ( $D_h$ ) for the drift which has been calculated as follows:

Area (A) of the drift with air enclosed is,

$$A = \frac{\theta}{\pi} \cdot \frac{\pi}{4} \cdot D^2 + \frac{1}{2} \cdot (2 \cdot x) \cdot y - \frac{\pi}{4} \cdot d^2 \quad (13)$$



Table 6 Boundary Conditions

No.of years	Heat flux q	Horizontal and vertical boundaries (T <sub>l</sub> )
0 years	270.0 W/m <sup>2</sup>	298.0 K
10 years	207.66 W/m <sup>2</sup>	371.0 K
30 years	146.76 W/m <sup>2</sup>	417.0 K
130 years	57.0 W/m <sup>2</sup>	437.0 K
600 years	20.66 W/m <sup>2</sup>	421.0 K

The wetted perimeter (P) is,

$$P = \frac{\theta}{\pi} \cdot \pi \cdot D + 2 \cdot x + \pi \cdot d \quad (14)$$

where,

$\theta$  = angle of the sector

x = half the width of the backfill

y = distance of the center of the waste container from the base of the  
backfill

D = diameter of the drift

d = diameter of the waste container

For this model,

$$\theta = 3.98 \text{ radians}$$

$$x = 3.047 \text{ m}$$

$$y = 1.355 \text{ m}$$

$$D = 6.67 \text{ m}$$

$$d = 1.67 \text{ m}$$

Therefore,  $A = 46.2 \text{ m}^2$

$$P = 37.88 \text{ m}$$

Hydraulic diameter is defined as,

$$D_h = \frac{4 \cdot A}{P} \quad (15)$$

Therefore,  $D_h = 4.878 \text{ m}$

Characteristic length (L) is defined as,

$$L = \frac{D_h - d}{2} \quad (16)$$

For this model,  $L = 0.52 \text{ m}$

Rayleigh numbers<sup>4</sup> are of the order of  $10^{10}$  indicating that the flow in the drift is still in the turbulent regime. Table 7 shows the Rayleigh numbers obtained at different years for different values of heat flux. The two equation k- $\epsilon$  model is used to model the turbulence viscosity, using the eddy viscosity concept.

The radiation heat transfer from the waste containers is governed by the emissivity of the waste container, backfill and the drift wall, the temperatures of each surface, and the view factor between the two surfaces. The air has been treated as a non-participating medium for the radiation problem. Grey body radiation has been

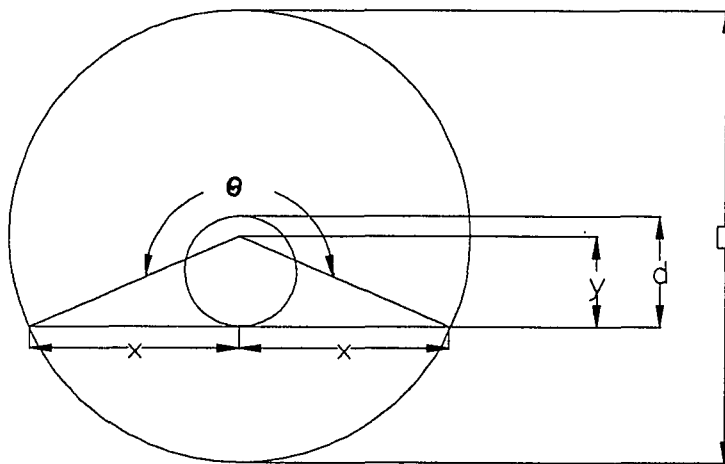


Figure 19 Calculation of Hydraulic Diameter

specified for the calculation of view factors. The emissivities<sup>2</sup> for the nuclear waste container, backfill and the walls of the drift have been taken as 0.6, 0.75 and 0.75 respectively. The simulation approach is discussed in chapter 4.

Paved mesh with quadrilateral elements has been generated. Figure 20 shows the mesh plot for this model. The total number of nodes is 2889 and the total number of elements 3084. Appendix 3 describes the input file to generate mesh and to obtain solution for the above problem.

Table 7 Rayleigh Numbers at Different Years

Years	Heat flux	Rayleigh Number
10	207.66 W/m <sup>2</sup>	3.488 x 10 <sup>10</sup>
30	146.76 W/m <sup>2</sup>	2.465 x 10 <sup>10</sup>
130	56.14 W/m <sup>2</sup>	9.432 x 10 <sup>9</sup>
600	20.66 W/m <sup>2</sup>	3.471 x 10 <sup>9</sup>
1000	13.26 W/m <sup>2</sup>	2.228 x 10 <sup>9</sup>

## Results

The results have been presented for four different cases:

Case 1: The initial heat of 30 kW is smeared over the entire length of 21.2 m (center distance between the waste containers) and a combined mode of heat transfer takes place between the waste container and the drift. Figure 21(a), 21(b), 21(c), and 21(d) show the

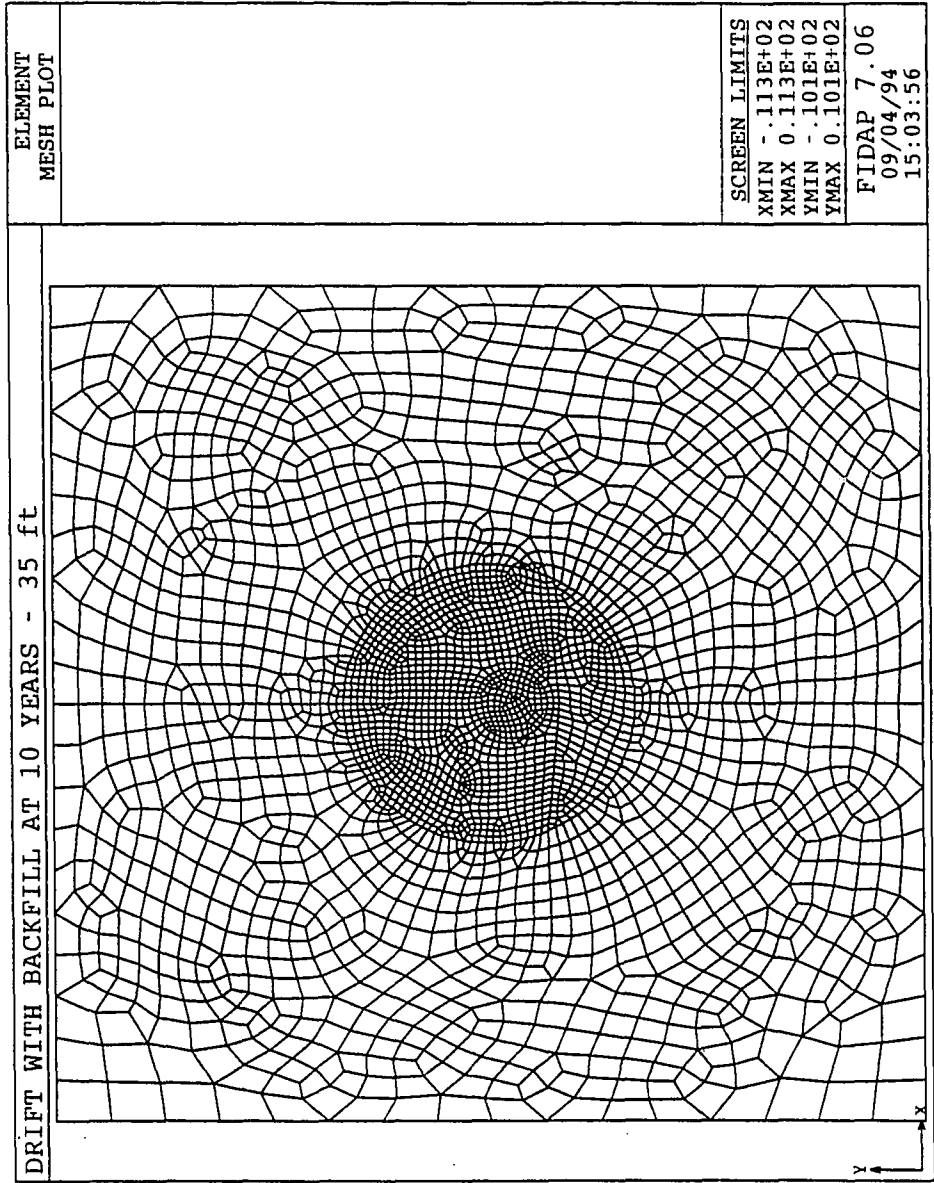


Figure 20 Mesh Plot

temperature contours at 10 years, 30 years, 130 years and 600 years respectively. Table 8 show maximum temperature inside the waste container and the peak temperature on the drift. The contour Q represents the average temperatures on the drift.

Case 2: The initial heat of 30 kW is smeared over the entire length of 21.2 m (center distance between the waste containers) but radiation is not a part of the heat transfer mechanism. Figure 22(a), 22(b), 22(c) and 22(d) show the temperature contours at 10 years, 30 years, 130 years and 600 years. Table 9 shows the maximum temperature inside the waste container and the peak temperature on the drift. The maximum temperature inside the container reaches  $189.1^{\circ}\text{C}$  but the drift reaches a peak temperature of  $173.4^{\circ}\text{C}$ .

Case 3: The initial heat of 30 kW is smeared over the length of 10.6 m (half the center distance between the waste containers) assuming that most of the waste heat will be concentrated around the waste container and a combined mode of heat transfer takes place between the waste container and the drift. Figure 23 shows the temperature contours at 10 years. The maximum temperature inside the container is  $272.6^{\circ}\text{C}$  while the drift reaches a peak temperature of  $248.0^{\circ}\text{C}$ . These temperatures are considerably high as compared to case 1.

Case 4: The initial heat of 30 kW is smeared over the length of 10.6 m (half the center distance between the waste containers) but radiation is not a part of the heat transfer mechanism. Figure 24 shows the temperature contours for this case. The maximum temperature inside the container raises to  $288.1^{\circ}\text{C}$  but the drift reaches a peak temperature of  $248.6^{\circ}\text{C}$ . At 10 years the temperatures for this case are the highest.

Table 8 Peak Temperatures on the Drift and Inside the Waste Container for Case 1

Years	Peak temperature on the drift	Peak temperature inside the waste container
10	173.4°C	185.7°C
30	201.0°C	209.1°C
130	184.8°C	189.3°C
600	155.5°C	156.5°C

Table 9 Peak Temperatures on the drift and inside the Waste Container for Case 2

Years	Peak temperature inside the drift	Peak temperature on the waste container
10	173.4°C	189.1°C
30	200.3°C	211.2°C
130	184.7°C	187.8°C
600	155.5°C	157.7°C

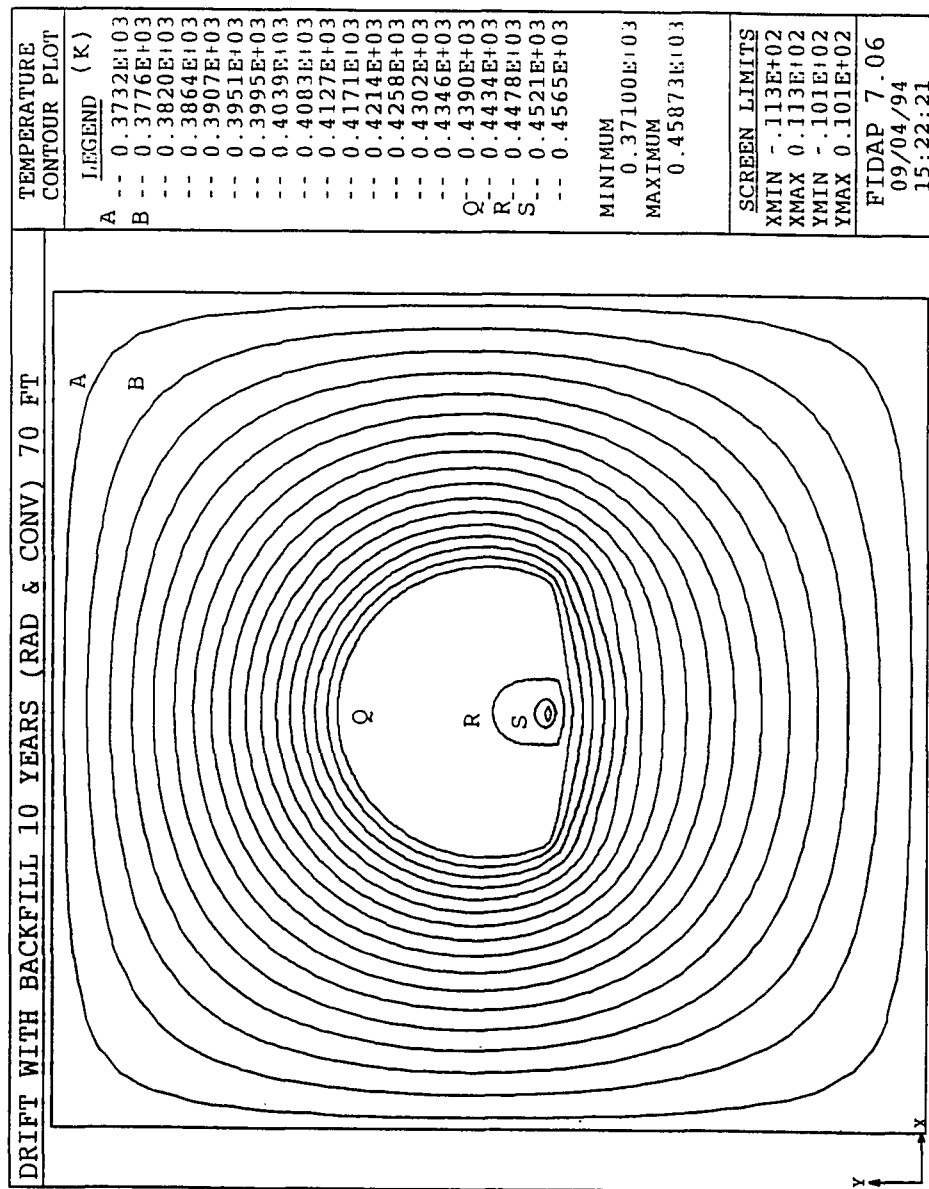


Figure 21(a) Temperature Contours at 10 Years for Case 1



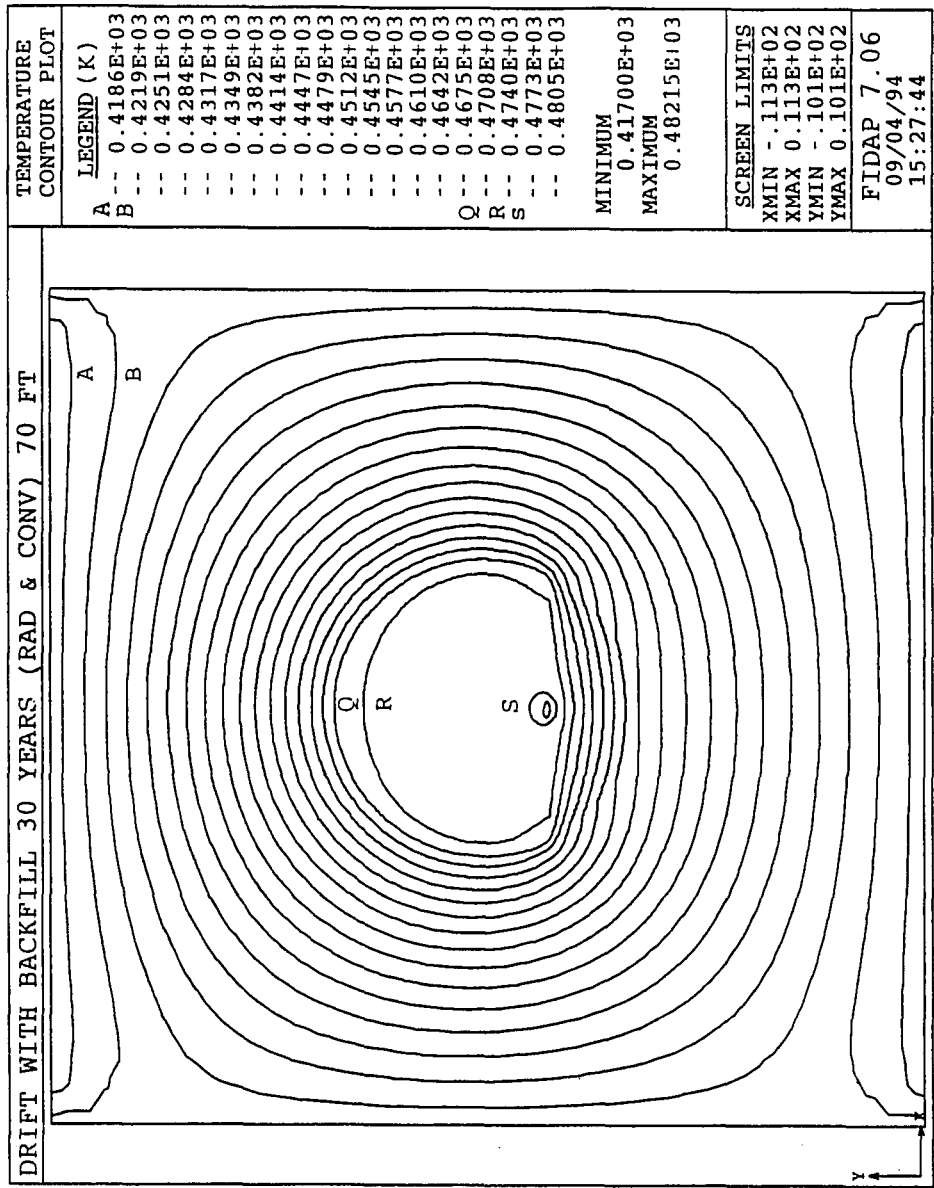


Figure 21(b) Temperature Contours at 30 Years for Case 1

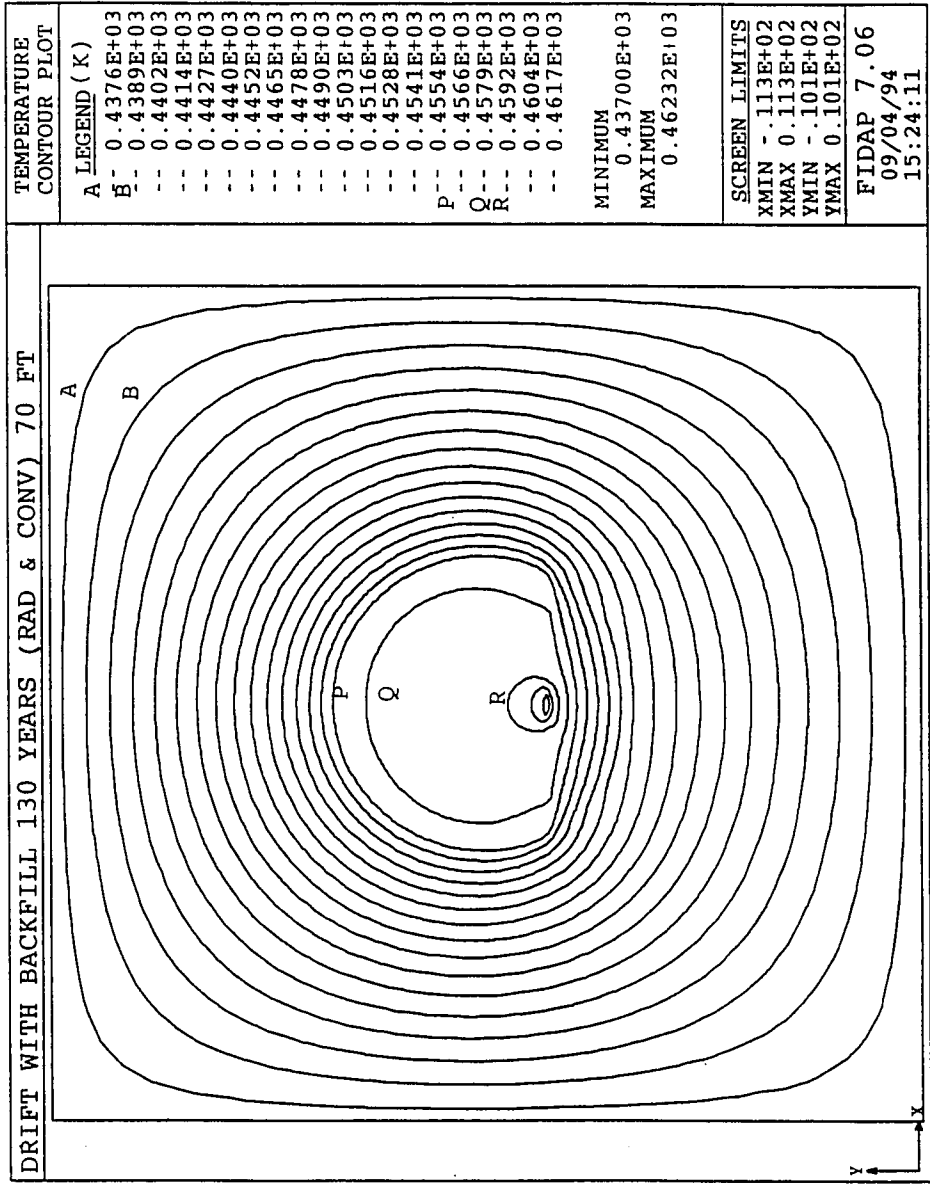


Figure 21(c) Temperature Contours at 130 Years for Case 1

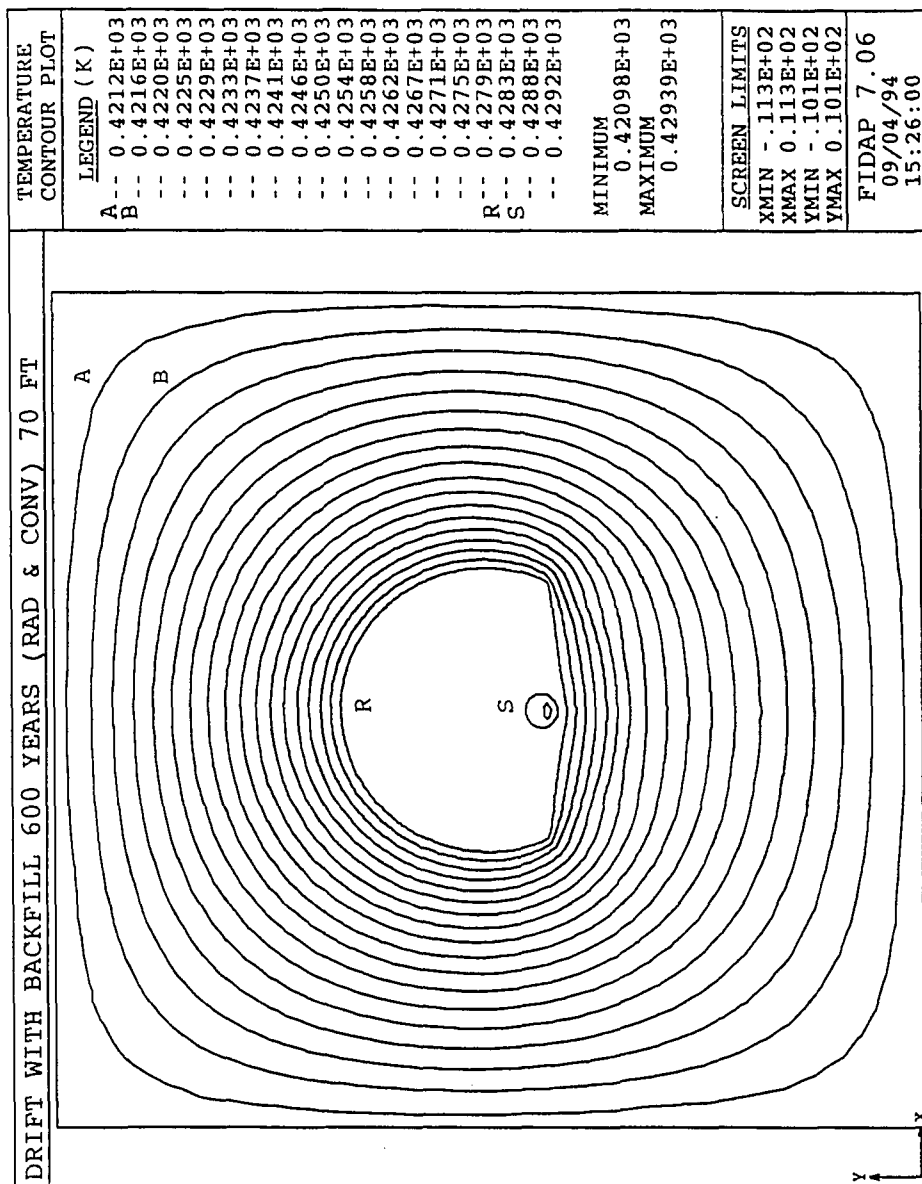


Figure 21(d) Temperature Contours at 600 Years for Case I

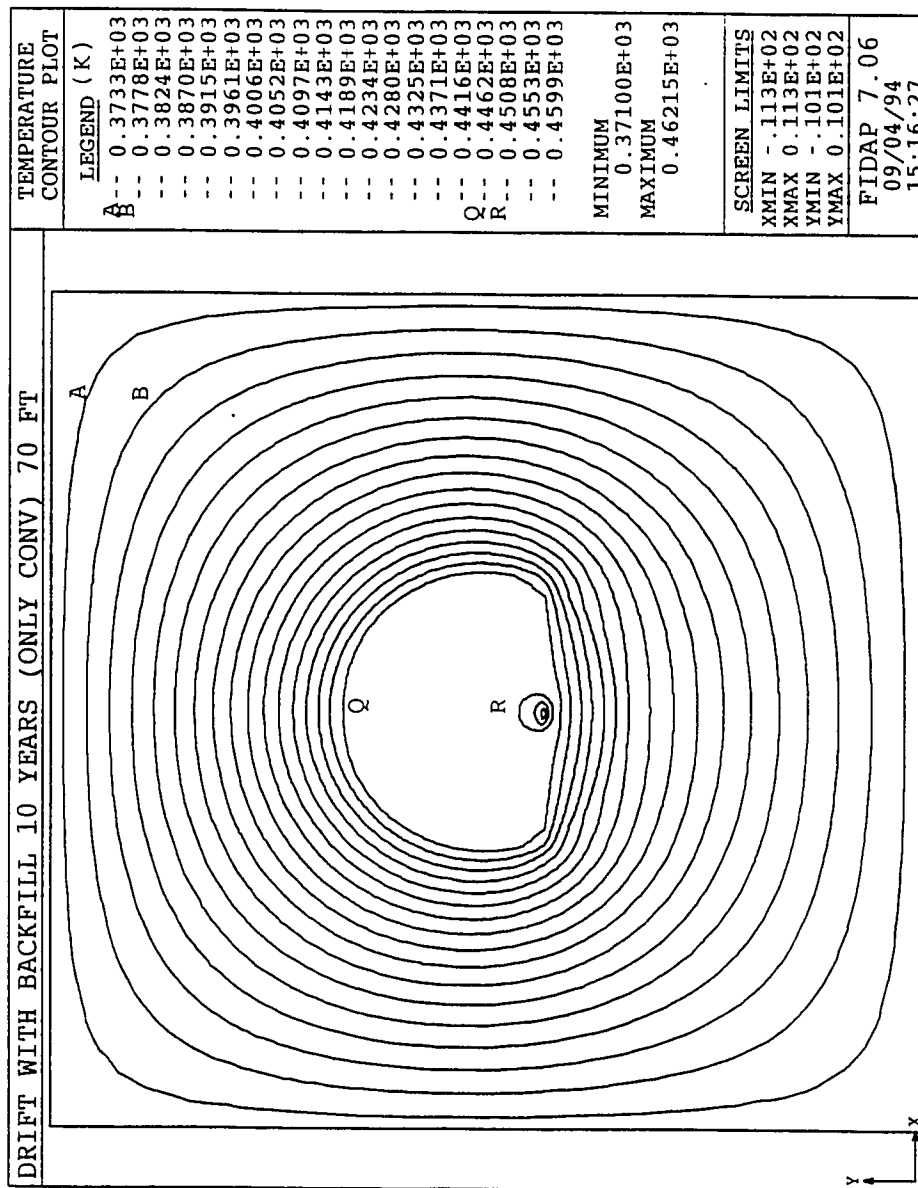


Figure 22(a) Temperature Contours at 10 Years for Case 2

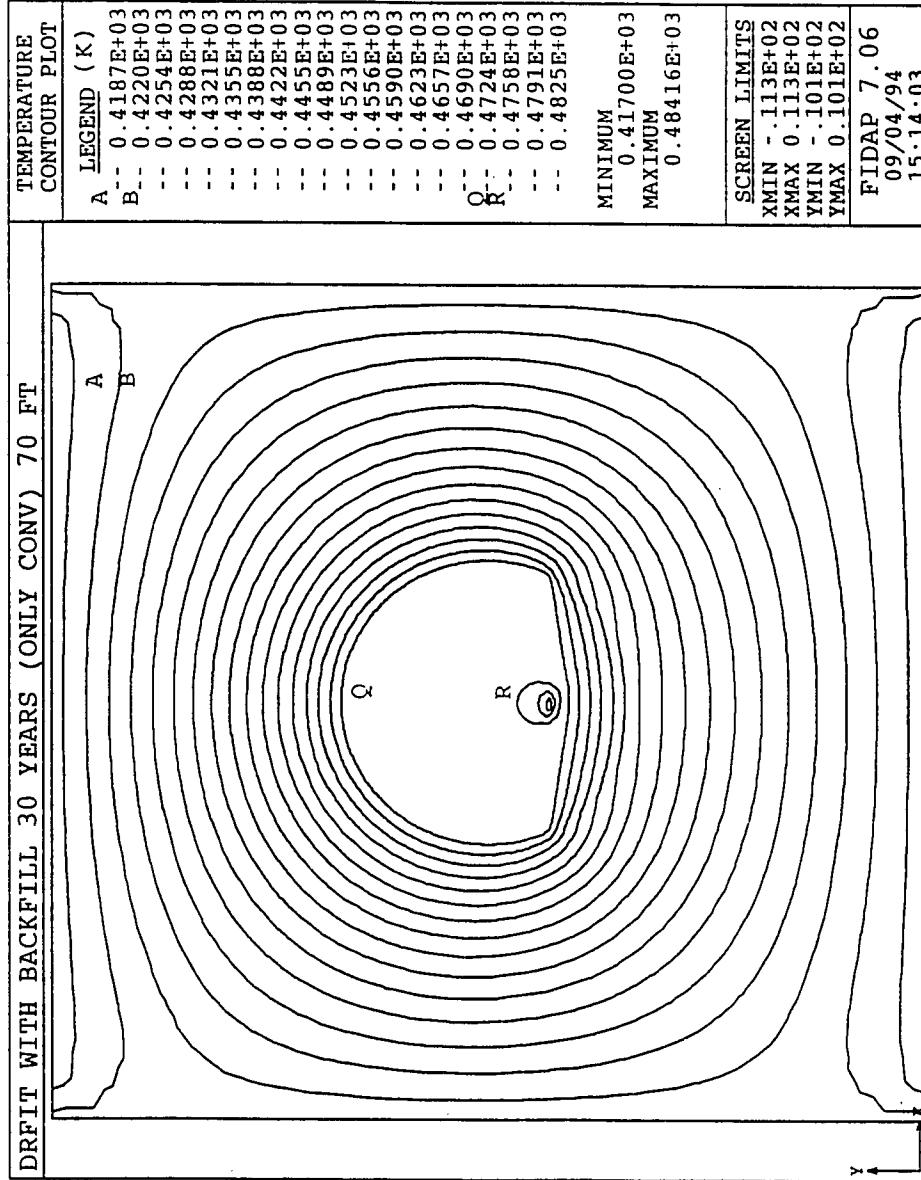


Figure 22(b) Temperature Contours at 30 Years for Case 2

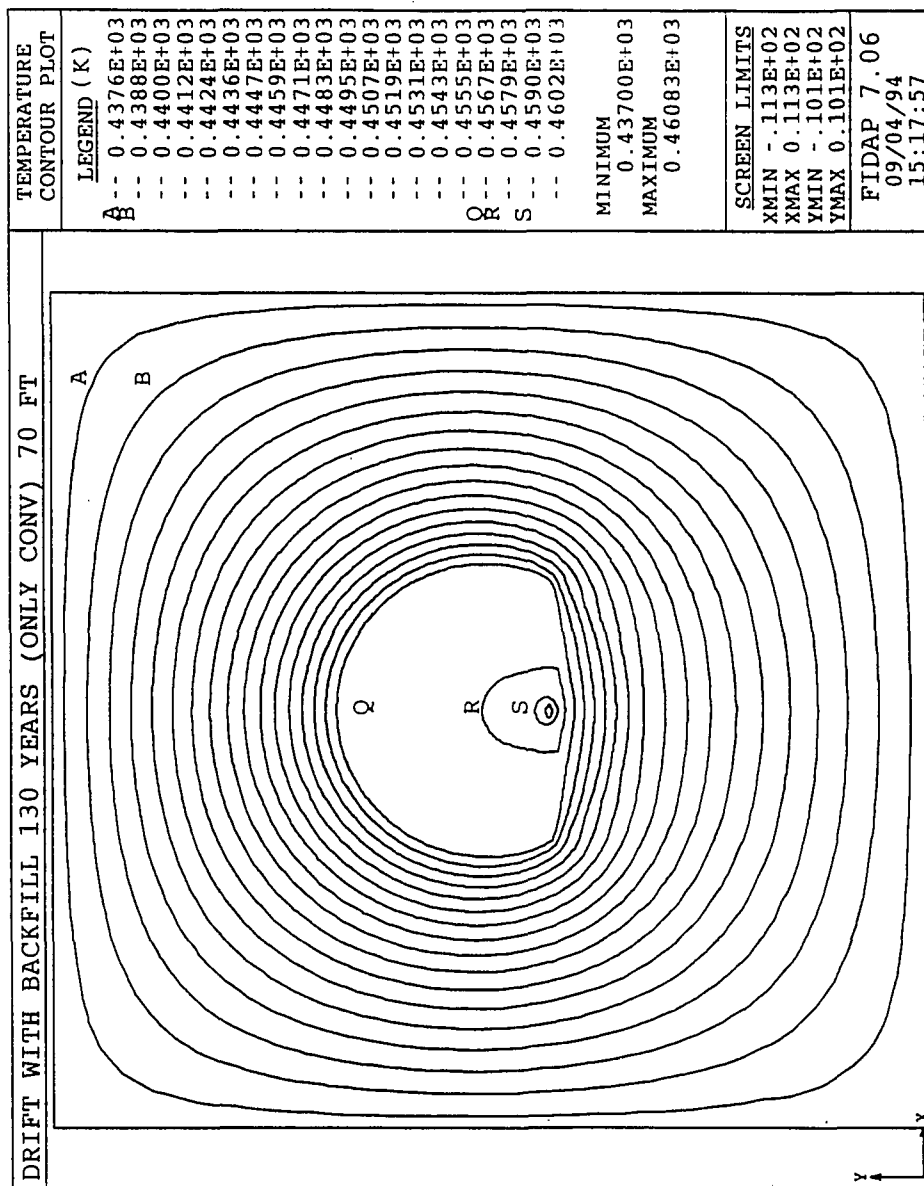


Figure 22(c) Temperature Contours at 130 Years for Case 2

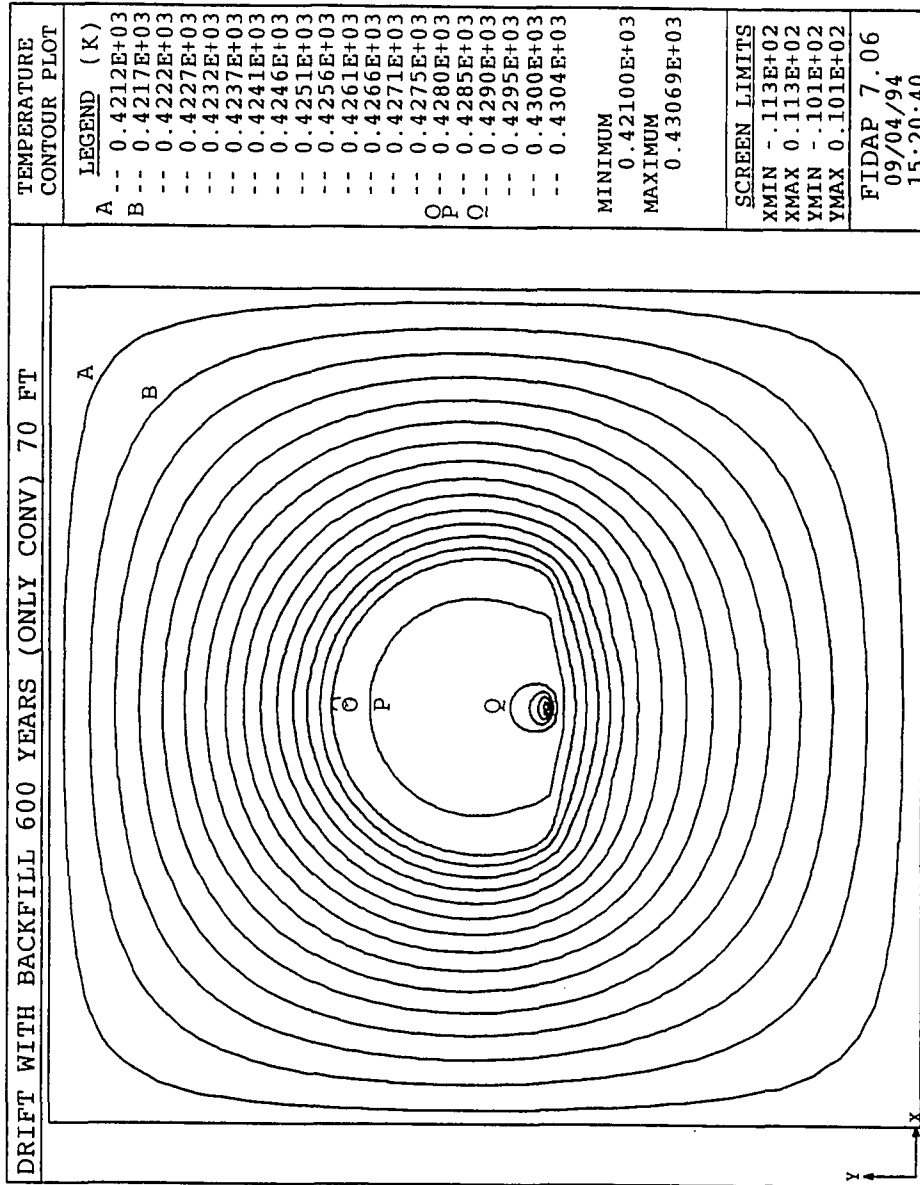


Figure 22(d) Temperature Contours at 600 Years for Case 2

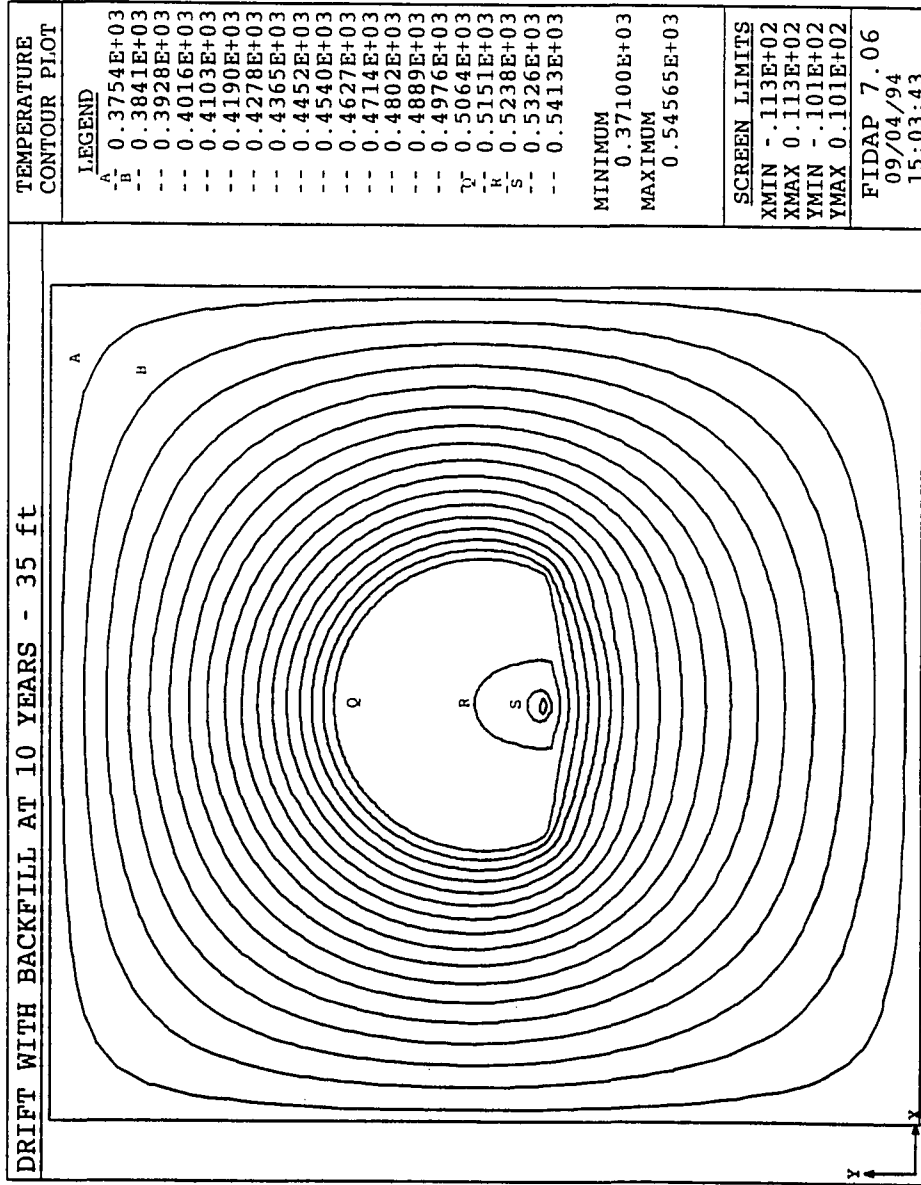


Figure 23 Temperature Contours at 10 Years for Case 3



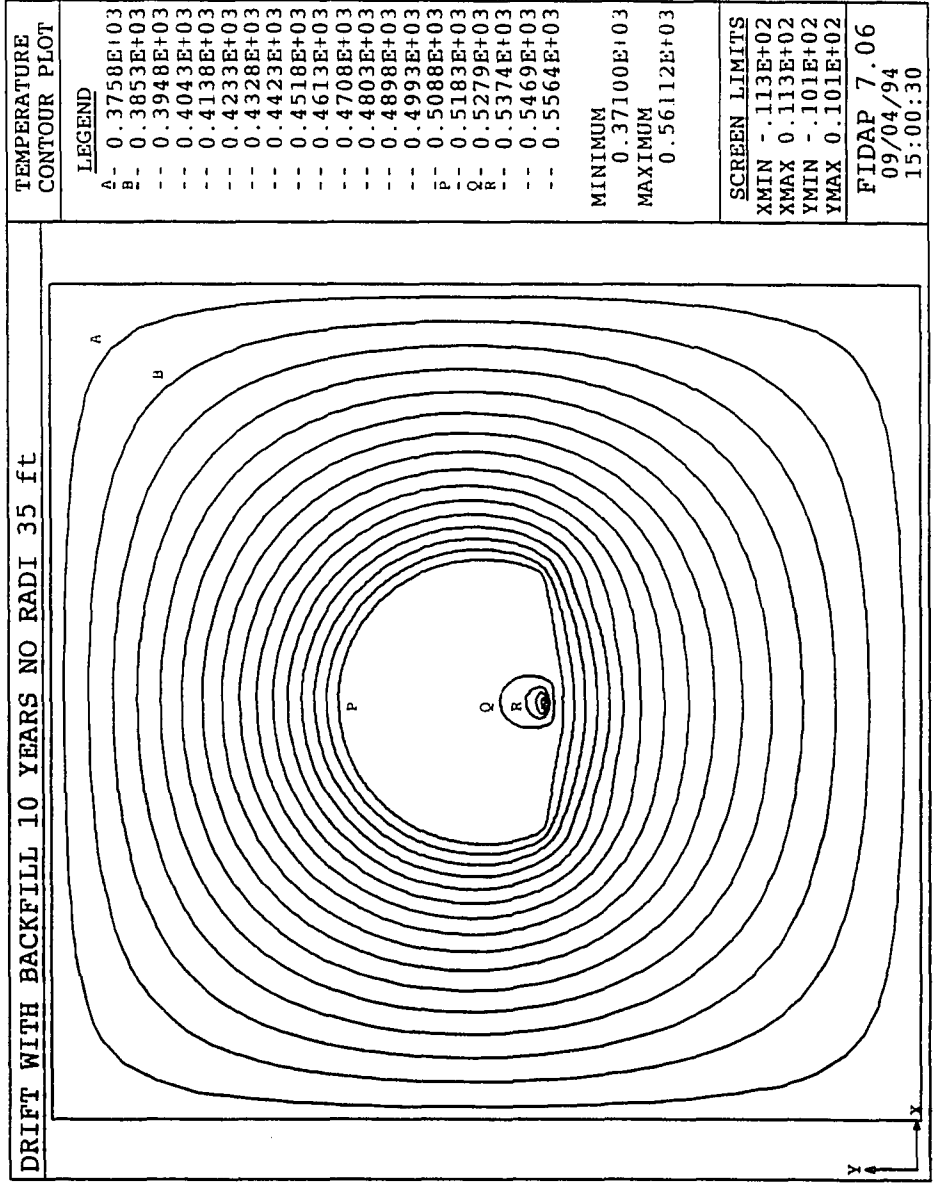


Figure 24 Temperature Contours at 10 Years for Case 4

A justification for presenting results for Case 1 versus Case 3 is the simple fact that the 2-D model is an approximation to the true 3-D model whereby the heat flux on the rock walls is not necessarily uniform. This gives a more realistic magnitude and importance of the mechanisms of heat convection and radiation which transfer heat from the waste container to the rock. A calculation of radiative heat flux to the overall heat flux using averaged temperature values for the drift wall and surface of the waste container and the formula

$$q_{rad} = \frac{\sigma (T_c^4 - T_d^4)}{\frac{1}{\epsilon_c} + \frac{1 - \epsilon_d}{\epsilon_d} \left( \frac{d}{D} \right)} \quad (17)$$

where,

$q_{rad}$  = radiative heat flux (W/m<sup>2</sup>)

$\epsilon_c$  = emissivity of the waste container

$\epsilon_d$  = emissivity of the drift wall

$\sigma$  = Stefan Boltzmann constant

$T_d$  = average temperature of the drift wall

$T_c$  = average temperature of the surface of the waste  
container

shows that for case 1 radiative heat flux accounts for 16% of the total heat transfer as opposed to 34% for the case 3 where the total length of smearing of the heat source has been shrunk from 21.2 m to 10.6 m. It is clear from these values that if the separation distance is further reduced, the heat radiation will become more prominent.

Obviously a distance between 21.2 m and 4.45 m (the length of the waste container) would tend to simulate appropriately the relative magnitudes of these two heat transfer mechanisms.

Figure 25 shows a vector plot obtained at 10 years for case 1. The maximum velocity achieved at this time is 0.018 m/s but the average velocity of the air is around 0.01 m/s. The velocities achieved at other times varies between 0.002 m/s to 0.102 m/s. The streamline plot shown in Figure 26 shows two cells obtained at 600 years. At all times two asymmetric cells were obtained.

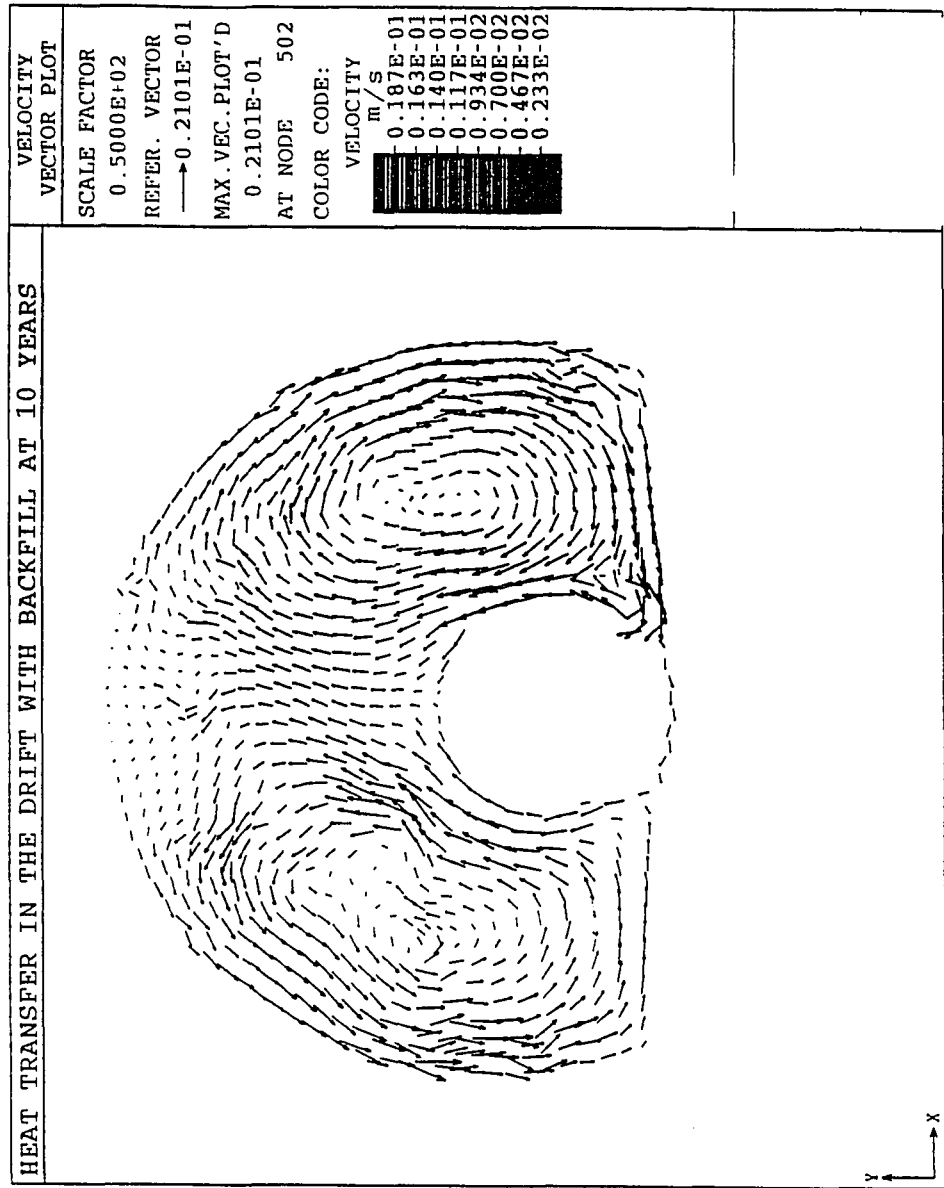


Figure 25 Vector Plot at 10 Years

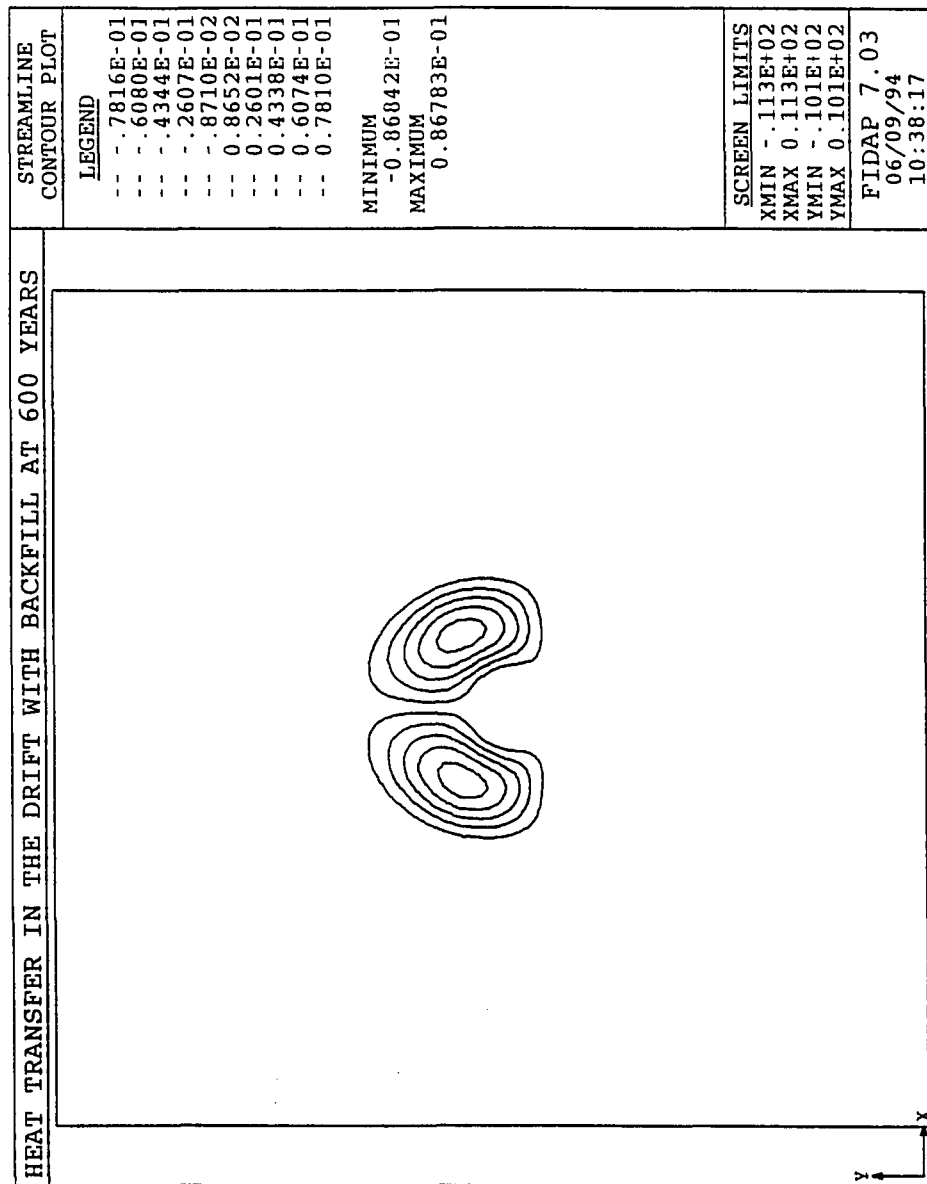


Figure 26 Streamline Plot

## CHAPTER 6

### CONCLUSION

Radiation and natural convection play an important role in the cooling of the nuclear waste containers. The 2-D model approach towards the smearing of the heat of the waste container affects the peak temperatures on the drift and inside the waste container to a great extent. In the early years the difference of temperatures between the drift and the surface of the waste container are significant but as the time progressed the temperature difference reduced considerably, thus reducing heat transfer due to radiation. It is also shown from the trends of the 2-D model that a 3-D model should be developed with the appropriate radiation boundary conditions to predict a more effect of radiation. This should produce a true temperature distribution on the drift especially in the vicinity of the waste container and waste container walls. The results for the transient conduction model have been compared with the results obtained by Ruffner<sup>2</sup>. The peak temperatures match with his case of 138 MTU/acre.

## APPENDIX 1

### INPUT FILE TO GENERATE MESH AND OBTAIN SOLUTION FOR THE TRANSIENT STATE CONDUCTION MODEL

```
TITLE
TRANSIENT CONDUCTION IN THE ROCK 70 FT
/ Generation of mesh using FI-GEN
FI-GEN( )
WINDOW(CHANGE= 1, MATRIX )
1.000000  0.000000  0.000000  0.000000
0.000000  1.000000  0.000000  0.000000
0.000000  0.000000  1.000000  0.000000
0.000000  0.000000  0.000000  1.000000
-10.00000  10.00000  -7.50000  7.50000  -7.50000  7.50000
/ generation of points
POINT( ADD, COOR, X = 0, Y = -3.335 )
POINT( ADD, COOR, X = -3.335, Y = 0 )
POINT( ADD, COOR, X = 0, Y = 3.335 )
POINT( ADD, COOR, X = 0, Y = 10 )
POINT( ADD, COOR, X = -20, Y = 10 )
POINT( ADD, COOR, X = 0, Y = 50 )
POINT( ADD, COOR, X = -20, Y = 50 )
POINT( ADD, COOR, X = 0, Y = 150 )
POINT( ADD, COOR, X = -20, Y = 150 )
POINT( ADD, COOR, X = 0, Y = 300 )
POINT( ADD, COOR, X = -20, Y = 300 )
POINT( ADD, COOR, X = 0, Y = -10 )
POINT( ADD, COOR, X = -20, Y = -10 )
POINT( ADD, COOR, X = 0, Y = -50 )
POINT( ADD, COOR, X = -20, Y = -50 )
POINT( ADD, COOR, X = 0, Y = -150 )
POINT( ADD, COOR, X = -20, Y = -150 )
POINT( ADD, COOR, X = 0, Y = -300 )
POINT( ADD, COOR, X = -20, Y = -300 )
/ Generation of arcs
POINT( SELE, ID, WIND = 1 )
1
```

```
2
3
CURVE( ADD, ARC )
POINT( SELE, ID, WIND = 1 )
3
4
CURVE( ADD, LINE )
POINT( SELE, ID, WIND = 1 )
1
12
CURVE( ADD, LINE )
POINT( SELE, ID, WIND = 1 )
5
13
CURVE( ADD, LINE )
POINT( SELE, ID, WIND = 1 )
4
6
CURVE( ADD, LINE )
POINT( SELE, ID, WIND = 1 )
5
7
CURVE( ADD, LINE )
POINT( SELE, ID, WIND = 1 )
12
14
CURVE( ADD, LINE )
POINT( SELE, ID, WIND = 1 )
13
15
CURVE( ADD, LINE )
POINT( SELE, ID, WIND = 1 )
6
8
CURVE( ADD, LINE )
POINT( SELE, ID, WIND = 1 )
7
9
CURVE( ADD, LINE )
POINT( SELE, ID, WIND = 1 )
14
16
CURVE( ADD, LINE )
POINT( SELE, ID, WIND = 1 )
```



```
15
17
CURVE( ADD, LINE )
POINT( SELE, ID, WIND = 1 )
8
10
CURVE( ADD, LINE )
POINT( SELE, ID, WIND = 1 )
9
11
CURVE( ADD, LINE )
POINT( SELE, ID, WIND = 1 )
16
18
CURVE( ADD, LINE )
POINT( SELE, ID, WIND = 1 )
17
19
CURVE( ADD, LINE )
POINT( SELE, ID, WIND = 1 )
4
5
CURVE( ADD, LINE )
POINT( SELE, ID, WIND = 1 )
12
13
CURVE( ADD, LINE )
POINT( SELE, ID, WIND = 1 )
6
7
CURVE( ADD, LINE )
POINT( SELE, ID, WIND = 1 )
14
15
CURVE( ADD, LINE )
POINT( SELE, ID, WIND = 1 )
8
9
CURVE( ADD, LINE )
POINT( SELE, ID, WIND = 1 )
16
17
CURVE( ADD, LINE )
POINT( SELE, ID, WIND = 1 )
```

```

10
11
CURVE( ADD, LINE )
POINT( SELE, ID, WIND = 1 )
18
19
CURVE( ADD, LINE )
/ Define surface
CURVE( SELE, ID, WIND = 1 )
24
16
12
8
4
6
10
14
23
13
9
5
2
1
3
7
11
15
SURFACE( ADD, WIRE, VISI, EDG1 = 1, EDG2 = 7, EDG3 = 1, EDG4 = 9 )
/ Define mesh edges
MEDGE( SETD, INTE = 3 )
MEDGE( SETD, INTE = 20 )
CURVE( SELE, ID, WIND = 1 )
1
MEDGE( ADD, INTE = 20 )
MEDGE( SETD, INTE = 10 )
CURVE( SELE, ID, WIND = 1 )
2
3
MEDGE( ADD, INTE = 10 )
MEDGE( SETD, INTE = 20 )
CURVE( SELE, ID, WIND = 1 )
4
MEDGE( ADD, INTE = 20 )
MEDGE( SETD, INTE = 30 )

```

```

CURVE( SELE, ID, WIND = 1 )
5
6
7
8
MEDGE( ADD, INTE = 30 )
MEDGE( SETD, INTE = 50 )
CURVE( SELE, ID, WIND = 1 )
9
10
11
12
MEDGE( ADD, INTE = 50 )
MEDGE( SETD, INTE = 80 )
CURVE( SELE, ID, WIND = 1 )
13
14
15
16
MEDGE( ADD, INTE = 80 )
MEDGE( SETD, INTE = 20 )
CURVE( SELE, ID, WIND = 1 )
17
18
19
20
MEDGE( ADD, INTE = 20 )
MEDGE( SETD, INTE = 16 )
CURVE( SELE, ID, WIND = 1 )
21
22
MEDGE( ADD, INTE = 16 )
MEDGE( SETD, INTE = 10 )
CURVE( SELE, ID, WIND = 1 )
23
24
MEDGE( ADD, INTE = 10 )
/ Define edge elements
MEDGE( SELE, ID, WIND = 1 )
1
ELEMENT( SETD, EDGE, NODE = 2 )
MEDGE( MESH, MAP, ENTI = "drift" )
MEDGE( SELE, ID, WIND = 1 )
23

```

```

MEDGE( MESH, MAP, ENTI = "top" )
MEDGE( SELE, ID, WIND = 1 )
24
MEDGE( MESH, MAP, ENTI = "bottom" )
/
/ define mesh loops
/
CURVE( SELE, ID, WIND = 1 )
1
2
17
4
18
3
MLOOP( ADD, PAVE, VISI )
CURVE( SELE, ID, WIND = 1 )
5
19
6
17
MLOOP( ADD, PAVE, VISI )
CURVE( SELE, ID, WIND = 1 )
9
21
10
19
MLOOP( ADD, PAVE, VISI )
CURVE( SELE, ID, WIND = 1 )
13
23
14
21
MLOOP( ADD, PAVE, VISI )
CURVE( SELE, ID, WIND = 1 )
7
18
8
20
MLOOP( ADD, PAVE, VISI )
CURVE( SELE, ID, WIND = 1 )
11
20
12
22

```

```

MLOOP( ADD, PAVE, VISI )
CURVE( SELE, ID, WIND = 1 )
15
22
16
24
MLOOP( ADD, PAVE, VISI )
/
/ define mesh faces
/
SURFACE( SELE, ID, WIND = 1 )
1
UTILITY( HIGH = 9 )
MLOOP( SELE, ID, WIND = 1 )
1
UTILITY( HIGH = 3 )
MFACE( ADD )
SURFACE( SELE, ID, WIND = 1 )
1
UTILITY( HIGH = 9 )
MLOOP( SELE, ID, WIND = 1 )
2
UTILITY( HIGH = 3 )
MFACE( ADD )
SURFACE( SELE, ID, WIND = 1 )
1
UTILITY( HIGH = 9 )
MLOOP( SELE, ID, WIND = 1 )
3
UTILITY( HIGH = 3 )
MFACE( ADD )
SURFACE( SELE, ID, WIND = 1 )
1
UTILITY( HIGH = 9 )
MLOOP( SELE, ID, WIND = 1 )
4
UTILITY( HIGH = 3 )
MFACE( ADD )
SURFACE( SELE, ID, WIND = 1 )
1
UTILITY( HIGH = 9 )
MLOOP( SELE, ID, WIND = 1 )
5
UTILITY( HIGH = 3 )

```

```

MFACE( ADD )
SURFACE( SELE, ID, WIND = 1 )
1
UTILITY( HIGH = 9 )
MLOOP( SELE, ID, WIND = 1 )
6
UTILITY( HIGH = 3 )
MFACE( ADD )
SURFACE( SELE, ID, WIND = 1 )
1
UTILITY( HIGH = 9 )
MLOOP( SELE, ID, WIND = 1 )
7
UTILITY( HIGH = 3 )
MFACE( ADD )
/ Define quadrilateral elements
MFACE( SELE, ID, WIND = 1 )
1
2
3
4
5
6
7
ELEMENT( SETD, QUAD, NODE = 4 )
MFACE( MESH, PAVE, ENTI = "solid" )
END( )
/ Generation of mesh is complete
/ Define the problem
FIPREP( )
PROBLEM( TRAN, NONL, NOMOMENTUM, ENERGY )
TIMEINTEGRATION( NSTE = 100, DT = 100000, VARI = 0.01 )
EXECUTION( NEWJ )
ICNODE( TEMP, CONS = 298, ALL )
SOLUTION( S.S. = 50, RESC = 0.1, ACCF = 0.8 )
CONDUCTIVITY( SET = 1, CONS = 3, ISOT )
DENSITY( SET = 1, CONS = 2640 )
SPECIFICHEAT( SET = 1, CONS = 800 )
BCNODE( TEMP, ENTI = "top", CONS = 298 )
BCNODE( TEMP, ENTI = "bottom", CONS = 308 )
BCFLUX( HEAT, ENTI = "drift", CONS = 1, CURV = 1, FACT = 0.0525 )
TMFUNCTION( SET = 1, NPOI = 18 )
/ Left column is time in seconds, right column is heat flux in W/m²
0, 1285

```



## APPENDIX 2

### INPUT FILE TO GENERATE MESH AND OBTAIN SOLUTION FOR STEADY STATE ANALYSIS INSIDE THE DRIFT WITHOUT BACKFILL

```
TITLE( )
HEAT TRANSFER INSIDE THE DRIFT WITHOUT BACKFILL
/ Generation of mesh using FI-GEN
FI-GEN( )
WINDOW(CHANGE= 1, MATRIX )
1.000000  0.000000  0.000000  0.000000
0.000000  1.000000  0.000000  0.000000
0.000000  0.000000  1.000000  0.000000
0.000000  0.000000  0.000000  1.000000
-10.00000  10.00000  -7.50000  7.50000  -7.50000  7.50000
/ Generation of points
POINT( ADD, COOR, X = 0, Y = -3.1826 )
POINT( ADD, COOR, X = -0.835, Y = -2.3476 )
POINT( ADD, COOR, X = 0, Y = -1.5126 )
POINT( ADD, COOR, X = 0.835, Y = -2.3476 )
POINT( ADD, COOR, X = 0, Y = -3.335 )
POINT( ADD, COOR, X = -3.335, Y = 0 )
POINT( ADD, COOR, X = 0, Y = 3.335 )
POINT( ADD, COOR, X = 3.335, Y = 0 )
POINT( ADD, COOR, X = 0, Y = -10 )
POINT( ADD, COOR, X = -10, Y = -10 )
POINT( ADD, COOR, X = -10, Y = 10 )
POINT( ADD, COOR, X = 0, Y = 10 )
POINT( ADD, COOR, X = 10, Y = 10 )
POINT( ADD, COOR, X = 10, Y = -10 )

/ Generation of arcs
POINT( SELE, ID, WIND = 1 )
```



```

1
2
3
CURVE( ADD, ARC )
POINT( SELE, ID, WIND = 1 )
1
4
3
CURVE( ADD, ARC )
POINT( SELE, ID, WIND = 1 )
5
6
7
CURVE( ADD, ARC )
POINT( SELE, ID, WIND = 1 )
5
8
7
CURVE( ADD, ARC )
POINT( SELE, ID, WIND = 1 )
7
12
CURVE( ADD, LINE )
POINT( SELE, ID, WIND = 1 )
3
7
CURVE( ADD, LINE )
POINT( SELE, ID, WIND = 1 )
1
5
CURVE( ADD, LINE )
POINT( SELE, ID, WIND = 1 )
9
10
CURVE( ADD, LINE )
POINT( SELE, ID, WIND = 1 )
10
11
CURVE( ADD, LINE )
POINT( SELE, ID, WIND = 1 )
11
12
CURVE( ADD, LINE )
POINT( SELE, ID, WIND = 1 )

```

```

12
13
CURVE( ADD, LINE )
POINT( SELE, ID, WIND = 1 )
13
14
CURVE( ADD, LINE )
POINT( SELE, ID, WIND = 1 )
14
9
CURVE( ADD, LINE )
POINT( SELE, ID, WIND = 1 )
5
9
CURVE( ADD, LINE )
/ Define surface
CURVE( SELE, ID, WIND = 1 )
13
8
9
10
11
12
SURFACE( ADD, WIRE, VISI, EDG1 = 2, EDG2 = 1, EDG3 = 2, EDG4 = 1 )
/ Define mesh edges
MEDGE( SETD, INTE = 3 )
MEDGE( SETD, INTE = 30 )
CURVE( SELE, ID, WIND = 1 )
1
MEDGE( ADD, INTE = 30 )
MEDGE( SETD, INTE = 30 )
CURVE( SELE, ID, WIND = 1 )
2
MEDGE( ADD, INTE = 30 )
MEDGE( SETD, INTE = 60 )
CURVE( SELE, ID, WIND = 1 )
3
MEDGE( ADD, INTE = 60 )
MEDGE( SETD, INTE = 60 )
CURVE( SELE, ID, WIND = 1 )
4
MEDGE( ADD, INTE = 60 )
MEDGE( SETD, INTE = 10 )
CURVE( SELE, ID, WIND = 1 )

```

```

5
MEDGE( ADD, INTE = 10 )
MEDGE( SETD, INTE = 20 )
CURVE( SELE, ID, WIND = 1 )
6
MEDGE( ADD, INTE = 20 )
MEDGE( SETD, INTE = 2 )
CURVE( SELE, ID, WIND = 1 )
7
MEDGE( ADD, INTE = 2 )
MEDGE( SETD, INTE = 10 )
CURVE( SELE, ID, WIND = 1 )
8
10
11
13
MEDGE( ADD, INTE = 10 )
MEDGE( SETD, INTE = 20 )
CURVE( SELE, ID, WIND = 1 )
9
12
MEDGE( ADD, INTE = 20 )
MEDGE( SETD, INTE = 10 )
CURVE( SELE, ID, WIND = 1 )
14
MEDGE( ADD, INTE = 10 )
/ Define edge elements
MEDGE( SELE, ID, WIND = 1 )
1
ELEMENT( SETD, EDGE, NODE = 2 )
MEDGE( MESH, MAP, ENTI = "rad1" )
MEDGE( SELE, ID, WIND = 1 )
2
ELEMENT( SETD, EDGE, NODE = 2 )
MEDGE( MESH, MAP, ENTI = "rad2" )
MEDGE( SELE, ID, WIND = 1 )
3
ELEMENT( SETD, EDGE, NODE = 2 )
MEDGE( MESH, MAP, ENTI = "rad3" )
MEDGE( SELE, ID, WIND = 1 )
4
ELEMENT( SETD, EDGE, NODE = 2 )
MEDGE( MESH, MAP, ENTI = "rad4" )
MEDGE( SELE, ID, WIND = 1 )

```

```

8
9
10
11
ELEMENT( SETD, EDGE, NODE = 2 )
MEDGE( MESH, MAP, ENTI = "rock" )
MEDGE( SELE, ID, WIND = 1 )
12
13
ELEMENT( SETD, EDGE, NODE = 2 )
MEDGE( MESH, MAP, ENTI = "side" )
/ Define mesh loops
CURVE( SELE, ID, WIND = 1 )
8
9
10
5
3
14
MLOOP( ADD, PAVE, VISI )
CURVE( SELE, ID, WIND = 1 )
13
14
4
5
11
12
MLOOP( ADD, PAVE, VISI )
CURVE( SELE, ID, WIND = 1 )
3
6
1
7
MLOOP( ADD, PAVE, VISI )
CURVE( SELE, ID, WIND = 1 )
6
4
7
2
MLOOP( ADD, PAVE, VISI )
CURVE( SELE, ID, WIND = 1 )
1
2
MLOOP( ADD, PAVE, VISI )

```

```

/
/ Define mesh faces
/
SURFACE( SELE, ID, WIND = 1 )
  1
UTILITY( HIGH = 9 )
MLOOP( SELE, ID, WIND = 1 )
  1
UTILITY( HIGH = 3 )
MFACE( ADD )
SURFACE( SELE, ID, WIND = 1 )
  1
UTILITY( HIGH = 9 )
MLOOP( SELE, ID, WIND = 1 )
  2
UTILITY( HIGH = 3 )
MFACE( ADD )
SURFACE( SELE, ID, WIND = 1 )
  1
UTILITY( HIGH = 9 )
MLOOP( SELE, ID, WIND = 1 )
  3
UTILITY( HIGH = 3 )
MFACE( ADD )
SURFACE( SELE, ID, WIND = 1 )
  1
UTILITY( HIGH = 9 )
MLOOP( SELE, ID, WIND = 1 )
  4
UTILITY( HIGH = 3 )
MFACE( ADD )
SURFACE( SELE, ID, WIND = 1 )
  1
UTILITY( HIGH = 9 )
MLOOP( SELE, ID, WIND = 1 )
  5
UTILITY( HIGH = 3 )
MFACE( ADD )
/ Define quadrilateral elements
MFACE( SELE, ID, WIND = 1 )
  1
  2
ELEMENT( SETD, QUAD, NODE = 4 )
MFACE( MESH, PAVE, ENTI = "solid" )

```

```

MFACE( SELE, ID, WIND = 1 )
3
4
ELEMENT( SETD, QUAD, NODE = 4 )
MFACE( MESH, PAVE, ENTI = "fluid" )
MFACE( SELE, ID, WIND = 1 )
5
ELEMENT( SETD, QUAD, NODE = 4 )
MFACE( MESH, PAVE, ENTI = "nuclear" )
END( )
/ Generation of mesh is complete
/ Define the problem
FIPREP( )
PROBLEM( STEA, NONL, TURB, BUOY )
EXECUTION( NEWJ )
PRESSURE( PENA = 1e-08, DISC )
SOLUTION( S.S. = 1000, RESC = 0.01, ACCF = 0.8 )
ICNODE( TEMP, CONS = 298.0, ALL )
ICNODE( KINE, CONS = 0.002, ALL )
ICNODE( DISS, CONS = 0.002, ALL )
GRAVITY( MAGN = 9.81 )
CONDUCTIVITY( SET = 1, CONS = 0.02816, ISOT )
CONDUCTIVITY( SET = 2, CONS = 3, ISOT )
CONDUCTIVITY( SET = 3, CONS = 2.79, ISOT )
DENSITY( SET = 1, CONS = 1.086 )
DENSITY( SET = 2, CONS = 2640.0 )
DENSITY( SET = 3, CONS = 4705.2 )
SPECIFICHEAT( SET = 1, CONS = 1006.0 )
SPECIFICHEAT( SET = 2, CONS = 800.0 )
SPECIFICHEAT( SET = 3, CONS = 422.8 )
VOLUMEXPANSION( SET = 1, CONS = 0.00307, REFT = 325.0 )
VISCOSITY( SET = 1, CONS = 1.962e-05, K.E. )
/ emissivity of the nuclear waste
EMISSION( SET = 1, CONS = 0.6, STEF = 5.669e-08 )
/ emissivity of the rock
EMISSION( SET = 2, CONS = 0.75, STEF = 5.669e-08 )
ENTITY( NAME = "fluid", FLUI, MDEN = 1, MVIS = 1, MSPH = 1, MCON = 1,
MEXP = 1 )
ENTITY( NAME = "rad1", RAD1, GREY, ATTA = "fluid", MEMS = 1 )
ENTITY( NAME = "rad2", RAD1, GREY, ATTA = "fluid", MEMS = 1 )
ENTITY( NAME = "rad3", RAD1, GREY, ATTA = "fluid", MEMS = 2 )
ENTITY( NAME = "rad4", RAD1, GREY, ATTA = "fluid", MEMS = 2 )
ENTITY( NAME = "solid", SOLI, MDEN = 2, MSPH = 2, MCON = 2 )
ENTITY( NAME = "nuclear", SOLI, MDEN = 3, MSPH = 3, MCON = 3 )

```

```

ENTITY( NAME = "rock", PLOT )
ENTITY( NAME = "side", PLOT )
RADIATION( NOPA, GREY )
RADSURFACE( ENTI = "rad1", INDI )
RADSURFACE( ENTI = "rad2", INDI )
RADSURFACE( ENTI = "rad3", INDI )
RADSURFACE( ENTI = "rad4", INDI )
VIEWFACTOR( SMOO )
OBSTRUCTION( LIST )
"rad1", "rad2"
DATAPRINT( CONT )
PRINTOUT( NONE, BOUN )
BCNODE( VELO, ENTI = "rad1", CONS = 0 )
BCNODE( VELO, ENTI = "rad2", CONS = 0 )
BCNODE( VELO, ENTI = "rad3", CONS = 0 )
BCNODE( VELO, ENTI = "rad4", CONS = 0 )
/The following three commands define the boundary
/conditions for the temperature and the heat flux at /different time steps
/These values are boundary conditions at 30 years
BCNODE( TEMP, ENTI = "rock", CONS = 417 )
BCNODE( TEMP, ENTI = "side", CONS = 423 )
BCFLUX( HEAT, ENTI = "rad1", CONS = 146 )
BCFLUX( HEAT, ENTI = "rad2", CONS = 146 )
END( )
CREATE( FISO )
END( )

```

### APPENDIX 3

INPUT FILE TO GENERATE MESH AND OBTAIN SOLUTION  
FOR THE STEADY STATE ANALYSIS INSIDE  
THE DRIFT WITH BACKFILL

```
TITLE( )
HEAT TRANSFER IN THE DRIFT WITH BACKFILL
/ Generation of mesh using FI-GEN
FI-GEN( )
WINDOW(CHANGE= 1, MATRIX )
1.000000  0.000000  0.000000  0.000000
0.000000  1.000000  0.000000  0.000000
0.000000  0.000000  1.000000  0.000000
0.000000  0.000000  0.000000  1.000000
-10.00000  10.00000  -7.50000  7.50000  -7.50000  7.50000
/ Generation of points
POINT( ADD, COOR, X = 0, Y = -1.335 )
POINT( ADD, COOR, X = -0.835, Y = -0.52 )
POINT( ADD, COOR, X = 0, Y = 0.315 )
POINT( ADD, COOR, X = 0.835, Y = -0.52 )
POINT( ADD, COOR, X = 0, Y = -3.335 )
POINT( ADD, COOR, X = -2.3811, Y = -2.335 )
POINT( ADD, COOR, X = -3.0473, Y = -1.335 )
POINT( ADD, COOR, X = -3.335, Y = 0 )
POINT( ADD, COOR, X = 0, Y = 3.335 )
POINT( ADD, COOR, X = 3.335, Y = 0 )
POINT( ADD, COOR, X = 3.0473, Y = -1.335 )
POINT( ADD, COOR, X = 2.3811, Y = -2.335 )
POINT( ADD, COOR, X = 0, Y = -10 )
POINT( ADD, COOR, X = -10, Y = -10 )
POINT( ADD, COOR, X = -10, Y = 10 )
POINT( ADD, COOR, X = 0, Y = 10 )
POINT( ADD, COOR, X = 10, Y = 10 )
POINT( ADD, COOR, X = 10, Y = -10 )
```



```

POINT( ADD, COOR, X = 0.0, Y = -1.6)
WINDOW(CHANGE= 1, MATRIX )
1.000000  0.000000  0.000000  0.000000
0.000000  1.000000  0.000000  0.000000
0.000000  0.000000  1.000000  0.000000
0.000000  0.000000  0.000000  1.000000
-14.00000  14.00000  -10.50000  10.50000  -21.00000  21.00000
/ Generation of arcs
POINT( SELE, ID = 1 )
POINT( SELE, ID = 2 )
POINT( SELE, ID = 3 )
CURVE( ADD, ARC )
POINT( SELE, ID = 3 )
POINT( SELE, ID = 4 )
POINT( SELE, ID = 1 )
CURVE( ADD, ARC )
POINT( SELE, ID = 7 )
POINT( SELE, ID = 19 )
CURVE( ADD, LINE )
POINT( SELE, ID = 19 )
POINT( SELE, ID = 11 )
CURVE( ADD, LINE )
POINT( SELE, ID = 5 )
POINT( SELE, ID = 6 )
POINT( SELE, ID = 7 )
CURVE( ADD, ARC )
POINT( SELE, ID = 5 )
POINT( SELE, ID = 12 )
POINT( SELE, ID = 11 )
CURVE( ADD, ARC )
POINT( SELE, ID = 7 )
POINT( SELE, ID = 8 )
POINT( SELE, ID = 9 )
CURVE( ADD, ARC )
POINT( SELE, ID = 9 )
POINT( SELE, ID = 10 )
POINT( SELE, ID = 11 )
CURVE( ADD, ARC )
POINT( SELE, ID = 13 )
POINT( SELE, ID = 14 )
CURVE( ADD, LINE )
POINT( SELE, ID = 13 )
POINT( SELE, ID = 18 )
CURVE( ADD, LINE )

```

```

POINT( SELE, ID = 15 )
POINT( SELE, ID = 16 )
CURVE( ADD, LINE )
POINT( SELE, ID = 16 )
POINT( SELE, ID = 17 )
CURVE( ADD, LINE )
POINT( SELE, ID = 14 )
POINT( SELE, ID = 15 )
CURVE( ADD, LINE )
POINT( SELE, ID = 17 )
POINT( SELE, ID = 18 )
CURVE( ADD, LINE )
POINT( SELE, ID = 9 )
POINT( SELE, ID = 16 )
CURVE( ADD, LINE )
POINT( SELE, ID = 5 )
POINT( SELE, ID = 13 )
CURVE( ADD, LINE )
POINT( SELE, ID = 9 )
POINT( SELE, ID = 3 )
CURVE( ADD, LINE )
POINT( SELE, ID = 1 )
POINT( SELE, ID = 19 )
CURVE( ADD, LINE )
/ Define surface
CURVE( SELE, ID = 13 )
CURVE( SELE, ID = 11 )
CURVE( SELE, ID = 12 )
CURVE( SELE, ID = 14 )
CURVE( SELE, ID = 10 )
CURVE( SELE, ID = 9 )
SURFACE( ADD, WIRE, VISI, EDG1 = 1, EDG2 = 2, EDG3 = 1, EDG4 = 2 )
/ Define mesh edges
MEDGE( SETD, INTE = 3 )
MEDGE( SETD, INTE = 20 )
CURVE( SELE, ID = 1 )
MEDGE( ADD, INTE = 20 )
CURVE( SELE, ID = 2 )
MEDGE( ADD )
MEDGE( SETD, INTE = 20 )
CURVE( SELE, ID = 3 )
MEDGE( ADD, INTE = 20 )
CURVE( SELE, ID = 4 )
MEDGE( ADD )

```

```

MEDGE( SETD, INTE = 20 )
CURVE( SELE, ID = 5 )
MEDGE( ADD, INTE = 20 )
CURVE( SELE, ID = 6 )
MEDGE( ADD )
MEDGE( SETD, INTE = 40 )
CURVE( SELE, ID = 7 )
MEDGE( ADD, INTE = 40 )
CURVE( SELE, ID = 8 )
MEDGE( ADD )
MEDGE( SETD, INTE = 10 )
CURVE( SELE, ID = 9 )
MEDGE( ADD, INTE = 10 )
CURVE( SELE, ID = 10 )
MEDGE( ADD )
CURVE( SELE, ID = 11 )
MEDGE( ADD )
CURVE( SELE, ID = 12 )
MEDGE( ADD )
MEDGE( SETD, INTE = 16 )
CURVE( SELE, ID = 13 )
MEDGE( ADD, INTE = 16 )
CURVE( SELE, ID = 14 )
MEDGE( ADD )
MEDGE( SETD, INTE = 20 )
CURVE( SELE, ID = 15 )
MEDGE( ADD, FRSTLAST, INTE = 20, RATIO=0.3 )
MEDGE( SETD, INTE = 20 )
CURVE( SELE, ID = 16 )
MEDGE( ADD, FRSTLAST, INTE = 20, RATIO=0.3 )
MEDGE( SETD, INTE = 20 )
CURVE( SELE, ID = 17 )
MEDGE( ADD, INTE = 20 )
MEDGE( SETD, INTE = 2 )
CURVE( SELE, ID = 18 )
MEDGE( ADD, INTE = 2 )
/ Define mesh loop
CURVE( SELE, ID = 1 )
CURVE( SELE, ID = 2 )
MLOOP( ADD, PAVE, VISI )
CURVE( SELE, ID = 3 )
CURVE( SELE, ID = 7 )
CURVE( SELE, ID = 17 )
CURVE( SELE, ID = 1 )

```

```

CURVE( SELE, ID = 18 )
MLOOP( ADD, PAVE, VISI )
CURVE( SELE, ID = 2 )
CURVE( SELE, ID = 17 )
CURVE( SELE, ID = 8 )
CURVE( SELE, ID = 4 )
CURVE( SELE, ID = 18 )
MLOOP( ADD, PAVE, VISI )
CURVE( SELE, ID = 3 )
CURVE( SELE, ID = 4 )
CURVE( SELE, ID = 6 )
CURVE( SELE, ID = 5 )
MLOOP( ADD, PAVE, VISI )
CURVE( SELE, ID = 9 )
CURVE( SELE, ID = 13 )
CURVE( SELE, ID = 11 )
CURVE( SELE, ID = 15 )
CURVE( SELE, ID = 7 )
CURVE( SELE, ID = 5 )
CURVE( SELE, ID = 16 )
MLOOP( ADD, PAVE, VISI )
CURVE( SELE, ID = 12 )
CURVE( SELE, ID = 14 )
CURVE( SELE, ID = 10 )
CURVE( SELE, ID = 16 )
CURVE( SELE, ID = 6 )
CURVE( SELE, ID = 8 )
CURVE( SELE, ID = 15 )
MLOOP( ADD, PAVE, VISI )
/ Define mesh face
SURFACE( SELE, ID = 1 )
UTILITY( HIGH = 9 )
MLOOP( SELE, ID = 1 )
UTILITY( HIGH = 3 )
MFACE( ADD )
SURFACE( SELE, ID = 1 )
UTILITY( HIGH = 9 )
MLOOP( SELE, ID = 2 )
UTILITY( HIGH = 3 )
MFACE( ADD )
SURFACE( SELE, ID = 1 )
UTILITY( HIGH = 9 )
MLOOP( SELE, ID = 3 )
UTILITY( HIGH = 3 )

```

```

MFACE( ADD )
SURFACE( SELE, ID = 1 )
UTILITY( HIGH = 9 )
MLOOP( SELE, ID = 4 )
UTILITY( HIGH = 3 )
MFACE( ADD )
SURFACE( SELE, ID = 1 )
UTILITY( HIGH = 9 )
MLOOP( SELE, ID = 5 )
UTILITY( HIGH = 3 )
MFACE( ADD )
SURFACE( SELE, ID = 1 )
UTILITY( HIGH = 9 )
MLOOP( SELE, ID = 6 )
UTILITY( HIGH = 3 )
MFACE( ADD )
/ Define edge elements
MEDGE( SETD, INTE = 8 )
MEDGE( SELE, ID = 1 )
ELEMENT( SETD, EDGE, NODE = 2 )
MEDGE( MESH, MAP, ENTI = "canister1" )
MEDGE( SELE, ID = 2 )
MEDGE( MESH, MAP, ENTI = "canister2" )
MEDGE( SELE, ID = 7 )
MEDGE( MESH, MAP, ENTI = "drift1" )
MEDGE( SELE, ID = 8 )
MEDGE( MESH, MAP, ENTI = "drift2" )
MEDGE( SELE, ID = 3 )
MEDGE( MESH, MAP, ENTI = "back1" )
MEDGE( SELE, ID = 4 )
MEDGE( MESH, MAP, ENTI = "back2" )
MEDGE( SELE, ID = 9 )
MEDGE( MESH, MAP, ENTI = "top" )
MEDGE( SELE, ID = 10 )
MEDGE( MESH, MAP, ENTI = "top" )
MEDGE( SELE, ID = 11 )
MEDGE( MESH, MAP, ENTI = "top" )
MEDGE( SELE, ID = 12 )
MEDGE( MESH, MAP, ENTI = "top" )
MEDGE( SELE, ID = 13 )
MEDGE( MESH, MAP, ENTI = "side" )
MEDGE( SELE, ID = 14 )
MEDGE( MESH, MAP, ENTI = "side" )
/ Define quadrilateral elements

```

```

MFACE( SELE, ID = 1 )
ELEMENT( SETD, QUAD, NODE = 4 )
MFACE( MESH, PAVE, ENTI = "nuclear" )
MFACE( SELE, ID = 2 )
ELEMENT( SETD, QUAD, NODE = 4 )
MFACE( MESH, PAVE, ENTI = "air" )
MFACE( SELE, ID = 3 )
ELEMENT( SETD, QUAD, NODE = 4 )
MFACE( MESH, PAVE, ENTI = "air" )
MFACE( SELE, ID = 4 )
ELEMENT( SETD, QUAD, NODE = 4 )
MFACE( MESH, PAVE, ENTI = "backfill" )
MFACE( SELE, ID = 5 )
ELEMENT( SETD, QUAD, NODE = 4 )
MFACE( MESH, PAVE, ENTI = "rock" )
MFACE( SELE, ID = 6 )
ELEMENT( SETD, QUAD, NODE = 4 )
MFACE( MESH, PAVE, ENTI = "rock" )
END( )
/ Generation of mesh complete
/ Define the problem
FIPREP( )
PROBLEM( STEA, NONL, TURB, BUOY )
EXECUTION( NEWJ )
PRESSURE( PENA = 1e-08, DISC )
SOLUTION( S.S. = 100, RESC = 0.01, ACCF = 0.8 )
ICNODE( TEMP, CONS = 298.0, ALL )
ICNODE( KINE, CONS = 0.002, ALL )
ICNODE( DISS, CONS = 0.002, ALL )
GRAVITY( MAGN = 9.81 )
CONDUCTIVITY( SET = 1, CONS = 0.02816, ISOT )
CONDUCTIVITY( SET = 2, CONS = 3.0, ISOT )
CONDUCTIVITY( SET = 3, CONS = 2.79, ISOT )
CONDUCTIVITY( SET = 4, CONS = 1.8, ISOT )
DENSITY( SET = 1, CONS = 1.086 )
DENSITY( SET = 2, CONS = 2640.0 )
DENSITY( SET = 3, CONS = 4705.2 )
DENSITY( SET = 4, CONS = 1584.0 )
SPECIFICHEAT( SET = 1, CONS = 1006.0 )
SPECIFICHEAT( SET = 2, CONS = 800.0 )
SPECIFICHEAT( SET = 3, CONS = 422.8 )
SPECIFICHEAT( SET = 4, CONS = 480.0 )
VOLUMEXPANSION( SET = 1, CONS = 0.00307, REFT = 325.0 )
VISCOSITY( SET = 1, CONS = 1.962e-05, K.E. )

```

```

EMISSION( SET = 1, CONS = 0.6, STEF = 5.669e-08 )
EMISSION( SET = 2, CONS = 0.75, STEF = 5.669e-08 )
BCNODE( VELO, ENTI = "drift1", CONS = 0 )
BCNODE( VELO, ENTI = "drift2", CONS = 0 )
BCNODE( VELO, ENTI = "canister1", CONS = 0 )
BCNODE( VELO, ENTI = "canister2", CONS = 0 )
BCNODE( VELO, ENTI = "back1", CONS = 0 )
BCNODE( VELO, ENTI = "back2", CONS = 0 )
ENTITY( NAME = "air", FLUID, MDEN = 1, MVIS = 1, MSPH = 1, MCON = 1,
MEXP = 1 )
ENTITY( NAME = "drift1",RADI, GREY, ATTA = "air", MEMS = 1 )
ENTITY( NAME = "drift2",RADI, GREY, ATTA = "air", MEMS = 1 )
ENTITY( NAME = "canister1",RADI,GREY,ATTA = "air",MEMS = 2 )
ENTITY( NAME = "canister2",RADI,GREY,ATTA = "air",MEMS = 2 )
ENTITY( NAME = "back1", RADI, GREY, ATTA = "air", MEMS = 1 )
ENTITY( NAME = "back2", RADI, GREY, ATTA = "air", MEMS = 1 )
ENTITY( NAME = "rock", SOLI, MDEN = 2, MSPH = 2, MCON = 2 )
ENTITY( NAME = "nuclear",SOLI, MDEN = 3,MSPH = 3, MCON = 3 )
ENTITY( NAME = "backfill",SOLI,MDEN = 4,MSPH = 4, MCON = 4 )
ENTITY( NAME = "top", PLOT )
ENTITY( NAME = "side", PLOT )
RADIATION( NOPA, GREY )
RADSURFACE( ENTI = "drift1", INDI )
RADSURFACE( ENTI = "drift2", INDI )
RADSURFACE( ENTI = "canister1", INDI )
RADSURFACE( ENTI = "canister2", INDI )
RADSURFACE( ENTI = "back1", INDI )
RADSURFACE( ENTI = "back2", INDI )
VIEWFACTOR( NOSMOO )
OBSTRUCTION( LIST )
"canister1","canister2"
DATAPRINT( CONT )
OPTIONS(UPWIN)
PRINTOUT( NONE, BOUN )
/ The following four commands define the boundary conditions for the temperatures
and the heat flux at different times
/ These values are boundary conditions at 30 years
BCNODE( TEMP, ENTI = "top", CONS = 417 )
BCNODE( TEMP, ENTI = "side", CONS = 423 )
BCFLUX( HEAT, ENTI = "canister1", CONS = 146.76 )
BCFLUX( HEAT, ENTI = "canister2", CONS = 146.76 )
END( )
CREATE( FISO )
END( )

```

## BIBLIOGRAPHY

1. F.P.Incropera, D.P.Dewitt, *Fundamentals of Heat Transfer*, 3rd ed., John Wiley and Sons, New York, NY, 1990.
2. D.J.Ruffner, J.A.Blink, T.W.Doering, Drift Emplaced Waste Package Thermal Response, "*Proceedings of International Conference High Level Radioactive Waste Management*", Las Vegas (May 1993), pp 538-543.
3. G.Danko, P.Mousset-Jones, The Analysis of Horizontal Cooling Enhancement for Nuclear Waste Container Emplacement, "*Proceedings of International Conference High Level Radioactive Waste Management*", Las Vegas (May 1993), pp 667-674.
4. B.Farouk, S.I.Guceri, Laminar and Turbulent Natural Convection in the Annulus Between Horizontal Concentric Cylinders, "*Journal of Heat Transfer*", (November 1992), Vol.104, pp 631-636.
5. *Fluid Dynamics International*, 500 Davis Street, Suite 600, Evanston, IL 60201.
6. J.F.Holland, The Results of Near-Field Thermal and Mechanical Calculations of Thermal Loading Schemes, "*Proceedings of International Conference High Level Radioactive Waste Management*", Las Vegas (May 1993), pp 868-873.
7. G.L.Johnson, Thermal Performance of a Buried Nuclear Waste Storage Container Storing a Hybrid Mix of PWR and BWR Spent Fuel Rods, "*Lawrence Livermore National Laboratory*", UCID-21414 Revision 1, Page 14.